Patrícia Alexandra Teles Martins

PASSIVE PERMEATION ACROSS THE BLOOD-BRAIN BARRIER

KINETICS AND THERMODYNAMICS OF CHLORPROMAZINE INTERACTION WITH LIPID BILAYERS REPRESENTATIVE OF ENDOTHELIAL CELL MEMBRANES

Janeiro 2013

· U C ·

Universidade de Coimbra

Faculdade de Ciências e Tecnologia da Universidade de Coimbra

Departamento de Química

Patrícia Alexandra Teles Martins

PASSIVE PERMEATION ACROSS THE BLOOD-BRAIN BARRIER.

KINETICS AND THERMODYNAMICS OF CHLORPROMAZINE INTERACTION WITH LIPID BILAYERS REPRESENTATIVE OF ENDOTHELIAL CELL MEMBRANES

Dissertação de Doutoramento em Química, especialidade Química Biológica, apresentada à Faculdade de Ciências e Tecnologia da Universidade de Coimbra, sob a orientação da Professora Doutora Maria João Pedrosa Moreno Silvestre e do Professor Doutor Winchil Luís Cláudio Vaz.

2013

Coimbra

Para o meu filho Pedro

Agradecimentos

Como todos os projectos que levam o tempo que este levou, também o meu projecto de doutoramento não teria sido possível concretizar sem a contribuição de algumas pessoas e entidades, às quais desejo agradecer.

Vim parar ao Grupo de Química dos Processos Biológicos em Janeiro de 2007, através de uma Bolsa de Investigação Científica, pelo que em primeiro lugar tenho a agradecer à FCT o financiamento, na forma de Bolsas de Investigação no âmbito dos projectos financiados, que permitiu a minha introdução nesta área científica. Agradeço ainda à FCT a bolsa de doutoramento que me foi concedida (SFRH/BD/38951/2007) e que me permitiu a continuação dos trabalhos, com vista à obtenção do grau académico de doutor e ao Departamento de Química da Faculdade de Ciências e Tecnologia que ao ser a minha instituição de acolhimento me proporcionou os meios físicos e as instalações, sem as quais não seria possível proceder a um estudo desta envergadura.

À Professora Maria João, orientadora e mestre não só deste trabalho mas em tantas outras situações. Uma amiga preciosa com quem espero manter a ligação/colaboração quer a nível profissional quer a nível pessoal.

Professor Winchil Vaz, co orientador e grande mestre. Pelas conversas de onde se bebe sabedoria.

Adrian Velazquez-Campoy, *expert* em calorimetria, que me ensinou em termos práticos a utilizar esta técnica em proveito do meu estudo. Que sempre se disponibilizou para me receber, para partilhar comigo as suas instalações e o seu equipamento além de me transmitir imenso conhecimento nesta área completamente nova para mim quando iniciei os estudos em calorimetria no final de 2008.

Estudantes do grupo de química biológica e de biologia de sistemas, pelo ambiente agradável e saudável em que juntos trabalhamos, pelas pausas divertidas e pelas conversas sobre os nossos temas de estudo que normalmente revelavam sempre pormenores importantes.

Estudantes e amigos que encontrei no BIFI nas pessoas: Sonia Veiga, que sempre se mostrou disponível para qualquer ajuda ou esclarecimento, Joaquin Sanz, Raquel Alvarez e Julia Poncela *mis compis de despacho* durante a estadia mais longa no BIFI, meus físicos queridos do coração que tornaram os últimos meses de 2009 e todas a idas subsequentes à

vossa cidade, períodos menos solitários e muito mais divertidos. Minha querida Julia, foi bom ganhar esta Amizade.

O ânimo não raras as vezes não vem apenas das relações laborais ou dentro do laboratório e são também algumas as pessoas a quem quero expressar o meu mais sentido agradecimento, pela presença, pelo apoio e por tornarem a minha vida mais bonita tornando tantas vezes mais fácil lidar com os desânimos e os dias menos bons que se encontram ao longo de um trabalho com esta dimensão.

Aos meus Amigos-que-são-como-família: Andreia Farinha, Catarina Gilo, Flávio Figueira, Nuno Moura, Vitor Borges e querida Ritinha (claro!), a minha *família* em Aveiro; Joana Real e Patrícia Dolores, a *família* em Coimbra. Porque no verdadeiro sentido de Família estão sempre presentes *no matter what*, um agradecimento muito especial por me abraçarem assim.

Aos Amigos, aqueles da família FCUL, que nos vêem acompanhando desde 2000 e nunca desitiram desta amizade à distância, muitos também no percurso do doutoramento e assim com tantos pontos em comum neste percurso: Alexandre Borges, Andreia Ruivo, Guida Galhetas, Helga Garcia, Pedro Carrapato, Sebastião Coelho, Sónia Neto.

Às minhas Amigas mais "antigas" que se têem mantido presentes, preocupadas e sempre com uma palavra ou um ombro amigo para os dias menos bons e sempre com um brinde nos dias melhores, Rute Brito, Sandra Mateus e Teresa Antunes.

As minhas ricas meninas e menino do 26, Marta Silva, Patrícia Mendonça, Soraia Mourato e Vila Rodrigues com quem partilhei um ano em Coimbra, na casa onde foi crescendo o meu filho dentro de mim e que me receberam e acompanharam com carinho nesse percurso.

Foi na família de sangue que cresci e onde recebi as maiores influências no desenvolvimento da pessoa que sou hoje em dia. Quero agradecer todas as influências positivas que recebi da minha família alargada e das quais me orgulho imenso, obrigada por contribuirem para a minha formação como pessoa ensinando-me a viver rodeada de valores e princípios que adapto na minha vida diária quer a nível profissional quer a nível pessoal. Agradeço imenso a todos os meus tios maternos, pelos exemplos de vida que são para mim, pela noção importante de fraternidade que transmitem, muito obrigada. Um agradecimento mais sentido à minha Madrinha Anabela Martins, pelo acompanhamento *quasi* maternal ao longo deste percurso e à minha prima Alexandra Vinhas, a minha irmã mais velha, um exemplo de determinação, um apoio constante. Aos restantes primos.

Ao longo dos últimos onze anos ganhei uma outra Família a quem estou também muito grata pela contribuição positiva e de estabilidade que me têem proporcionado: D. Emília, Sr. Lopes, Sr. Eduardo, Avó Maria, Heitor, Sónia (e Carolininha, claro!). Obrigada!

É a primeira vez que tenho oportunidade de agradecer pública e formalmente às pessoas mais importantes da minha existência:

Obrigada, Pai! Obrigada, Mãe!

Por tudo, mesmo tudo, por me terem educado e proporcionado a vida que me trouxe aqui, pelo carinho, pelo incentivo, pelo orgulho que sentem em mim e que nem sempre estou segura de ser merecedora. Obrigada!

Obrigada meu Irmão Tiago, meu mano pequenino, meu miúdo! Por existires, por seres a minha Amizade mais pura, mais cheia de tudo-do-bom-e-do-mau, mas mais forte. Porque a tua existência faz-me querer ser uma pessoa melhor, ser a Mana mais velha, um pequenino exemplo, uma voz consciente e me faz tentar sempre agir e ser de acordo com isso.

À Família que construí(mos). Eddy, é impossível arranjar palavras para o reconhecimento e o sentimento de realização que associo à nossa existência. Já existíamos antes de iniciar este percurso "com vista à obtenção do grau de doutor", mas foi durante este percurso que crescemos, que atingimos novos patamares, que nos tornamos uma Família nos bons e nos maus momentos, que amadurecemos e que demos fruto (e que fruto delicioso!). E é um orgulho maior que o mundo olhar para vocês e saber-vos tão aí, de pedra e cal, fortes alicerces tão prontos para continuarmos esta construção, juntos. Amo-vos.

Acknowledgments

The work presented in this Ph.D. thesis would not be possible without the contribution of some people and entities to which I want to express my gratitude:

First of all, I want to express thanks to the "Fundação para a Ciência e Tecnologia" (FCT) for the financing of my PhD scholarship, granted in 2008, which allowed me to perform the work during these last years.

To the Department of Chemistry of the Faculty of Sciences and Technology, I sincerely appreciate the allowance and granted use of its physical facilities and technical installations, without which it would not have been possible to engage a study of this magnitude.

To Professor Maria João, my scientific supervisor and master, not only for the support in this work but also regarding all kind of situations in and outside the laboratory. She is a precious friend with whom I hope to maintain a connection/collaboration at a professional as well as personal level.

To Professor Winchil Vaz, my co-supervisor and great master, for the fruitful conversations, where one can drink wisdom.

To Adrian Velazquez-Campoy, expert in calorimetry, who taught me in practical terms how to properly use this technique in order to make it advantageous for my work. He always made himself available to receive me, to share with me their facilities and equipment, besides sharing with me his immense knowledge, in an area that was completely new to me when I first started working with calorimetry in the late 2008.

To the students that are now or have been part of the biological chemistry and biological systems groups in the Chemistry Department of Coimbra, for the good and healthy working environment and for the good and productive conversations and debates.

To the students I met in BIFI, who openly received me at their institute and made me comfortable and welcome in a new town and country.

To all my friends living in Aveiro, Coimbra, Lisboa and Barreiro, for all the support, unconditional friendship and presence, for making my life prettier and easier to deal with, especially in the moments of discouragements and less good days that can occur along the way.

To all my enlarged family, aunts, uncles, cousins and relatives-in-law, thank you for contributing for the person I became, for the life example you were and are for me and for the all the support.

To my father, mother and brother. You are the most important persons of my existence. For the life you provided me in order to achieve what I am today, for the love, the affection, the education you provided and for the pride you feel for me, even if sometimes I'm not sure I'm worthy. Thank you.

To the family we built. It is impossible to get words for the recognition and sense of fulfillness I associate to our existence. We grew during this process and we became a Family, we developed and we gave fruit (and what a delicious fruit!). And it's with a sense of pride, bigger than the world, that I look at you and know that you are there, cast in stone, strong and prepared foundations for life, to continue our growth, together. Thank you, for all the joy you bring to my life. I love you.

Dissertation Abstract

Passive transport across cell membranes is the major route for the permeation of xenobiotics through tight endothelia such as the blood–brain barrier. The rate of passive permeation through lipid bilayers for a given drug is therefore a critical step in the prediction of its pharmacokinetics. In this work, we present a detailed study on the kinetics and thermodynamics for the interaction of chlorpromazine, an antipsychotic drug used in the treatment of schizophrenia, with lipid membranes composed of different lipid mixtures. We use isothermal titration calorimetry, a very powerful technique for the study of molecular interactions that allows the measurement of the partition coefficient as well as the thermodynamic parameters for the interaction.

The complexity of the membranes used in this study was progressively increased, from the simple pure POPC bilayer towards lipid compositions characteristic of the outer and inner leaflets of the endothelial cells. The effect of charge, presence of cholesterol (Chol), ethanolamine phospholipids (POPE) and sphingomyelin (SpM), as well as phase coexistence, on the interaction of CPZ with the lipid bilayers was evaluated.

The introduction of 10 molar % of the negatively charged POPS into POPC membranes increases the partition of CPZ, due to the electrostatic attraction between the opposite charges, and the enthalpy variation becomes more favourable. On the other hand, the presence of Chol increases the order of the bilayers and strongly decreases the affinity of CPZ for the bilayer, both in terms of the amount of CPZ that associates with the membrane and on the interaction enthalpy that becomes unfavourable. For membranes in the liquid ordered phase (POPC:SpM:Chol 1:5:4) it is observed a much smaller partition coefficient, than for membranes in the l_d phase, with a very unfavourable enthalpy contribution. From the parameters obtained for all lipid bilayers studied, we observe that the partition of CPZ towards membranes in the liquid disordered phase has a significant favourable enthalpy contribution while the association of CPZ with membranes in the liquid ordered phase is only driven by entropy increase in the system.

The partition coefficients obtained allow the calculation of the affinities of CPZ towards the different membranes in the cell and the prediction of the relative concentration of CPZ in each lipid pool at equilibrium.

The rate of passive permeation through lipid bilayers depends on the affinity of the drug for the membrane and also on the rate constants for the interaction (insertion, desorption and translocation). In this work we have developed methodology that allows the

quantitative characterization of the rate of translocation through membranes in the liquid-disordered phase using ITC. We also give preliminary results regarding the use of this technique to obtain the rate constants for insertion into, and desorption from, lipid bilayers in the liquid-ordered phase.

Additionally, this work provides important insight regarding phase heterogeneity of the lipid mixtures characterized. The results obtained with the POPC:SpM:Chol mixtures studied allow the critical evaluation of the phase diagrams available in the literature. We have also found strong evidence for the coexistence of a liquid-disordered and a liquid-ordered phase in the quaternary mixture representative of the cytoplasmic leaflet of the plasma membrane POPC:Chol:POPE:POPS 4:3:2:1. Evidence for structural rearrangements induced by the partition of cationic amphiphiles, such as CPZ, for membranes with POPS and/or POPE was also encountered. Those results may be relevant to elucidate the structural communication between the outer and inner leaflets of plasma membranes in the light of the "raft" hypothesis. Additionally, they may also contribute to the understanding of CPZ effects on the activity of membrane transporters such as P-glycoprotein.

Resumo da Dissertação

A difusão passiva através da membrana celular é a principal via para a permeação de xenobióticos através de endotélios *tight*, tais como a barreira hemato-encefálica. A velocidade da permeação passiva através de bicamadas lipídicas de um dado fármaco é, portanto, um passo crítico na previsão da sua farmacocinética. Neste trabalho, foi realizado um estudo detalhado sobre a cinética e a termodinâmica da interacção da clorpromazina, um antipsicótico utilizado no tratamento da esquizofrenia, com membranas lipídicas compostas por diferentes misturas de lípidos. Utilizámos a calorimetria de titulação isotérmica, uma técnica muito eficiente para o estudo de interacções moleculares, que permite a medição do coeficiente de partição de moléculas entre o meio aquoso e a membrana, bem como dos parâmetros termodinâmicos associados a esta partição.

A complexidade das membranas utilizadas neste estudo foi aumentada progressivamente, desde a bicamada simples de POPC puro até composições de lípidos características das monocamadas exterior e interior das células endoteliais. Os efeitos da presença de carga, de colesterol (Chol), de fosfolípidos com etanolamina (POPE) e de esfingomielina (SPM), bem como da coexistência de fases, foram avaliados na interacção de CPZ com as bicamadas lipídicas.

A introdução de 10% molar de POPS carregado negativamente em membranas de POPC aumenta a partição da CPZ, devido à atracção electrostática entre as cargas opostas, sendo que a variação de entalpia torna-se mais favorável. Por outro lado, a presença de Chol aumenta a ordem das bicamadas e diminui fortemente a afinidade da CPZ para com a bicamada, tanto em termos da quantidade de CPZ que se associa com a membrana bem como da entalpia de interacção, que se torna desfavorável. Para membranas na fase líquida ordenada (POPC:SPM:Chol 1:5:4) observa-se um coeficiente de partição muito mais pequeno do que para as membranas na fase líquida desordenada, com uma contribuição entalpica muito desfavorável. A partir dos parâmetros obtidos para todas as bicamadas lipídicas estudadas, observa-se que a partição de CPZ em membranas na fase líquida desordenada tem uma contribuição entalpica significativamente favorável, enquanto que a associação de CPZ com membranas na fase líquida ordenada é somente impulsionada pelo aumento de entropia no sistema.

Os coeficientes de partição obtidos permitiram o cálculo das afinidades de CPZ para com as diferentes membranas da célula e a previsão da concentração relativa de CPZ em cada *pool* de lípidos em equilíbrio.

A permeação passiva através de bicamadas lipídicas depende da afinidade do fármaco para com a membrana e também das constantes de velocidade para a interacção (inserção, desorpção e translocação). Neste trabalho, desenvolvemos uma metodologia que permite a caracterização quantitativa da constante de translocação através das membranas na fase líquida desordenada, usando ITC. Apresentamos também resultados preliminares sobre o uso desta técnica para obter as constantes de velocidade para inserção em e desorção de bicamadas lipídicas na fase líquida ordenada.

Além disso, este trabalho oferece uma visão importante sobre a heterogeneidade de fases das misturas lipídicas caracterizadas. Os resultados obtidos com as misturas estudadas de POPC:SPM:Chol permitem a avaliação crítica dos diagramas de fases disponíveis na literatura. Também foram encontradas fortes evidências para a coexistência de fase líquida desordenada e líquida ordenada na mistura quaternária representante da monocamada citoplasmática da membrana, POPC:Chol:POPE:POPS 4:3:2:1. Adicionalmente, foram encontradas evidências de rearranjos estruturais nas membranas com POPS e/ou POPE, induzidos pela partição de compostos anfifílicos catiónicos, como a CPZ. Estes resultados podem ser relevantes para elucidar a comunicação estrutural entre as monocamadas exterior e interior da membrana plasmática, em função da hipótese da existência de *rafts*. Além disso, podem também contribuir para o entendimento dos efeitos da CPZ sobre a actividade dos transportadores de membrana, tais como a P-glicoproteína.

Table of Contents

Tables Summary

Figures Summary

Abbreviations

A_i – Cross area of specie *i*

AJ – Adherent junction

BBB – Blood Brain Barrier

BM – Basement Membrane

CAC – Critical Aggregation Concentration

Chol – Cholesterol

CMC – Critical Micellar Concentration

CNS – Central Nervous System

CPZ – Chlorpromazine

CSF – Cerebrospinal fluid

e_0 – Elemental electrostatic charge

DMPC – 1,2 dimyristoyl-sn-glycero-3-phosphocholine

DMPE – 1,2 dimyristoyl-sn-glycero-3-phosphoethanolamine

EDTA – Ethylenediamine tetra-acetic acid

e. g. – do latim: *exempli gratia*, por exemplo

F – Faraday constant

HEPES – 4-(2-hydroxyethyl)-1-piperazineethanesulfonic acid

i. e. – do latim: *id est*, isto é, ou seja

ISF – Interstitial Fluid

ITC – Isothermal Titration Calorimetry

K_a – Ionization constant

K_P^{obs} – Observed Partition Coefficient

K_P - Intrinsic Partition Coefficient

k_+ – Insertion rate constant

k_- – Desorption rate constant

k_f – Translocation rate constant

L – Lipid

LUV – Lipid Unilamellar Vesicle (LUVs for plural)

MDCK – Madin-Darby Canine Kidney

MLV – Multilamellar Vesicle (MLVs for plural)

NBD-C16 – 7-nitrobenz-2-oxa-1,3-diazol-4-yl with an alkyl chain of 16 carbons

NDB-DMPE – 7-nitrobenz-2-oxa-1,3-diazol-4-yl 1,2 dimyristoyl-*sn*-glycero-3-phosphoethanolamine

Pc - Pericyte

PC – Phosphatidylcholine

PE – Phosphatidylethanolmamine

PS – Phosphatidylserine

POPC – 1-palmitoyl-2-oleoyl phosphatidylcholine

POPE – 1-palmitoyl-2-oleoyl phosphatidylethanolamine

POPS – 1-palmitoyl-2-oleoyl phosphatidylserine

R – Ideal gas constant

SpM – Sphingomyelin

TEER – Transendothelial Electrical Resistance

TJ – Tight Junctions

TPP^+ - Tetraphenylphosphonium

UV-Vis – Ultraviolet-visible spectroscopy

$\overline{V_L}$ - Molar volume

z_i – Charge of specie *i*

Greek Alphabet

β - Characteristic rate constant

ε - Dielectric constant

γ - Equilibration factor

η - Viscosity

λ - Wavelength

σ - Bilayer charge density

τ - Characteristic time

ξ - Zeta potential

Ψ_0 – Electrostatic potential at the bilayer surface

Chapter I:

Literature Review

Biological membranes

The biological membrane is a crucial cell structure playing an important role on the function of all cells. The main function of membranes is to define boundaries to different biological compartments like cells and cell organelles offering a physical barrier with low and specific permeability that provides directional transport of species into and out of the cell.

The barrier functions attributed to biological membranes allow maintaining a non-equilibrium ion distribution between the external and internal sides of the cell, which is crucial for cell function. Destruction of the cell membrane results in cell necrosis.

There are numerous types of specialized plasma membranes and many other distinct types of membranes that create different intracellular organelles. These types of membranes differ in lipid and protein composition. Their distinct chemical composition, in particular that of the lipid fraction, defines their physical properties and results in specific biological properties.

In addition to its structural and barrier functions, the proteins present in biomembranes are responsible for a number of biological reactions vital to cell function from bioenergetics to cell signaling.

Historical perspective

From the mid-nineteenth century the plasma membrane at the surface of cells is recognized as a discrete structure. The period starting in 1885 and lasting for more than forty years was dominated by the view that the plasma membrane is an inert envelope surrounding the cell and this was the "paradigm" embraced by the community of membrane physiologists (Schultz, 1998). During these decades a lot was done in the fields of biochemistry, physical chemistry and membrane physiology that allowed a growing knowledge on the structure and dynamics of the cell membrane. The beginning of the twentieth century brings to light the classic work of Overton (see Kleinzeller, 1997) showing that the ease with which a large number of solutes permeate cell membranes is closely correlated with their olive oil-to-water partition coefficients (*i.e.,* lipid solubility) leading to the speculation on the lipid nature of the membrane. Twenty five years later, Gorter and Grendel (1925) demonstrated that there is sufficient lipid in the erythrocyte membrane to form an envelope where lipids would be arranged in a bimolecular leaflet or lipid bilayer, as they conclude:

> *It is clear that all our results fit in well with the supposition that the chromocytes are covered by a layer of fatty substances that is two molecules thick.* (Gorter & Grendel, 1925)

Although the interpretation of the results is only correct in its conclusions (Bar et al., 1966) the work done by Gorter and Grendel is of huge historical relevance since the concept of the lipid bilayer as the structural base of membrane has been established ever since and is known to be correct. Some years later, Danielli and Davson (1935) proposed the lipoprotein model (Figure I.1 A), in which it was postulated that proteins coat the surfaces of the lipid bilayer.

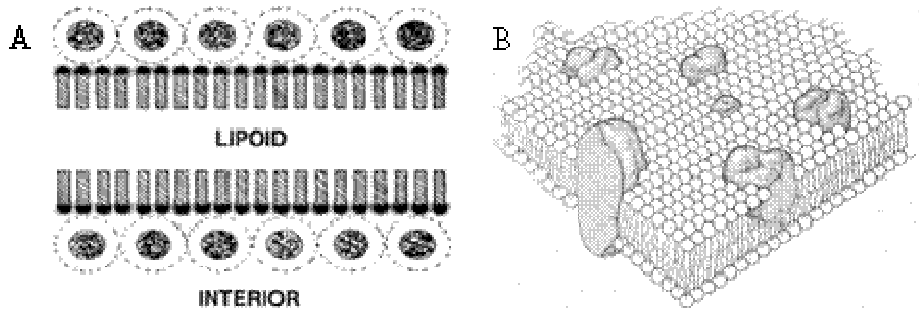

Figure I.1: A: Davson-Danielli model of the cel membrane (From Danielli and Davson (1935)). B: Fluid mosaic model (From Singer and Nicolson (1972))

During the succeeding decades, the enormous diversity of membrane functions was becoming clear, and the basic Davson-Danielli model was modified by numerous other workers to account for this functional diversity (see, for example: Stein and Danielli, 1956; Finean, 1962; Lucy and Glauert, 1964; Vandenheuval, 1965). The decade of 1960's and the beginnings of 1970's were fruitful in the characterization of membrane proteins and revealed the fluid nature of the lipid bilayer (See references Branton, 1966; Branton, 1971; Green and Perdue, 1966; Green and Fleischer, 1963; Vanderkooi and Green, 1970; Lenard and Singer, 1966; Wallach and Zahler, 1966; Richardson et al., 1964; Frye and Editin, 1970). Singer and Nicholson combined these ideas into the fluid mosaic model (Figure I.1 B), which basically pictures the membrane as ''a two dimensional oriented solution of integral proteins (…) in the viscous phospholipid bilayer'' (Singer and Nicholson, 1972; Singer, 1974).

Much of the focus in membrane research since than has been directed at the dynamics of the membrane, and the relationship between this dynamics and membrane function. The

emphasis of the fluid mosaic model has undergone modification and will continue to due so. In particular, it is now evident that membrane proteins do not all diffuse freely in the fluid lipid bilayer (Jacobson, 1983) and there is evidence for differentiated lateral domains within membranes (Jain, 1983). Thirty years passed from the fluid mosaic model, Vereb and co-workers (2003) compile experimental data on the compartmentalization of membrane components and present a "dynamically structured mosaic model" (Figure I.2).

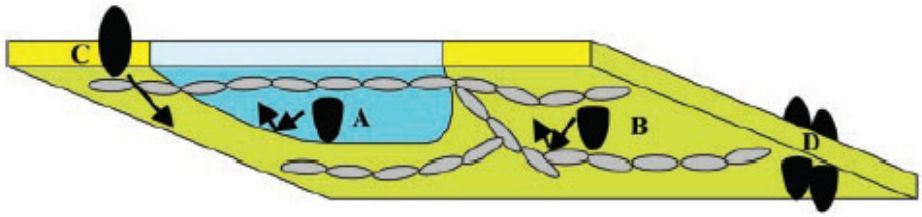

Figure I.2: Schematic representation of the "dynamically structured mosaic model" presented by Vereb et al. (2003)

This new ''dynamically structured mosaic model'' maintains the overall mobility of molecular elements of the membrane with restrictions at the level of the lipid domain structure, cytoskeletal interactions or associations with integral proteins, considering the membrane "a heavily compartmentalized, quasi-two dimensional structure, which is more mosaic-like than fluid" (Vereb et al., 2008).

Structure and composition

Biological membranes are mainly constituted by lipids and proteins. Less than 10 % of the total content is composed of carbohydrates covalently attached to the lipids or to the proteins (glycolipids and glycoproteins, respectively).

According to the fluid mosaic model, the lipids form a two-dimensional sheet that consists of two layers of closely packed lipids, in which hydrophobic tails are directed toward the centre of the sheet, while the hydrophilic head groups are oriented toward the aqueous phase (Singer and Nicolson, 1972).

The proteins are imbedded in this lipid matrix or adsorbed to the hydrophilic surface. Membrane proteins play important functional roles in a cell as ionic channels, transporters and receptors. Certain proteins also play an important structural role such as the maintenance of a membrane cytoskeleton. The content of proteins in the membrane varies

from almost 20 weight % for membranes of myelin to almost 80 % for inner membranes of mitochondria (Gennis, 1989).

Membrane proteins are divided into three main groups: peripheral proteins, integral proteins (see Figure I.1 B) and structural proteins. Peripheral proteins are localized at the membrane surface and are connected with the membrane either by means of electrostatic interactions or by a short hydrophobic chain that allows anchoring in the membrane. Integral proteins are spanned across the lipid bilayer. These proteins contain a hydrophilic part which contacts with the aqueous environment and a hydrophobic part that is solvated by the apolar interior of the membrane, being more tightly connected with the membrane than peripheral proteins. Membrane architecture and membrane protein function are determined by protein-lipid interactions. Structural proteins form the membrane cytoskeleton. These proteins do not belong exactly to the above membrane proteins group, but are connected to the membrane through integral proteins.

Enzymes are also present in membranes and can be integral or peripheral as well as receptors and immunoproteins. The receptor proteins are usually connected to additional proteins in cytoplasmic side of the membrane for transfering signals inside the cell.

Both glycolipids and glycoproteins play important role in the cell recognition. The hydrocarbons are localized at outer part of all cell membranes and thus together with the different chemical composition of lipids at both membrane monolayers contribute to the membrane asymmetry (see below).

Membrane lipids

The lipid bilayer is a self assembled structure formed from lipids in an aqueous environment. The non polar acyl chains of tend to escape from the aqueous phase as a result of the hydrophobic effect (Tanford, 1980). Lipids are amphiphilic, i.e. contain two distinct parts differing in their solubility properties. The hydrophilic part of the molecule has an affinity for polar solutes, such as water, and the hydrophobic part of the molecule has an affinity for non-polar solutes, such as hydrocarbons. In the presence of water amphiphilic molecules spontaneously come together in an arrangement that allows each component to interact with its favored environment, forming micelles, vesicles or other self assembled structures. The geometry of these structures depends on three packing constrains: *i)* the optimal area occupied by polar interface (S_0), *ii)* the maximum length of the alkyl chain (l) and *iii)* the molecular volume of the hydrocarbon portion of the

amphiphilic molecule (v). These parameters, together, define the critical packing parameter (CPP) (eq. I.1), which can be used to predict for a particular amphiphilic molecule, the preferential aggregate shape (Vaz, 2008). Lipid bilayers are formed when CPP ≈ 1 which is the case for the most abundant phospholipids in biological membranes.

$$\mathrm{CPP} = \frac{v}{l.S_0} \qquad \text{eq. I.1}$$

Lipids that constitute bilayers may be divided into three main classes: phospholipids, glycolipids and sterols.

Phospholipids are the most predominant lipids in cell membranes and can be subdivided into two major classes: glycerophospholipids and sphingophospholipids. Glycerophospholipids consist of a polar head group and two hydrophobic chains of fatty acids connected to the glycerol backbone. Both length and saturation of the acyl chains can differ as well as the polar head group, being phosphatidylcholine (PC), phosphatidylethanolamine (PE), phosphatidylserine (PS), phosphatidylinositol (PI) and phosphatidylglycerol (PG) the most biologically common representatives of glicerophospholipids (Fig I.3).

The structures of glycerophospholipids and sphingophospholipids differ considerably in the interfacial and hydrophobic part (compare structure of PC and SpM on Figure I.3). They contain the same kinds of polar substituents but in sphingophospholipids the hydrophobic group is a ceramide. Sphingomyelin (SpM) is formed by a phosphorylcholine attached to the ceramide and is widely found in animal cell plasma membranes.

Phospholipids play dominantly a structural role in the membrane, participating on the formation of a barrier for passive permeation of ions and other polar species through the membrane and providing a special environment for membrane proteins function. Some phospholipids have also a functional role. For example, phosphatidylinositol (PI) is localized in the cytoplasmic side of the membrane and is important in cell signalling; and SpM, in addition to the structural role, participates also in cell signalling. Products of SpM metabolism, like ceramide sphingosine and sphingosine-1-phosphate are important cellular effectors and give SpM a role in cellular functions like apoptosis, ageing and development (Ramstedt and Slotte, 2002).

Most of the generally called glycolipids are glycosphingolipids (cerebosides, gangliosides and globosides). Another important glycolipid is glycophosphatidylinositol (GPI). They are localized exclusively at extracellular side of plasmatic membrane with the sugar residues exposed to the external part of the cell and create the protective film, which surrounds most of the living cells, the glycocalix (Gennis, 1989). As examples, monogalactosyldiglyceride (MG) and galactosylceramide (GC) are shown on Figure I.3.

Sterols are found in many plant, animal and microbial membranes. Cholesterol (Chol) constitutes about 30 % of the mass of the membrane lipids in many animal cell plasma membranes. This molecule is a compact and rigid hydrophobic entity with a polar hydroxyl group (Gennis, 1989). In higher plants and eukaryotic organisms, Chol is substituted by phytosterols (sitosterol and stigmasterol (ST) and ergosterol (ES), respectively. (Figure I.3).

Glycerophospholipids

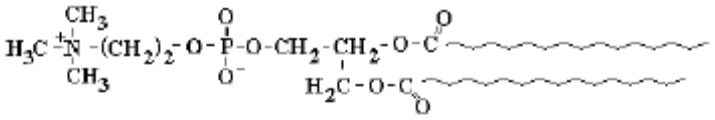

PC

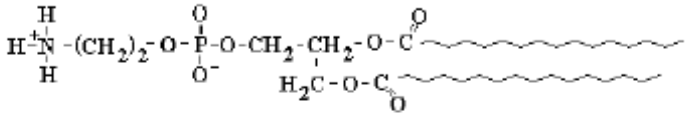

PE

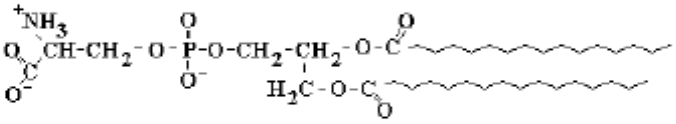

PS

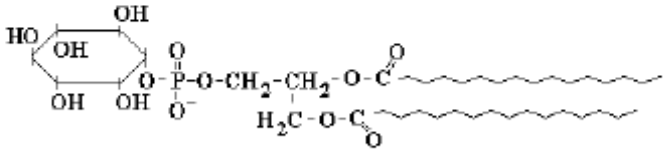

PI

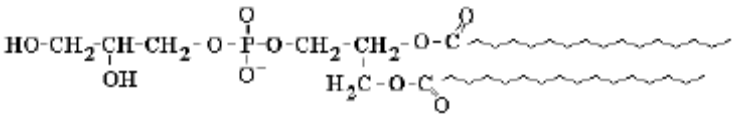

PG

Sphingophospholipids

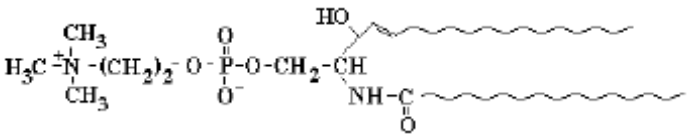

SpM

Glycolipids

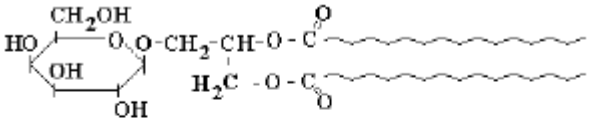

MG

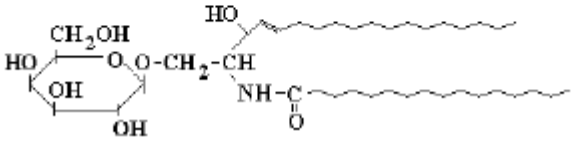

GC

Cardiolipin

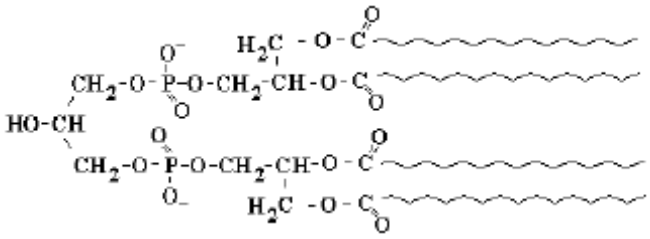

DPG

Sterols

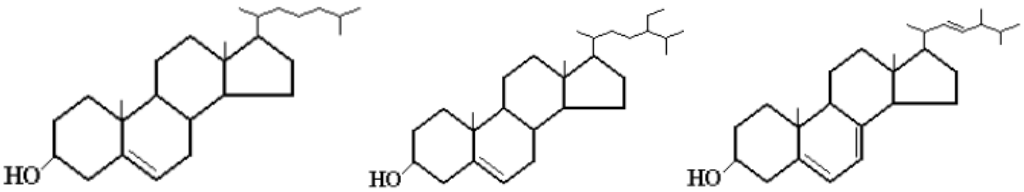

Chol ST ES

Figure I.3: Structural formula for some of the most relevant lipids present in biomembranes. PC: phosphatidylcholine, PE: phosphatidylethanolamine, PS: phosphatidylserine, PI: phosphatidylinositol, PG: phosphatidylglycerol, SpM: sphingomyelin, MG: monogalactosyldiglyceride, GC: galactosylceramide, DPG: diphosphatidylglycerol (cardiolipin), Chol: cholesterol, ST: stigmasterol and ES: ergosterol. Adapted from Hianik, 2006.

In addition to the above there are other lipids that occur less frequently in membranes. Among these we can mention plasmalogens, phosphoglycerides where one of the hydrocarbon chains is linked via a vinyl ether linkage to glycerol; cardiolipin (diphosphatidylglycerol, DPG), a dimeric phospholipid and an important component of the mitochondrial membrane; sulphospholipids, found in cyanobacteria where the nitrogen is replaced by sulphate and diphytanoyl glycerolethers, present in thermophilic and methane

producing bacteria with the fatty acid chains covalently connected in the middle plane of the membrane offering higher stability against disruption (Hianik, 2006).

Lipid and proteins asymmetry in biological membranes

The two faces of membranes are exposed to different environments, one leaflet exposed to the inner part of the compartment enclosed by the membrane and another leaflet exposed to the outer environment. In laboratory, a lipid bilayer prepared by hydration of lipids will result in an identical composition of both monolayers (Gregoriadis, 1995) but this is not the case for biological membranes. All biomembranes are asymmetric with regard to the lipids and protein distribution of each monolayer that constitutes the membrane (Gennis, 1989). Glycolipids, for example, are exclusively located at outer monolayer of the membrane and the lipid composition on the erythrocyte shows that almost every type of lipid is present on both sides of the bilayer but in different amounts (Verkleij et al., 1973).
How transverse asymmetry is originated and maintained in biological membranes is still not entirely clear but an important contribution certainly comes from the vectorial nature of lipid biosynthesis in cell organelles. Physical forces such as those caused by extreme curvature may be important in some cases as well as cytoskeleton interactions. The asymmetric chemical composition of the aqueous compartments on the two sides of the membrane and the slow transmembrane translocation of lipids in lipid bilayers are important to maintain this asymmetry (Vaz, 2008). In addiction to the physical driving forces, living cells maintain membrane transverse asymmetry actively, using 'flippases' (Devaux, 1988; Daleke, 2007). Uncatalysed exchange of lipid molecules between monolayers is very slow (probably does not exist for proteins) because it requires the insertion of the polar groups into the nonpolar region and the exposure of the apolar groups to the polar region (Hianik, 2006) as an intermediate "transition state" with an activations free energy ($\Delta G^{\ddagger}$) on the order of 100 $kJ \cdot mol^{-1}$ (Vaz, 2008, Moreno et al., 2006).
In addiction to transverse asymmetry, it is now clear that biomembranes can have lateral inhomogeneities. Many eukaryotic cell surfaces are highly polarized and exhibit distinct macroscopic domains. These domains maintain different functions and compositions, and are physically separable (detergent resistant membranes). Macroscopic lateral domains may be maintained by specific protein-protein interactions between membranes (e.g. tight junctions (TJ)), by specific structures within the membrane (e.g. interactions with cytoskeletal elements), or by protein aggregation in the plane of the membrane (Gennis,

1989). Additionally, lateral asymmetry may be caused by lipid-lipid immiscibility leading to microscopic lipid domains within membranes, defined as small regions within the bilayer with distinct physical properties and composition. In general these distinct membrane domains are called "rafts", enriched in certain lipids, cholesterol and proteins (Simons and Vaz, 2004). Lateral organization of biomembranes has been suggested to be important in its physiological function (Vaz and Almeida, 1993; Prenner et al., 2000).

Lipid bilayers as model systems for biological membranes

From a biophysical perspective, biological membranes are anisotropic and inhomogeneous structures with similar properties to liquid crystals of smectic type. The study of physical and electrochemical properties of biomembranes is strongly compromised by their complicated structure, small size of the cell, small thickness, anisotropy and inhomogeneity. Additionally, it is very difficult to separate the properties of lipid bilayer and the influence of the proteins present.

In order to understand the simplest phenomena that govern biological functions attributed to biomembranes, it is necessary to reduce the complexity of the system to its basic constituents. Therefore, several models of biomembranes have been developed, for use in biophysical studies, such as micelles, lipid monolayers, multilayers, bilayer lipid membranes, multi and unilamellar vesicles and solid supported lipid films.

The first models of membrane structure were lipid monolayers, very important in establishing the bilayer nature of the membranes in the early XX century. Stable bilayer lipid membranes have been reported by Mueller and co-workers (1962) and finally, in 1965, Bangham and Horne described the formation of lipid vesicles, which became the most popular and widely used model system to study the physical properties of biomembranes.

Lacking the complexity of living organisms, in both composition and surrounding environment, model membranes are not able to reproduce all properties found in real membranes. The simplest model systems are composed of pure lipids and the complexity of the models may be increased progressively by adding different lipids, like cholesterol and charged lipids, or incorporating integral or peripheral proteins. Therefore, the model membranes can be designed in a way that mimics the structure and properties of biomembranes, preserving the main biophysical and biochemical characteristics.

Liposomes

The word liposome derives from two Greek words: *lipo* (fat) and *soma* (body) and can be defined as any lipid bilayer structure which encloses a volume. The primary uses of liposomes are (1) as model membranes and (2) to encapsulate solutes for such uses as drug delivery systems. Application of liposomes as models for biomembranes has been discussed in several reviews and monographs (See Rosoff, 1996).

Many phospholipids when dispersed in water spontaneously form a heterogeneous mixture of vesicular structures which contain multiple bilayers forming a series of concentric shells with diameters that can go up to cm. These were the first liposomes to be described by Alec Bangham (1964) and are now termed multilamellar vesicles (MLV). MLVs are structurally poor-defined systems and their use in biological studies has been neglected in favor of unilamellar vesicles, which can be prepared by a variety of methods.

Unilamellar vesicles can be generally characterized as small unilamellar vesicles (SUV), with diameters in the range 200 Å to 500 Å and large unilamellar vesicles (LUV) with diameters from 500 Å to 500 nm (Gennis, 1989). Giant unilamellar vesicles (GUV) can also be prepared and used as model membranes and have diameters as large as 300 μm.

SUV are usually prepared by sonication and result in a homogeneous distribution with average diameter ~250 Å. Although the population homogeneity is advantageous, the small size can be a disadvantage since the high curvature results in packing constraints for the lipids. For liposomes composed of one lipid species, the bilayer packing defects are highest for small vesicles. In SUV, the surface area of the outer monolayer is almost twice that of the inner monolayer and therefore about 70 % of the lipids are in the outer leaflet. Lipids with an “inverted cone” shape (CPP > 1) will preferably partition into the outer leaflet, resulting in lipid asymmetry.

The need for larger vesicles became obvious in the 1970s and since then numerous procedures have been devised to produce LUVs. The method of choice may depend on the lipid composition but certainly depends on the intended use of the liposomes. The average bilayer curvature in LUVs is practically the same as for planar membranes when considering curvature at the molecular level (Gennis, 1989), but the choice of lipid compositions is limited, as not all lipids or lipid mixtures form planar membranes which are pre requisite for homogenous LUV formation.

Physical properties

Dynamics and organization

Lipid bilayers are highly dynamic structures. From a functional point of view, the most important motions that must be considered can be divided into four categories: conformational, describing intramolecular motions; translational diffusion, rotational diffusion, both indicating the lateral position of the molecule in the plane of the membrane; and translocation, describing the movement between the bilayer leaflets (Vaz, 2008). Another important movement is the spontaneous desorption and insertion of amphiphilic molecules, a type of movement also relevant for the interaction of other molecules with biomembranes.

Lipid dynamics depends on many factors, such as alkyl chain length, number of *cis*-double bonds, temperature, pressure and degree of hydration (Kinnunen et al., 1994).

The anisotropic nature of phospholipid bilayers implies that the phospholipid conformational and orientational movements have some anisotropic restrictions and occur at diverse time scales (Blume, 1993), from ~10^{14} s^{-1} (for the vibrational dynamics of single bonds in the lipid molecules) to ~10^{-5} s^{-1} for trans-membrane translocation ("flip-flop") of a lipid molecule (Vaz, 2008).

The membrane fluidity results from the weak forces that held its molecular components together and leads to a relatively high mobility of the components within the plane of the cell membrane. The fluidity of membranes allows movement of molecules within its plane, providing the basis for lipid–lipid, lipid–protein and protein–protein interactions (Hu et al., 2003).

Phase behaviour and phase transition in lipid bilayers

In lipid bilayers at low temperatures, the alkyl chains are characterized by a high *trans/gauche* configurational ratio. The chains, viewed along their long axes, are packed parallel to each other in a hexagonal lattice and the bilayers are characterized by a high degree of conformational, rotational and translational order. These bilayers are said to be in the "gel" phase. In gel phases, the alkyl chain axes may be oriented normal to the bilayer plane (the L_β phase) or be slightly tilted relative to this plane (the $L_{\beta'}$ phase) as a result of the reorientation of the lipid in order to accommodate the two acyl chains in the slightly

higher cross sectional area of its head group. Depending on the chemical identities of the lipids and at very low temperatures an even more ordered state may be found, the "sub-gel" or L_c (or $L_{c'}$ when the chains are tilted relative to the bilayer normal) phase. In the L_c phase a crystalline ordering of the lipid molecules may be observed. In some ordered bilayers, at higher temperatures, is possible to find the "rippled" or $P_{\beta'}$ phase that is characterized by a zig-zag ripple in the bilayer plane. The acyl chain order in the $P_{\beta'}$ phase is lower that in the L_β (or $L_{\beta'}$) and L_c (or $L_{c'}$) phases.

Phase transition in ordered lipid bilayers occur at characteristic temperatures that depend on the chemical identity of the lipids and their acyl chain lengths. The conversion of the ordered or gel phase into the so called "liquid-crystalline", "fluid" or L_α phase, occurs when raising the temperature above a characteristic temperature, *T*m. In the L_α phase the acyl chain configuration is characterized by a low *trans/gauche* configurational ratio and are still packed in a more or less hexagonal lattice but with a low coherence length. Lipid bilayers in the L_α phase have a low conformational, rotational and translational order. The chain melting transition at Tm is observed in all lipid bilayers regardless of the chemical identity of the constituent lipid.

Increasing temperature in some lipid bilayers already in the L_α phase will convert the hydrated lipid aggregate into one of several other phases such as inverted hexagonal and cubic phases (Vaz, 2008)

The characteristic "chain-melting" or main phase transition temperature in a lipid bilayer, *T*m, depends on the nature of the polar head group, the length of the acyl chains and their degree and type of unsaturation (See Huang and Li, 1999). Bulkier head groups result in lower values of *T*m for equivalent acyl chains and for homologous head groups with two identical acyl chains, *T*m increases with increasing acyl chain length. Lipids with one *cis* unsaturated acyl chain have *T*m values that are considerably lower than their fully saturated homologs, the reduction being larger when the position of the double bond is roughly in the middle of the acyl chain (Vaz, 2008).

As expected, the lipid bilayer phase transitions from a more ordered to a less ordered state are endothermic in nature and can be followed by differential scanning calorimetry (DSC) (Chapman et al., 1967). The enthalpies of the sub-transitions ($L_c \rightarrow L_\beta$) and of the pre transition ($L_\beta \rightarrow P_{\beta'}$) have been found to be essentially the same for bilayers prepared from different lipids irrespective of acyl chain lengths or head group structures. However, the enthalpy of the main transition ($L_\beta \rightarrow L_\alpha$) is strongly dependent on the acyl chain length

and the degree and type of unsaturation of the lipid that forms the bilayer being similar, for similar chain lengths in bilayers formed from lipids with different head groups (Vaz, 2008).

Phase coexistence

The phospholipid bilayer of biological membranes is composed of several distinct lipids and therefore, the properties of mixed lipid bilayers are very important for the understanding of biomembranes.

Since the 70's, bilayers formed from binary lipid mixtures are studied in detail and recently some phase diagrams are described for lipid bilayers prepared from ternary mixtures including cholesterol (See, for example, Mabrey and Sturtevant, 1976, Vaz et al., 1989; Bultmann at a., 1991; Almeida et al., 1992, Simons and Vaz, 2004, de Almeida et al., 2003 and Zhao et al., 2007).

The general observation is that lipids in a bilayer are not very miscible with each other in the gel phase but they are essentially miscible when in the fluid phase.

Lipid bilayers that contain Chol are particularly interesting from a biological perspective since the plasma membrane of animals contain very large molar fractions of this lipid (typically 30-50 %). Chol has a condensing effect on phosphatidylcholine in bilayers, i. e., increases the *trans/gauche* ratio and the conformational order in the acyl chains of the phospholipid to values significantly higher than those typical for the cholesterol-free L_α phase (Vaz, 2008). Chol-rich bilayers also show slower translational diffusions when compared with cholesterol-free bilayers. In 1987, Ipsen and co-workers proposed that cholesterol forms an Lα phase with lipids in which the lipid chains are ordered conformationally. This phase, which was denominated the liquid-ordered (l_o) phase is distinct from the Lα phase with conformationally disordered chains (the l_d phase) observed in cholesterol-free lipid bilayers at temperatures above *T*m. The formation of the l_o liquid-ordered phase is the consequence of the flat and rigid cholesterol structure that maximizes its interaction with the lipid acyl chains in a $L\alpha$ phase bilayer by forcing these into a predominantly all-*trans* conformation. A compromise solution is to retain the all-*trans* configuration of the chains and simultaneously maintain the translational order of the fluid phase. Thus, in lipid bilayers enriched in Chol, two fluid phases may coexist in the lipid bilayer.

Cholesterol is also an important constituent of lipid "rafts", lipid assemblies at the bilayer plane that provide fluid platforms that segregate membrane components and dynamically

compartmentalize membranes. These assemblies are thought to be composed mainly of sphingolipids (like SpM) and cholesterol (Simons and Vaz, 2004).

SpM forms more stable complexes with Chol in comparison with other phospholipids. Results obtained during the last decade show a substantial lateral organization of both lipids and proteins in biomembranes. Sphingolipids, including SpM, together with Chol, have been shown as important factors in formation of lateral domains or .rafts in biological membranes. These domains have been suggested to take part in cellular processes, such as signal transduction, membrane tracking and protein sorting. The formation of lateral rafts in biological membranes is supposed to be driven by lipid-lipid interactions, which are largely dependent on the structure and biophysical properties of the lipid components (Ramstedt and Slotte, 2002; London, 2002).

Electrical Properties

The electrical profile associated with the membrane strongly influences the interaction (insertion, translocation and desorption) of a charged molecule with a membrane (Estronca et al, 2002): anions bind with higher affinity and translocate more rapidly across bilayers than structurally similar cations (Flewelling and Hubbell, 1986).

The electrical profile associated with a lipid membrane consists of three components: the transmembrane potential, the surface potential and the dipole potential.

The transmembrane potential represents a difference in the electrical potential of the two bulk aqueous phases separated by the membrane i.e. there is a difference in ionic strength between the aqueous phases of both sides of the membrane. This transmembrane potential, due to different membrane permeability of the ions present in the bulk phase or generated by active processes that create a charge separation across the membrane (Gennis, 1989), has an important role in the regulation of protein function (Peterson et al, 2002). At the cytoplasmic surface we find over 90% of the phosphatidyl serine and inositol which constitute 12-20% of the total phospholipids and 24-40% of the cytoplasmic, half of the bilayer. These negatively charged lipids cause a very high density of negative charges on the cytoplasmic surface (0.5-0.8 charge/nm^2), although these negative are partially neutralized by mobile counterions distributed in the aqueous phase.

The surface potential is an electrical potential near the membrane surface, given by the surface density charge and concentration of ions in bulk solution described by the Gouy-Chapman theory (for a detailed treatment see Trauble, 1976).

Membranes have a considerable internal dipole (300 mV), i.e., it is positive in the center of the hydrocarbon moiety, which is known to affect both ion transport processes across model lipid membranes and protein insertion (Flewelling and Hubbell, 1986). Although to generate a dipolar potential that is positive inside we would expect the choline group to be closer to the center of the bilayer, the fact is that it is known this is not the case: the orientation of the phosphate → choline vector is almost parallel to the bilayer plane, but pointing towards the aqueous phase. This dipole results from the orientation of water dipole on the interface, the orientation of fatty ester carbonyls of each phospholipid molecule and the dipole moment of the terminal methyl groups in the chains.

Even though transmembrane and surface potential are negligible, the dipolar potential is one relevant property for the insertion of fluorescent amphiphiles in neutral lipid bilayers (e.g. POPC bilayers). Studies suggest that this dipolar potential has an important role in solubility of fluorescence lipid amphiphiles (FLA) in different membrane phases because of their different dipole magnitudes and orientations (Estronca et al, 2002).

Permeability

Regardless of their chemical and structural differences, all membranes act as highly selective permeability barriers separating two aqueous compartments.

The ability of small molecules to cross the bilayer passively is directly proportional to their ability to partition into hexadecane or olive oil from an aqueous solution, as was first observed by Overton and is commonly referred as the "Overton's Law". The solubility-diffusion mechanism, based on Overton simple laws of permeation, treats the membrane as a thin static slab of hydrophobic matter surrounded by two bulk aqueous environments (Paula et al, 1996). To permeate the membrane, a molecule must partition into the hydrophobic region on the bilayer, diffuse across it, and leave the membrane, partitioning into the aqueous phase on the other side on the bilayer. In this case, the permeability coefficient, P, is given by:

$$P = \frac{K_P D_m}{d} \qquad \text{eq. I.2}$$

Where, K_P and D_m are the partition and diffusion coefficients of the permeant molecule, respectively, and d is the bilayer thickness. It has been generally considered that the

properties of the hydrophobic interior of the membrane are approximated by those of octanol or other long chain hydrocarbons and therefore, partition between water and those organic solvents is usually taken to estimate the permeability coefficient. Undoubtedly, this is a good first approximation and was the experimental basis for the development of this rule. However, several discrepancies between the predicted permeation coefficient and the measured one have been reported in the literature (Paula et al, 1996). One example is the case of small charged molecules where it is not possible to establish a correlation between the permeability and the water to octanol partition coefficient (Donna Bassolino-Klimas et al, 1995).

To account for those discrepancies, a pore mechanism has been proposed,which considers the formation of transient water-filed pores across the bilayer due to density fluctuations. The permeant molecule is then assumed to diffuse through the bilayer via these transient pores, overcoming the Born energy required to pass a charge through the hydrophobic centre of the lipid bilayer. This is the permeation mechanism adopted by protons and hydroxyl groups. The pore mechanism is also the dominant route for other ions but the permeation mechanism depends on the thickness of the bilayer. As bilayers become thicker the number of pores due to thermal fluctuations decreases, and the partition-diffusion mechanism may become dominant (Paula et al, 1996). Uncharged, small polar molecules such as water, glycerol, and urea permeate bilayers, regardless of their thickness, via the solubility-diffusion mechanism (Vaz, 2008).

Blood brain barrier

The brain (and central nervous system (CNS) in general) requires a level of homeostasis and protection against circulating toxins in the blood, greater than most others tissues of the body. The complex neural function occurring in the brain is therefore protected by physiological barriers that separate the blood from the brain interstitial fluid (ISF) at three interfaces: the blood-brain barrier (BBB), the choroid plexus epithelium (blood-cerebrospinal fluid (CSF) barrier) and the arachnoid epithelium. These three barriers possess mechanisms to regulate the molecular traffic between blood and brain. The BBB, formed by the endothelial cells lining the micro vessels, is the largest barrier in surface area and has the shortest diffusion distance to neurons, being the most important in regulating drug permeability to the brain (Abbot et al., 2006).

Function

Being responsible for the influx and efflux of molecules into and from the brain, the BBB supplies essential nutrients, like amino acids and glucose, and mediates the efflux of waste and harmful products. It has specific ion transporters and channels to regulate ion traffic, restricting ion and fluid movement between the blood and the brain and thus producing an optimal ISF for neuronal function. ISF is similar in composition to blood plasma but with a much lower protein, K^+ and Ca^{2+} concentrations and higher levels of Mg^{2+} (Abbot et al., 2006). Moreover, the BBB protects the brain from fluctuation in ionic composition that occur abruptly after a meal or exercise, which would disturb synaptic and axonal signalling. Like with ions, the BBB helps to keep separate pools of neurotransmitters and neuroactive agents that can be used by the CNS and the peripheral nervous system in separate. BBB has a predominant role in regulating the brain microenvironment, together with the choroid plexus epithelium (Chodobski and Szmydynger-Chodobska, 2001). Continual turnover and drainage of CSF and ISF by bulk flow helps to clear larger molecules and brain metabolites, also assisting homeostasis of the brain microenvironment (Abbot et al., 2004)

Characteristics

The BBB is formed by the endothelial cells that line cerebral micro vessels. The main physical difference between this endothelium and most other endothelia in the organism is the absence of fenestrations and the presence of complex and more extensive tight junctions (TJ) between adjacent endothelial cells that force most of the molecular traffic to take a transcellular route across the cells monolayer rather than moving paracellularly through the junctions (Wolburg and Lippoldt, 2002; Hawkins and Davis, 2005). In addition to endothelial cells, the BBB is composed of the capillary basement membrane (BM), astrocyte end-feet casing the vessels, and pericytes (PCs) embedded within the BM (Figure I.4) (Ballabh et al., 2004). It is believed that all the components of the BBB are essential for the normal function and stability of the BBB.

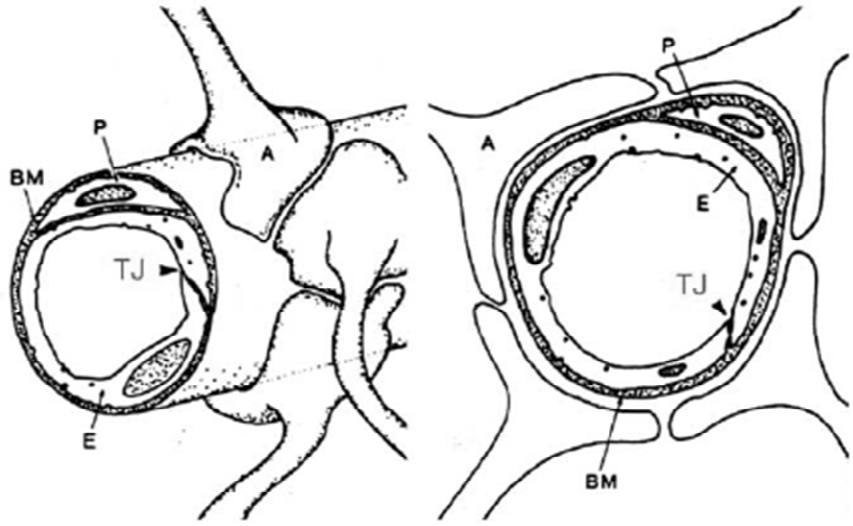

Figure I.4: Cellular constituents of the blood-brain barrier shown in three dimensions (left) and as a transverse section (right). A: astrocyte, BM: basement membrane, E: endothelial cell, P: pericyte and TJ: tight junction. Adapted from Abbot, 2004.

The specific junctions in the BBB are formed by the TJ and adherens junctions (AJ). These junctions restrict even the movement of small ions such as Na^+ and Cl^- so that the transendothelial electrical resistance (TEER) can be over 500 times higher in brain endothelium compared to peripheral capillaries (Wolburg and Lippoldt, 2002). TJ consists of three transmembrane protein classes, namely: i) occludin, that play an important role in the regulation of TJs, ii) claudins, that to contribute to the high TEER and iii) junctional adhesion molecules, involved in the formation and maintenance of the TJs (Abbot et al., 2006). The transmembrane proteins are connected on the cytoplasmic side to a complex array of peripheral membrane proteins that link these transmembrane complexes to actin, which is the primary cytoskeleton protein for the maintenance of structural and functional integrity of the endothelium (Ballabh et al, 2004). Cell-cell interaction in the junctional zone is stabilized by AJ, composed of a cadherin–catenin complex and its associated proteins (Ballabh et al., 2004).

The TJ has a preponderant role not only in restricting paracellular permeability but also in segregating the apical and basal domains of the cell membrane so that the endothelium can assume the polarized properties more commonly found in epithelia (Wolburg, 2006), related mainly with the polarized transport function.

Transport across the BBB

The brain endothelial TJ restrict the penetration of polar solutes trough the intercellular cleft forcing molecular traffic between blood and brain to take a largely transcellular route (Figure I.5). Gaseous molecules such as O_2 and CO_2 can diffuse freely across plasma membranes along their concentration gradient (passive diffusion) (Grieb et al., 1985). This is also the route for permeation of small lipophilic agents including many CNS drugs that diffuse passively through the apical and basal endothelial cell membranes (Bodor and Buchwald, 2003).

The presence of specific transport systems on the cell membranes regulates the transcellular traffic of small hydrophilic molecules (carrier mediated transport), providing a selective barrier, allowing the entry of required nutrients, such as glucose and amino acids, and excluding or effluxing potentially harmful compounds (Begley and Brightman, 2003). Some molecules, such as peptides and proteins, too large for carrier-mediated transport are generally excluded but are able to cross the endothelium to a limited degree (metabolically regulated) via a vesicular route, either by specific receptor-mediated transcytosis (*e.g.* insulin) or following a non specific adsorption of cationic molecules to the membrane surface, adsorptive-mediated transcytosis (Pardridge, 2003). Nevertheless, the brain endothelium has a much lower degree of endocytosis/transcytosis activity than has peripheral endothelium, which contributes to the transport barrier property of the BBB (Abbot et al., 2004).

The barrier function of the endothelium is not only related to the specific mechanisms to cross the cell membrane but includes also a combination of intra and extracellular enzymes that provide a metabolic barrier, metabolizing some peptides and/or inactivating many neuroactive and toxic compounds (El-Bacha and Minn, 1999).

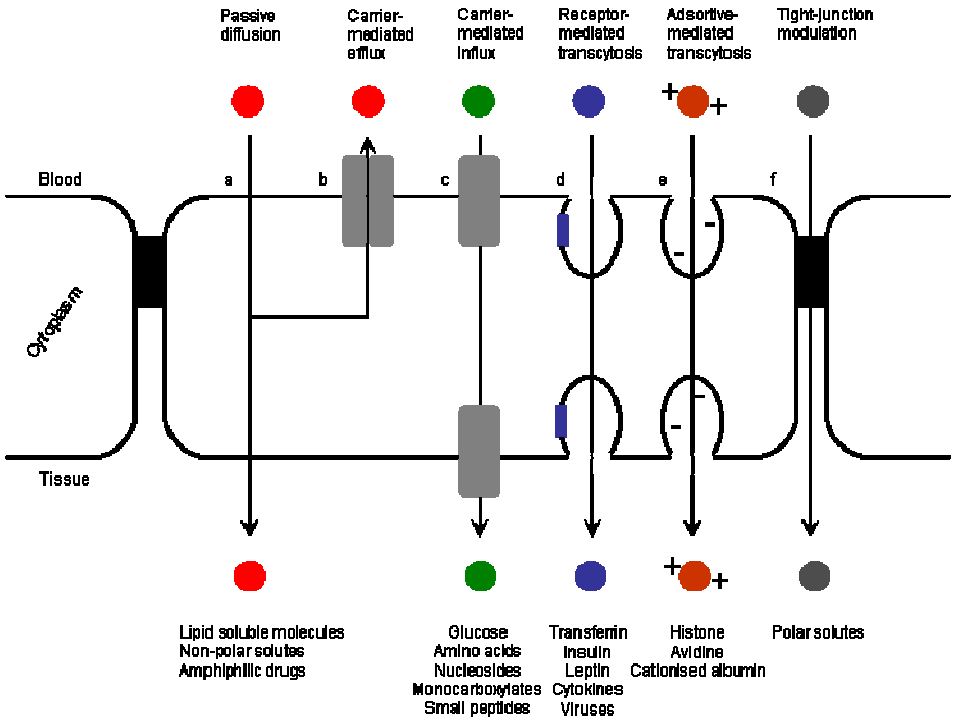

Figure I.5: Main routes for molecular traffic across the brain endothelium forming the blood-brain barrier. (a) Passive diffusion of solutes through the cell membrane for lipid soluble molecules. (b) Interception of some of these passively penetrating molecules by active efflux carriers that pump them out of the endothelial cell. (c) Carrier mediated influx for the transport of many essential polar nutrients and nucleosides, into the CNS. (d) Receptor mediated transcytosis can transport macromolecules such as proteins and peptides and (e) adsorptive mediated transcytosis induced by positively charged molecules to be transported across the BBB. (g) Tight junction modulation may also occur, which relaxes the junctions and wholly or partially opens paracellular aqueous diffusional pathway. (Modified from Abbot et al., 2004).

Brain-Drug delivery

Despite the enormous amount of information on brain biochemistry and available drugs that to some extent can enter the brain, there are still few effective treatments for disorders of the CNS, such as epilepsy, neurodegenerative disorders and brain tumours.

For designing the most effective strategy for drug delivery to the CNS, it will be necessary to take into account not only the properties of the useful routes to cross the endothelium (described above) but also those of mechanisms capable of impeding drug penetration, such as the TJ and the efflux mechanisms present in the BBB endothelium, that severely restrict the entry of hydrophilic drugs.

Most drugs produce their pharmacological response in a concentration-dependent manner and, to be effective, the drug needs to reach and maintain a therapeutic concentration at its target site for sufficient time.

The two main routes for drugs to enter the CNS are by crossing the BBB endothelia cells, the transcellular pathway, or going between these cells, the paracellular pathway. TJ severely restrict the paracellular pathway and the ability of drugs to use the passive transcellular pathway is governed largely by their lipid solubility. Strategies to increase the passive entry of drugs into the CNS could involve either increasing the paracellular permeability of the BBB interfaces or increasing the lipid solubility of drug molecules to allow them to use the passive transcellular pathway (Habgood et al., 2000)

Traditional modes of drug delivery to the brain use strategies that are invasive and require access to the brain by either a neurosurgeon or an interventional radiologist. Among these techniques are the direct injection of therapeutic agents into the brain and cerebrospinal fluid, application of intracranial implants, osmotic disruption of the BBB and chemical modulation of the TJ. These methods present major drawbacks and are not very efficient. For example, the distribution of drug into brain parenchyma is limited when intracerebral implants are used, whether because the efficacy of diffusion is inversely proportional with the square of the distance to the target or because highly diffusible molecules will exit the brain immediately by transport across local capillaries following release from the implanted site (Pardridge, 1998).

Using a systemic administration of drugs implies that these drugs will have to undergo transport through the CNS microvascular endothelial wall, which comprises the BBB, in order to be delivered to the brain. Some strategies may be applied to increase this pathway, making use of the specific transporters present in the BBB endothelium and developing drugs that contain a region recognized by these transporters. One of the problems associated with the transcellular route is the active efflux system present. Some drugs such as AZT are transported across the BBB at reduced rates but are effluxed at a much greater rate. The discovery and co-administration of inhibitors to the active efflux systems is one of the strategies to increase drug delivery into the brain (Pardridge, 1998).

Certain drugs appear to possess appropriate molecular characteristics that allow them to passively pass through the BBB. If these characteristics can be identified and quantified it may be possible to design drugs that incorporate the appropriate features that enable them to pass through the BBB barrier by passive diffusion alone. The major factor affecting the ability of therapeutic agents to use the passive transcellular pathway for entry into the CNS appears to be lipid solubility. Drugs may be altered chemically to increase lipid solubility of the compound and BBB transport of the drug may be increased in direct proportion to

lipid solubility, providing the molecular mass of the drug does not exceed a threshold of 400-600 Da (Pardridge, 1998).

It is possible to increase lipid solubility and consequently the capability to permeate the BBB by reducing the overall balance of polar: nonpolar groups on a drug molecule, either by removing polar groups or by adding nonpolar groups at sites that do not interfere with pharmacological function.

Strategies for increasing lipid solubility of individual drugs have the distinct advantage, over osmotic disruption of the BBB, that the entry of only the therapeutic agent is increased and not all other solutes in the blood at the time, as happens when TJ are disrupted (Habgood et al., 2000).

More specific targeting of the CNS may be possible if the active forms of the drugs are designed to interact only with receptors that are present, or expressed to a greater degree, in the CNS.

The permeation of the BBB and the development of new and more efficient active drugs on the CNS has been the subject of extensive scientific research (Pardridge, 1998; Habgood et al., 2000 and Abbott, 2004). Given the complexity of BBB function at the endothelial cell and the influence of surrounding cells like astrocytic glia, neurons, pericytes and perivascular macrophages, the development of *in vitro* models of the BBB is restricted. Therapeutic agents are usually not substrates for active transporters but cross the brain endothelium by passive permeation. It is therefore, of extreme pharmaceutical and medical importance to quantitatively understand the physical chemical characteristics of the mechanisms by which these agents are passively transported.

In that sense, to study the interaction of model drug molecules with model membranes that mimic the BBB endothelium may be a simplistic way to recover the physicochemical information relevant for a better understanding of drug delivery into the CNS.

References

Abbot, N. J. (2004) Prediction of blood-brain barrier permeation in drug discovery from *in vivo*, *in vitro* and *in silico* models. *Drug Discovery Today: Technologies*, 1 407-416

Abbot, N. J., Rönnbäcj, L. and Hansson, E. (2006) Astrocyte-endothelial interactions at the blood-brain barrier. *Nature Reviews: Neuroscience*, 7, 41-53

Almeida, P. F. F., Vaz, W. L. C. and Thompson, T. E. (1992) Lateral diffusion in the liquid phases of dimyristoylphosphatidylcholine/cholesterol lipid bilayers: a free volume analysis. *Biochemistry*, 31, 6739-6747

Ballabh, P., Braun, A. and Nedergaard, M. (2004) The blood-brain barrier: an overview. Structure, regulation and clinical implication. *Neurobiology of Disease*, 16, 1-13

Bangham, A. D. and Horne, R. W. (1964) Negative staining of phospholipids and their structural modification by surface active agents as observed in electron microscope. *Journal of Molecular Biology*, 8, 660-668

Bar, R.S., D.W. Deamer, and D. G. Cornwell, (1966), Surface area of human erythrocyte lipids: reinvestigation of experiments on plasma membrane. *Science*, 153, 1010-1012

Bassolino-Klimas, D., Alper, H.E. and Stouch, T.R. (1995) Mechanism of solute diffusion through lipid bilayer membranes by molecular dynamics simulation. *Journal of the American Chemical Society*, 117, 4118-4129

Begley, D. J. and Brightman, M. W. (2003) Structural and functional aspects of the blood–brain barrier. *Progress in Drug Research*, 61, 40-78

Blume, A. (1993) Dynamic Properties. In Cevc, G. (Ed.) Phospholipids Handbook. (pp 455-510) New York, Marcel Dekker, Inc.

Bodor, N. and Buchwald, P. (2003) Brain-targeted drug delivery – experiences to date. *American Journal of Drug Delivery*, 1, 13-26

Branton, D. (1966) Fracture faces of frozen membranes. *Proceedings of the National Academy of Sciences USA*, 55, 1048-1056

Branton, D. (1971) Freeze-etching studies of membrane structure. *Philosophical Transactions of the Royal Society of London B*, 261, 133-138

Bultmann, T., Vaz, W. L. C. Melo, E. C. C., Sisk, R. B. and Thompson, T. E. (1991) Fluid-phase connectivity and translational diffusion in a eutectic two-component, two-phase phosphatidylcholine bilayer. *Biochemistry*, 30, 5573-5579

Chapman, D., Williams, R. M. and Ladbrooke, B. D. (1967) Physical studies of phospholipids. VI. Thermotropic and lyotropic mesomorphism of some 1,2-diacylphosphatidylcholines (lecithins). *Chemistry and Physics of Lipids*, 1, 445-475

Chodobski, A. and Szmydynger-Chodobska, J. (2001) Choroid plexus: target for polypeptides and site of their synthesis. *Microscopy Research and Technique*, 52, 65-82

Daleke, D. L. (2007) Phospholipid flippases. *The Journal of Biological Chemistry*, 282, 821–825

Danielli, J. F. and Davson, H. (1935) A contribution to the theory of permeability of thin films. *Journal of Cellular and Comparative Physiology*, 5, 495-508

de Almeida, R. F. M., Fedorov, A. and Prieto, M. (2003) Sphingomyelin/phosphatidulcholine/cholesterol phase diagram: boundaries and composition of lipid rafts. *Biophysical Journal*, 85, 2406-2416

Devaux, P. F. (1988) Phospholipid flippases. *FEBS Letters*, 234, 8-12

El-Bacha, R. S. and Minn, A. (1999) Drug metabolizing enzymes in cerebrovascular endothelial cells afford a metabolic protection to the brain. *Cell and Molecular Biology*, 45, 15-23

Estronca, L. M. B. B., Moreno, M. J., Abreu, M. S. C., Melo, E. And Vaz, W. L. C. (2002) Solubility of amphiphiles in membranes: influence of phase properties and amphiphile head group. *Biochemical and Biophysical Research Communications*, 296, 596-603

Finean, J. B., (1962) The nature and stability of the plasma membrane. *Circulation*, 26, 1151-1162

Flewelling, R.S. and Hubbell, W.L. (1986) The membrane Dipole Potential in a Total Membrane Potential Model. *Biophysical Journal*, 49, 541-552

Frye, L. D. and Editin, M. (1970) The rapid intermixing of cell surface antigens after formation of mouse-human heterokaryons. *Journal of Cell Science*, 7, 319-335

Gennis, R.B. (1989) Biomembranes: Molecular Structure and Function, New York, Springer-Verlag.

Gorter, E. and Grendel, F. (1925) On bimolecular layers of lipoids on the chromocytes of the blood. *Journal of Experimental Medicine*, 41, 439-443

Green, D. E. and Fleischer; S. (1963) The role of lipids in mitochondrial electron transfers and oxidative phosphorilation. *Biochimica et Biophysica. Acta*, 70, 554-582

Green, D. E. and Perdue, J. F. (1966) Correlation of mitochondrial structure and function. *Annals of the New York Academy of. Sciences*, 137, 667-684

Gregoriadis, G. (1995) Engineering liposomes for drug delivery: progress and problems. *Trends in Biotechnology*, 13, 527-537

Grieb, P., Forster, R.E., Strome, D., Goodwin, C.W. and Pape, P.C. (1985) O_2 exchange between blood and brain tissues studied with $^{18}O_2$ indicator dilution technique. *Journal of Applied Physiology*, 58, 1929-1941

Habgood, M. D., Begley, D. J. and Abbott, N. J. (2000) Determinants of passive entry into the cerebral nervous system. *Cellular and Molecular Neurobiology*, 20, 231-253

Hawkins, B. T. and Davis, T. P. (2005) The blood–brain barrier/neurovascular unit in health and disease. *Pharmacological Reviews*, 57, 173-185

Hu, W. Y., Jones, P. D., DeCoen, W., King, L., Fraker, P., Newsted, J. and Giesy, J. P. (2003) Alterations in cell membrane properties caused by perfluorinated compounds. *Comparative Biochemistry and Physiology*, 135, 77-88

Huang, C. H. and Li, S. S. (1999) Calorimetrics and molecular mechanics studies of the thermotropic phase behaviour of membrane phospholipids. *Biochimica et Biophysica Acta*, 1422, 273-307

Ipsen, J. H., Karlström, G., Mouritsen, O. G., Wennerström, H. and Zuckermann, M. J. (1987) Phase equilibria in the phosphatidylcholine-cholesterol system. *Biochimica et Biophysica Acta*, 905, 162-172

Jacobson, K. (1983) Lateral diffusion in membranes. *Cell Motility*, 3, 367-373

Jain, M. K. (1983) Non-random lateral organization in bilayers and biomembranes. In Aloia, R. C. (Ed.) Membrane fluidity in biology. Vol. 1, pp. 1-37. New York, USA, Academic Press

Kinnunen, P. K. J., Kôiv, A., Lehtonen, J.Y.A. and Mustonen, P. (1994) Lipid dynamics and peripheral interactions of proteins with membrane surfaces. *Chemistry and Physics of Lipids*, 73, 181-207

Kleinzeller, A. (1997). Ernest Overton's contribution to the cell membrane concept: a centennial appreciation. *Physiology*, 12, 49-53

Knoll, W. K., Ibel, K. and Sachmann, E. (1981) Small-angle neutron scattering study of lipid phase diagrams by the contrast variation method. *Biochemistry*, 20, 6379-6383

Lenard, J. and Singer, S. J. (1966) Protein conformation in cell membrane preparations as studied by optical rotatory dispersion and circular dichroism. *Proceedings of the National Academy of Sciences USA*, 56, 1828-1835

London, E. (2002) Insights into lipid rafts structure and formation from experiments in model membranes. *Current Opinion in Structural Biology*, 12, 480

Lucy J. A., and A. M. Glauert (1964) Structure and assembly of macromolecular lipid complexes composed of globular micelles. *Journal of Molecular Biology*, 8, 727-748

Marbrey, S. and Sturtevant, J. M. (1976) Investigation on the phase transitions of lipids and lipid mixtures by high sensitivity differential scanning calorimetry. *Proceedings of the Natural Academy of Sciences USA*, 73, 3862-3866

Moreno, M. J., Estronca, L. M. B. B. and Vaz, W. L. C. (2006) Translocation of phospholipids and dithionite permability in liquid-ordered and liquid-disordered membranes. *Biophysical Journal*, 91, 873-881

Mueller, P., Rudin, D. O., Ti Tien, H. And Wescott, W. C. (1963) Methods for the formation of single bimolecular lipid membranes in aqueous solution. *Journal of Physical Chemistry*, 67, 534-535

Pardridge, W. M. (1998) CNS drug design based on principles of blood-brain barrier transport. *Journal of Neurochemistry*, 70, 1781-1792

Pardridge, W.M. (2003) Blood-brain barrier drug targeting: the future of brain drug development. *Molecular Interventions*, 3, 90-105

Paula, S., Volkov, A. G., Van Hoek, A. N., Haines, T. H. and Deamer, D. W. (1996) Permeation of protons, potassium ions, and small polar molecules through phospholipid bilayers as a function of membrane thickness. *Biophysical Journal*, 70, 339-348

Peterson, U., Mannock, D.A., Lewis, N.A.H and Pohl, P. (2002) Origin of membrane dipole potential: Contribution of the phospholipid fatty acid chains. *Chemistry and Physics of Lipids*, 117, 19-27

Prenner, E., Sommer, A., Maurer, N., Glatter, O., Gorges, R., Paltauf, F. and Hermetter, A. (2000) Lateral microheterogeneity of diphenylhexatriene-labeled choline phospholipids in the erythrocyte ghost membrane as determined by Time-Resolved Fluorescence Spectroscopy. *The Journal of Membrane Biology*, 174, 237-243

Ramstedt, B. and Slotte, J. P. (2002) Membrane properties of sphingomyelins. *FEBS Letters*, 531, 33-37

Richardson, S. H., Hultin, H. O. and Fleischer, S. (1964) Interactions of mitochondrial structural protein with phospholipids. *Archives of Biochemistry and Biophysics*, 105, 254-260

Rosoff, M. (Ed.) Vesicles. Marcel Dekker, Inc., New York, 1996

Schultz, S. G. (1998). A century of (epithelial) transport physiology: from vitalism to molecular cloning. *American Journal of Physiology - Cell Physiology*, 274, C13-C23

Simons, K. and Vaz, W. L. C. (2004) Model Systems, lipid rafts and cell membranes. *Annual Review of Biophysics and Biomolecular Structure*, 33, 269-295

Singer, S. J. and Nicolson, G. L. (1972) The fluid mosaic model of the structure of cell membranes. *Science*, 175, 720-731

Singer, S. J., (1974) The molecular organization of membranes. *Annual Review of Biochistry*, 43, 805-833

Stein, W. D. and Danielli, J. F. (1956) Structure and function in red cell permeability. *Discussions of the Faraday Society*, 21, 238-251

Tanford, C. (1980) The hydrophobic effect: formation of micelles and biological membranes John Wiley and Sons, Inc. New York, USA

Trauble, H., Teubner, M., Woolley, P. and Eibl, H. (1976) Electrostatic interactions at charged lipid membranes. 1. Effects of pH and univalent cations on membrane structure. *Biophysical Chemistry*, 4, 319-342

Vandenheuval, F. A., (1965) Study of biological structure at the molecular level with stereomodel projections. II. The structure of myelin in relation to other membrane systems. *The Journal of the American Oil Chemists' Society*, 42, 481-492

Vanderkooi, G. and Green, D. E. (1970) Biological membrane structure. I. The protein crystal model for membranes. *Proceedings of the National Academy of Sciences USA*, 66, 615-621

Vaz, W. L. C., Melo, E. C. C. And Thompson, T. E. (1989) Translational diffusion and fluid domain connectivity in a two-component, two-phase phospholipid bilayer. *Biophysical Journal*, 56, 869-875

Vaz, W. L. C. and Almeida, P. F. F. (1993) Phase topology and percolation in multi-phase lipid bilayers: is the biological membrane a domain mosaic? *Current Opinion in Structural Biology*, 3, 482-488

Vaz, W. L. C. (2008) Lipid Bilayers: Properties, Wiley Encyclopedia of Chemical Biology, John Wiley & Sons, Inc

Vereb, G., Szöllõsi, J., Matkó, J., Nagy, P., Farkas, T., Vígh, L., Mátyus, L., Waldmann, T. A. and Damjanovich S. (2003) Dynamic, yet structured: the cell membrane three decades after the Singer-Nicolson model. *Proceedings of the National Academy of Sciences USA*, 100, 8053-8058

Verkleij, A. J., Zwaal, R. F. A., Roelofsen, B., Comfurius, P., Kastelijn, D. and Van Deenen, L. L. M. (1973) The asymmetric distribution of phospholipids in the human red cell membrane. *Biochimica et Biophysica Acta*, 323, 178-193

Wallach, D. F. H. and Zahler, P. H. (1966) Protein conformations in cellular membranes. *Proceedings of the National Academy of Sciences USA*, 56, 1552-1559

Wolburg, H. and Lippoldt, A. (2002) Tight junctions of the blood–brain barrier: development, composition and regulation. *Vascular Pharmacology*, 38, 323-337

Wolburg, H. (2006) The endothelial frontier. In Dermietzel, R., Spray, D. and Nedergaard, M. (Eds.) Blood-brain interfaces – from ontogeny to artificial barriers (pp. 77-107) Weinheim, Germany, Wiley-VCH Verlag GmbH & Co.

Zhao, J., Wu, J., Heberle, F. A., Mills, T. T., Klawitter, P., Huang, G., Constanza, G. and Feigenson, G. W. (2007) Phase studies of model biomembranes: complex behaviour of DSPC/DOPC/Cholesterol. *Biochimica et Biophysica Acta*, 1768, 2764-2776

Chapter II:

Kinetics and thermodynamics of chlorpromazine interaction with lipid bilayers: Effect of charge and cholesterol

Introduction

Passive transport across cell membranes is the major route for the permeation of xenobiotics through tight epithelia, such as the vascular endothelium that constitutes the BBB. The rate of passive permeation through lipid bilayers, a critical step in the prediction of pharmacodynamics, is usually evaluated from the drug hydrophobicity with little consideration for the rate of insertion/desorption or translocation through the lipid bilayer. However, in most cases, the rate of the interaction (rather than the equilibrium partition) is the most relevant parameter, (Kramer et al., 2009; Sawada et al., 1999; Jing and Amemiya, 2009) and therefore it is very important to have kinetic details.

Chlorpromazine (CPZ) (Figure II.1), recommended in psychiatric disorders as neuroleptic sedative, is a phenothiazine derived antipsychotic agent. CPZ is amphiphilic and self-aggregates at a critical concentration, forming micelle-like structures, which undergo temperature and concentration dependent phase transitions (Attwood, 1995). Critical micelle concentrations (CMC) of CPZ are scattered over a range of 2 orders of magnitude (from 10^{-5} to 10^{-3} M). It should be noted that CPZ has a tertiary amine ($pK_a = 9.35$) (Kitamura et al., 1991), and therefore intermolecular interactions depend strongly on the solution pH and ionic strength (Wajnberg et al., 1988). At conditions similar to those used in this study (22 ℃, 10 mM phosphate buffer at pH 7.3, with 140 mM NaCl), the CMC was found to be 2×10^{-4} M, by Wajnberg and co-workers (1988). Aggregation of CPZ at concentrations well below its CMC is well supported by literature, (Attwood et al., 1992; Attwood et al., 1994) and the structure of a dimer has actually been proposed by Attwood (1995). To guarantee that CPZ is predominantly in the monomeric form, its concentration in the aqueous solution at pH ≈ 7 must be maintained below 3×10^{-5} M (Luxnat and Galla, 1986).

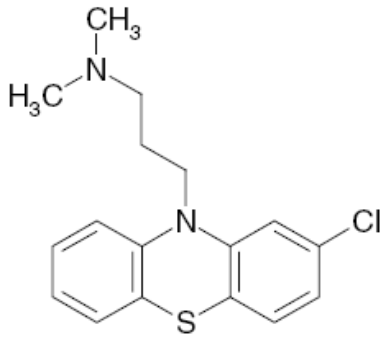

Figure II.1: Chlorpromazine structure.

The mechanism of action of CPZ involves interaction with membrane proteins, but effects mediated by the lipid bilayer must also be considered. In fact, some authors concluded that CPZ does not interact with proteins in the erythrocyte membrane, since the binding affinity of CPZ for erythrocyte ghost was found to be the same as for neutral membranes (Welti et al., 1984; Kitamura et al., 1998). Several studies of the interaction of CPZ with lipid bilayers prepared from phosphatidylcholines have been performed, and there is evidence for a location of the charged amine group in the phosphate region, while the tricyclic ring inserts in the lipid bilayer affecting mostly the properties of the carbonyl and first methylene groups of the lipid (Kuroda and Kitamura, 1984). The ionization properties of CPZ are somewhat affected by insertion in the lipid bilayer with a decrease in the value of pK_a to 8.3 in phosphocholine (lecithin) from egg yolk (egg PC) with or without cholesterol (Kitamura et al., 2004). A more interfacial location of CPZ has been argued for the case of negatively charged membranes based on a larger area expansion of lipid monolayers upon interaction with CPZ (Agasosler et al., 2001). It has also been established that CPZ affects the properties of lipid bilayers. At very high CPZ concentrations, well above its CMC, the membrane is completely dissolved due to the formation of mixed micelles and at lower concentrations membrane leakage and loss of lipid asymmetry is increased (Ahyayauch et al., 2010; Rosso et al., 1988; Schrier et al., 1992). Other effects include: depression in the main transition temperature of PC membranes at CPZ concentrations above 5 mol % (Luxnat and Galla, 1986; Jutila et al., 2001); induction of phase separation and domain morphology changes in membranes prepared from mixtures of neutral and negative lipids, (Jutila et al., 2001; Hidalgo et al., 2004; Hanpft and Mohr, 1985); and stabilization of PE lamellar phases (Hornby and Cullis, 1981). Suppression of multi drug resistance by CPZ has been reported (Wadkins and Houghton, 1993) and has received special attention recently (Michalak et al., 2006; Hendrich et al., 2003). The mechanism of this important effect of CPZ in biomembranes is yet to be established. The interpretation of the different effects of CPZ in lipid membranes is very difficult because its local concentration is usually not explicitly considered and most of the times it is impossible to calculate because the K_P at the conditions of the experiments is not known. The K_P of CPZ between the aqueous medium and lecithin bilayers has been accurately measured by Kitamura and co-workers in several works (1998; 1995; 1999) and others (Luxnat and Galla, 1986; Welti et al., 1984). A decrease in the K_P with the total concentration of CPZ, from 5 to 100 μM, was observed. At a total concentration of 10 μM

and pH ≈ 7, the reported values for the K_P of CPZ between water and egg PC are 9.9×10^3 (Welti et al., 1984) and 6.8×10^3 (Kitamura et al., 1995) being 5.4×10^3 for association with 1,2- dimyristoylphosphocholine (DMPC) (Luxnat and Galla, 1986). The value of pH was shown to affect significantly the affinity to the lipid bilayer that increases at higher values of pH (Welti et al, 1984), indicating a higher K_P for the neutral form. No quantitative interpretation was given for the dependence of the K_P on CPZ concentration, although aggregation of CPZ in the aqueous phase was evoked. In this work, we will readdress this question taking into account the charge imposed in the bilayer by the cationic CPZ according to the Gouy–Chapman theory as was done previously for sodium dodecyl sulphate (Moreno et al., 2010; Tan et al., 2002). The introduction of Chol in the membrane was shown to decrease the K_P of CPZ, (Luxnat and Galla, 1986; Takegami et al., 1999) while the addition of negatively charged lipids increases the affinity of CPZ for the membrane (Takegami et al., 2005). We will characterize the effect of Chol and negative charge in the lipid bilayer in an attempt to give a quantitative interpretation to the variations observed.

The methodology used in the characterization of CPZ interaction with membranes is mostly based on changes in the second derivative of CPZ absorption in the UV, (Welti et al., 1984; Kitamura et al., 1995; Takegami et al., 1999; 2003; 2005) but physical separation of the aqueous and membrane phases has also been used (Luxnat and Galla, 1986). In this work, we use isothermal titration calorimetry (ITC), a very powerful technique that allows the measurement of the K_P as well as the thermodynamic parameters for the interaction. The ITC technique has been generally used with high concentrations of ligands, and under those conditions saturation of the membrane may occur for the case of ligands with a high K_P. Additionally, those high concentrations are not appropriate for ligands with a tendency to aggregate in the aqueous phase. We have recently shown that with the high sensitivity of modern ITC equipment, the ligand concentration may be reduced to levels previously accessible only by spectroscopic techniques, (Moreno et al., 2010) allowing the direct characterization of partition to unperturbed membranes. Additionally, protocols have been recently developed that allow the qualitative evaluation of the kinetics of ligand translocation across the bilayers (Tsamaloukas et al., 2007; Heerklotz, 2004; Heerklotz et al., 1999). This parameter is of fundamental importance in the quantitative characterization of the association of ligands with lipid bilayers because it is necessary to know the amount of membrane phase that is accessible to the ligand (only the outer monolayer or both) and

also because this is usually considered the rate-limiting step in their permeation through membranes (Andreas and Peter, 2009). In this work, we introduce new approaches that allow the quantitative measurement of the translocation rate constant using ITC.

We report here the kinetics and thermodynamics of the interaction of CPZ with LUVs prepared from pure POPC, POPC:POPS (9:1), and POPC:Chol:POPS (6:3:1) using ITC. The effect of CPZ concentration on the K_P observed is quantitatively interpreted in terms of the charge imposed by CPZ in the membrane using the Gouy-Chapman theory. The relative rate of the insertion/desorption and translocation processes was obtained using the uptake and release protocols (Tsamaloukas et al., 2007). A quantitative evaluation of the translocation rate is also performed, for the case of the membranes in the l_o phase studied, following an innovative methodology based on the kinetics of the heat evolved upon association of CPZ with the membranes. The equilibration of aqueous CPZ with the outer monolayer of LUVs occurs faster than the time resolution of the ITC, but a much slower process is observed due to translocation of CPZ into the inner monolayer of LUVs, which leads to the association of additional CPZ with the outer monolayer. The mathematical model to describe this biphasic heat variation was developed, and the rate constant of translocation was obtained as a function of both temperature and pH.

Partition Model

The predicted heat evolved in titration step i, $q(\mathrm{i})$, is calculated by eq II.1, and the best fit of the model to the experimental values was obtained through minimization of the square deviations between the experimental and the predicted heat per injection for all of the titration steps, as described previously (Moreno et al., 2010):

$$q(\mathrm{i}) = \Delta H\left(n_{\mathrm{CPZ\_L}}(\mathrm{i}) - n_{\mathrm{CPZ\_L}}(\mathrm{i}-1)\left(1-\frac{V(\mathrm{i})}{V_{\mathrm{cell}}}\right)\right) + q_{\mathrm{dil}} \qquad \text{eq II.1}$$

Where $V(\mathrm{i})$ is the injection volume, V_{cell} is the volume of the calorimetric cell, and q_{dil} is the "heat of dilution" (residual heat due to nonbinding phenomena). The amount of CPZ associated with the lipid bilayer is calculated assuming simple partition between the aqueous and the lipid phase (kinetic scheme I).

Kinetic Scheme I: Interaction of CPZ with the liposomes considered as a lipid phase:

$$\mathrm{CPZ_W} \xleftrightarrow{K_P^{obs}} \mathrm{CPZ_L}$$

The observed partition coefficient (K_P^{obs}) is given by the ratio of the concentrations of CPZ in each phase, calculated with respect to the volume of the respective phase, and is given by the upper line of eq II.2, where n_{CPZ_T} is the total number of moles of CPZ of which n_{CPZ_W} are in the aqueous and n_{CPZ_L} are in the lipid phase.

$$K_P^{obs} = \frac{n_{CPZ\_L}/V_L}{n_{CPZ\_W}/V_W} = \frac{n_{CPZ\_L}/\left([L]\overline{V}_L V_T\right)}{n_{CPZ\_W}/V_T}$$
$$n_{CPZ\_L} = n_{CPZ\_T}\frac{K_P^{obs}[L]\overline{V}_L}{1+K_P^{obs}[L]\overline{V}_L} \qquad \text{eq. II.2}$$

In eq. II.2, V_T is the total volume, and V_L and V_W are the volumes of the lipid and aqueous phases, respectively. The molar volumes, $\overline{V}_L$, considered for the lipids used in this work were 0.795 dm^3 mol^{-1} for POPC (Wiener and White, 1992) and POPS and 0.325 dm^3 mol^{-1} for cholesterol (Krivanek et al., 2008). Values of the adjustable parameters, K_P^{obs} and ΔH, are generated by the Microsoft Excel Add-In Solver, and the corresponding heat evolved at each injection is calculated using eq II.1 and the lower line of eq II.2. This is compared to the experimental values obtained in the titration, and the square difference is minimized. Depending on the relative rates of translocation and insertion/desorption, CPZ may or may not be equally distributed between the two bilayer leaflets. This requires the substitution of CPZ concentration by its effective concentration, [CPZ]*, which depends on the effective lipid concentration, [L]*, according to eq II:3. This introduces the equilibration factor, γ, which is a measure of the fraction of lipid accessible to CPZ during the titration experiment, with values of 1 for fully permeable (fast translocation of ligand) and 0.5 for impermeable membranes (slow translocation of ligand).

For experiments following the uptake protocol (addition of lipid to ligand in the aqueous phase), all ligand is accessible for partition, and the effective lipid concentration is either equal to its total concentration (case of fast translocation) or is reduced to the lipid in the outer monolayer (case of slow translocation), according to eq. II.3. In this type of

experiments, if γ is unknown, the uncertainty is propagated to the K_P, but the calculated ΔH is accurate. On the other hand, in experiments following the release protocol, both the lipid effective concentration and the available moles of ligand must be calculated from eq. II.3. In this situation, both K_P and ΔH are affected by the uncertainty in γ. The combination of both protocols allows the calculation of the γ and, therefore, the accurate measurement of K_P and ΔH and a qualitative estimation of the translocation rate constant.

$$[\mathrm{L}]^*(i) = [\mathrm{L}]^*(i-1)\left\{1-\frac{V(i)}{V_{\mathrm{cell}}}\right\}+\gamma\left\{[\mathrm{L}]^{\mathrm{Syr}}\frac{V(i)}{V_{\mathrm{cell}}}\right\}$$
$$n^*_{\mathrm{CPZ\_T}}(i) = n^*_{\mathrm{CPZ\_T}}(i-1)\left\{1-\frac{V(i)}{V_{\mathrm{cell}}}\right\}+\left\{\gamma[\mathrm{CPZ}]_{\mathrm{L}}^{\mathrm{Syr}}\right\}V(i) \qquad \text{eq. II.3}$$

where the index *i* refers to the injection number, the superscript Syr indicates concentrations in the syringe, and the subscripts L and W indicate the phase where CPZ is dissolved, being L for the lipid and W for water (T for the sum of both).

Correction for the electrostatic effect

The partition coefficient obtained directly from the ratio of the concentrations in both phases, K_P^{obs}, is dependent on the total concentration of ligand in the bilayer due to the charge introduced by it and is related to the intrinsic partition coefficient (for an uncharged bilayer, K_P) via the electrostatic potential at the bilayer surface, Ψ_0, as described previously (Moreno et al., 2010; Tan et al., 2002; Keller et al., 2006) and shown in eq. II.4. The bilayer charge density, σ, is related to the electrostatic potential at the bilayer surface, Ψ_0 (eq. II.5, first line), and may be calculated from the surface density of charged molecules in the bilayer (eq. II.5, second line). The difference between the values of σ calculated from both approaches is minimized by changing the values of the surface potential and intrinsic partition coefficient, allowing the computation of the best value for those two parameters.

$$K_P^{obs} = K_P e^{-zF\Psi_0/RT} \qquad \text{eq. II.4}$$

$$\sigma = \frac{\Psi_0}{|\Psi_0|}\sqrt{2000\varepsilon RT\sum_i C_i\left(e^{-z_i F\Psi_0/RT}-1\right)}$$
$$\sigma = e_0\frac{\sum z_i\left(n_i/n_{\mathrm{L}}\right)}{\sum A_j\left(n_j/n_{\mathrm{L}}\right)} \qquad \text{eq. II.5}$$

where ε is the dielectric constant, R is the ideal gas constant, F is the Faraday constant, C_i is the concentration of the charged species *i*, with the charge z_i, e_0 is the elemental electrostatic charge, A_j is the area of the *j* component of the lipid bilayer (being 68 Å^2 for POPC and POPS (Tan et al., 2002), 25 Å^2 for Chol (do Canto et al., 2011) and 39 Å^2 for CPZ (Agasosler et al., 2001)), n_j (n_i) is the number of moles of the membrane component *j* (*i*), and n_{L} is the number of moles of lipid. The charge considered for POPS was −1, and that of CPZ inserted in lipid bilayers at pH = 7.4 was +0.89 (considering its pK_{a} = 8.3 (Kitamura et al., 2004)).

Results and Discussion

Effect of Ligand Concentration

To obtain the partition of small molecules into lipid bilayers, the usual protocol is to titrate the ligand with increasing amounts of lipid (Moreno et al., 2010; Heerklotz, 2004; Sampaio et al., 2005). One important factor is the eventual effects of ligand in the membrane (Moreno et al., 2010; Matos et al., 2004) and this was evaluated through the dependence of the observed partition coefficient on the total CPZ concentration when titrated with 5 mM POPC, assembled as 100 nm LUVs, at 25 °C. Given the positive charge on CPZ at the pH used (pH 7.4), a small rate of translocation is anticipated, and therefore the accessibility factor was assumed to be 0.5. The results obtained are shown in Figures II.2 and II.3.

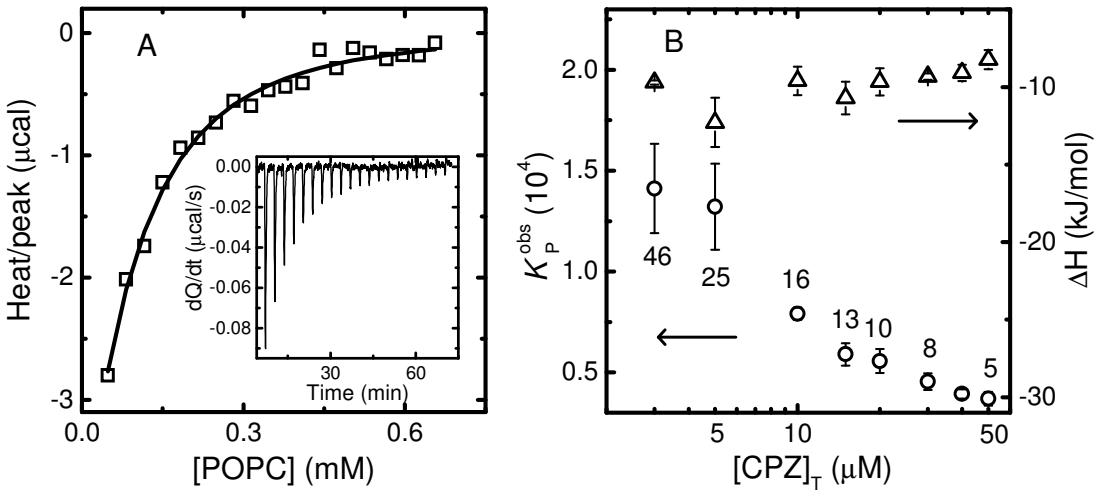

Figure II.2: Titration of CPZ at different total concentrations with 5 mM POPC at 25 ºC. Plot A: Typical titration curve obtained for $[CPZ]_T$ = 5 μM. The line is the best fit obtained with eq. II.1 and II.2. Plot B: Observed partition coefficients (K_P^{obs} , ○) and molar enthalpy change (ΔH, △) obtained by the best fit of eq. II.1 and II.2 to the experimental results. The numbers indicated are the ratio of lipid molecules per bound CPZ after the first 10 μL injection.

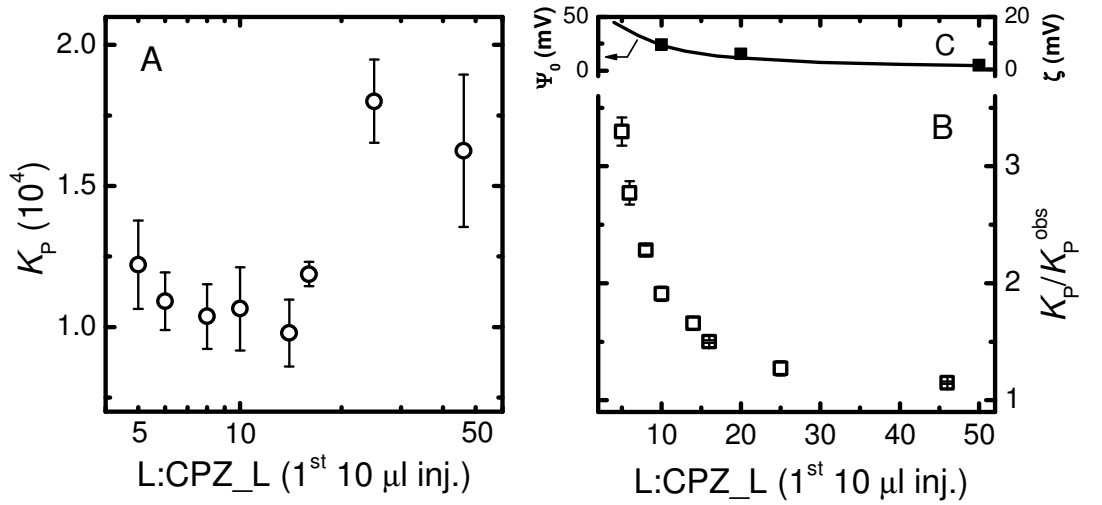

Figure II.3: Effect of CPZ concentration on its partition to POPC bilayers at pH = 7.4 and 25 ºC. Plot A: Intrinsic partition coefficients (K_P , ○) obtained for titration of CPZ at different total concentrations in the aqueous phase, between 2.5 and 50 μM, with POPC 5 mM. The results are indicated as a function of the lipid to bound CPZ ratio after the first 10 μL injection. Ideal conditions correspond to high values in this parameter, while they corresponded to low ligand concentrations in Figure II.2. Plot B: Ratio between the values of the intrinsic and observed partition coefficients as a function of the local concentration of CPZ in the POPC bilayer. Plot C: Surface potential predicted by the Gouy−Chapman theory (Ψ_0), eq. II.2−II.5, and the measured zeta potential (ζ) at the indicated ratios of POPC to CPZ.

Figure II.2, plot A, shows a typical titration of CPZ at a total concentration of 5 μM. The interaction parameters, obtained with eq. II.1 and II.2, are represented in Figure II.2, plot B, together with the parameters obtained for all of the concentrations of CPZ studied. The

numbers indicated in plot B are the ratio of lipid per bound CPZ after the first 10 μL injection. This ratio increases as the titration proceeds due to the increase in the lipid concentration.

The observed partition coefficient (K_P^{obs}) is independent of local concentration of CPZ for very small molar fractions of ligand (smaller than 4%, that is, over 25 lipid molecules per bound CPZ). For larger local concentrations of CPZ, the observed partition coefficient shows a significant decrease.

This result was expected due to the positive charge imposed by CPZ in the bilayer, and it may be accounted for using eq.II.4 and II.5 from which the intrinsic partition coefficient K_P may be obtained (Figure II.3, plot A).

Some dependence of K_P on the local concentration of CPZ is still observed, although it is much smaller than that observed for K_P^{obs}, reflecting deviations from ideal behaviour. The small increase in K_P observed for very small and very large local concentrations of CPZ may reflect an overestimation of the membrane surface potential by the Gouy-Chapman theory due to the limitations of this approach, which does not consider the discreteness-of-charge (Keller et al., 2006; Torrie et al., 1982; Murray et al., 1999; Shapovalov et al., 2006; Heerklotz, 2008). Additionally, the binding of sodium and chloride to POPC was not taken into account, although it is not expected to significantly influence the results due to the small binding constants reported for the binding of those ions to phosphocoline membranes and the similar affinities of both ions (Tatulian, 1987). The abrupt variation of K_P between 1:25 and 1:10 (CPZ:lipid molecules) possibly indicates a distinct mode of interaction between CPZ and the POPC bilayer, suggesting the formation of aggregates in the membrane. Significant effects of CPZ in the properties of membranes have been observed at comparable CPZ concentrations (Luxnat and Galla, 1986; Ahyayauch et al., 2010; Rosso et al., 1988; Schrier et al., 1992; Jutila et al., 2001).

The ratio between the observed and the intrinsic partition coefficient is represented in Figure II.3 plot B, and it may be seen that the two parameters converge for low local concentrations of CPZ (less than 4% molar ratio), giving $K_P = (1.7 \pm 0.2) \times 10^4$ with $\Delta H = -12 \pm 2$ kJ·mol^{-1} and $K_P^{obs} = (1.5 \pm 0.4) \times 10^4$ with $\Delta H = -13 \pm 1$ kJ·mol^{-1} at 25 °C. The parameters obtained are very similar to those reported in the literature for partition of CPZ to EggPC SUVs using small ligand concentrations where the partition was followed

through the variations in CPZ absorption spectra ($K_P^{obs} = 1.5 \times 10^4$ t 37 °C (Welti et al., 1984) with a van't Hoff enthalpy of −9.5 kJ mol^{-1} (Takegami et al., 2003)).

When the local concentration of CPZ is high, the calculation of the intrinsic partition coefficient is strongly dependent on the electrostatic model used. To have some indication on the adequacy of eq. II.4 and II.5, we have measured the ζ potential of POPC LUVs loaded with CPZ at a ligand to lipid molar ratio of 1:50, 1:20, and 1:10. The dependence of ζ on the local concentration of CPZ is similar to that of the surface potential predicted from the Gouy−Chapman theory, but the magnitude of the ζ potential is significantly smaller, Figure II.3 plot C. Some difference was expected because ζ is the potential at the hydrodynamic shear plane and not at the bilayer surface, which is the potential predicted by the equations used in this work and felt by CPZ when inserted in the bilayer (Jones, 1995).

Since it is difficult to correct for the electrostatic effects, there is uncertainty associated with the parameters required, and data analysis is complex, it is preferable to use the lowest concentration of ligand that generates a good signal-to-noise ratio (5 μM) and analyze the results in terms of the partition coefficient directly obtained experimentally, K_P^{obs}. A total concentration of CPZ corresponding to a lipid to CPZ bound ratio of at least 25, in the first 10 μL injection, was used throughout the rest of the work.

At the pH used in the experiments, 99% of CPZ is in the protonated state (pKa = 9.35 (Kitamura et al., 1991)), and based on the reported value of the ionization constant for CPZ inserted in lipid bilayers (pKa = 8.3 (Kitamura et al., 2004)), 89% remains in the charged protonated state after interaction with the membranes. Because of the importance of this process in the interpretation of the interaction enthalpies obtained, we have performed titrations in buffers with different ionization enthalpies to evaluate the fraction of protons released upon partition to the POPC bilayers (Beschiaschvili et al., 1992). No significant dependence of ΔH on the ionization enthalpy of the buffer was observed, an indication that the fraction of protons released or bound upon association with the membrane is ≤0.1 (results not shown).

Translocation of CPZ in Membranes Prepared with POPC

As considered in the previous section, CPZ translocation was slower than the characteristic time for the titration; this assumption was required for the preliminary experiments to

identify the most appropriate ligand and lipid concentrations. The rate of translocation was then evaluated, using the selected best CPZ and lipid concentrations, and this was first attempted through the global best fit of titrations performed according to the uptake and release protocols (Tsamaloukas et al., 2007).

ITC uptake and release curves obtained at 25 °C for CPZ titration with POPC LUVs are represented in Figure II.4. The uptake experiment was performed injecting aliquots of 5 mM POPC into 5 μM CPZ in buffer, while in the release experiment aliquots of 15 mM POPC preloaded with 0.15 mM CPZ (POPC:CPZ molar ratio equal to 100) were injected into the buffer containing sample cell, both spaced by 200 s between injections.

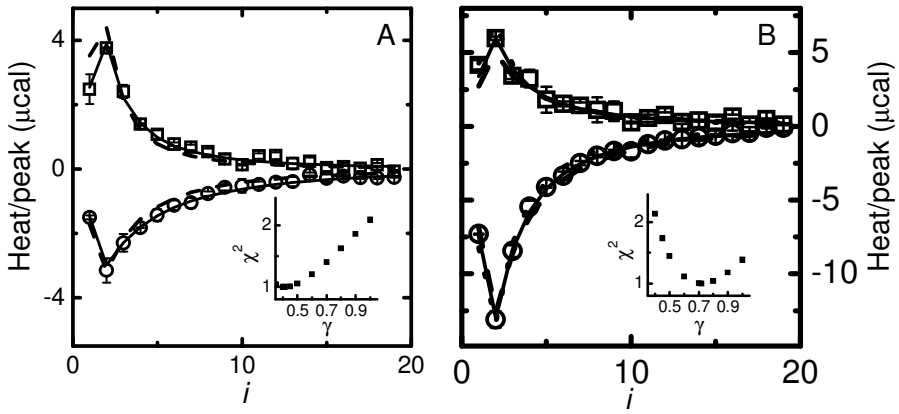

Figure II.4: Titration curves obtained for the uptake (○) and release (□) protocols with POPC membranes. Plot A: Experiments at 25 °C. The lines are the best fit using $\gamma = 0.5$ (continuous line) and $\gamma = 1$ (dashed line). Plot B: Experiments at 37 °C. The lines are the best fit obtained with $\gamma = 0.5$ (−−−), $\gamma = 1$ (- - -), and $\gamma = 0.7$ (−). The insets show the dependence of the square deviation between the global best fit and the experimental results (χ^2) as a function of γ.

The experiment performed at 25 °C was well fitted by eq. II.1-II.5, using a lipid accessibility factor of $\gamma = 0.5$ in eq. II.3, and the average thermodynamic parameters found previously for titrations of CPZ at 5 μM using the uptake protocol. In contrast, if an accessibility factor of 1 was imposed, the best global fit of the uptake and release experiments was not acceptable (Figure II.4 plot A). The variation of the global fit χ^2 on the accessibility factor is shown in the inset with a minimum for $\gamma = 0.4–0.5$ and increasing sharply for $\gamma \geq 0.55$. This indicates that translocation of CPZ between the two bilayer leaflets is negligible during the time scale of the experiment at 25 °C. Those results show, additionally, that the fraction of lipid exposed to the aqueous media outside the LUVs is between 40% and 50% and, conversely, that the fraction of lipid present in inner bilayers is

smaller than 20%. This is in agreement with the results obtained by other methods for the multilamellarity of the LUVs used in this work (see Material and Methods).

The results obtained in the experiments at 37 °C are shown in Figure II.4 plot B. In this case, the best global fit for the uptake and release experiments leads to $\gamma \approx 0.7$, and a good fit could not be obtained in any of the two thermodynamically meaningful cases ($\gamma = 0.5$ or 1); see inset in the figure. Intermediate values of accessibility factors reflect translocation rates comparable to the titration experiment, but a quantitative characterization of this parameter cannot be performed using this approach (Keller et al., 2006).

Aiming to separate the processes of equilibration of CPZ between the outer monolayer and the aqueous phase and its translocation across the bilayer, the time between injections was increased from 200 to 3600 s in an uptake experiment. The results obtained are shown in Figure II.5 where it can be seen that most heat is evolved during the first minutes with an additional slower step being also present that extends up to 40 min (see inset of plot A). The fast process corresponds to the partition of CPZ into the outer monolayer of LUVs, and the slower step was attributed to the entry of new CPZ into the outer monolayer due to translocation of CPZ from the outer into the inner monolayer. It should be noted that translocation in itself does not originate any heat change because both initial and final states are energetically equivalent. However, as CPZ leaves the outer monolayer, due to translocation into the inner, some additional CPZ partitions between the aqueous phase and the outer monolayer of the LUVs, according to kinetic scheme II and eq. II.6.

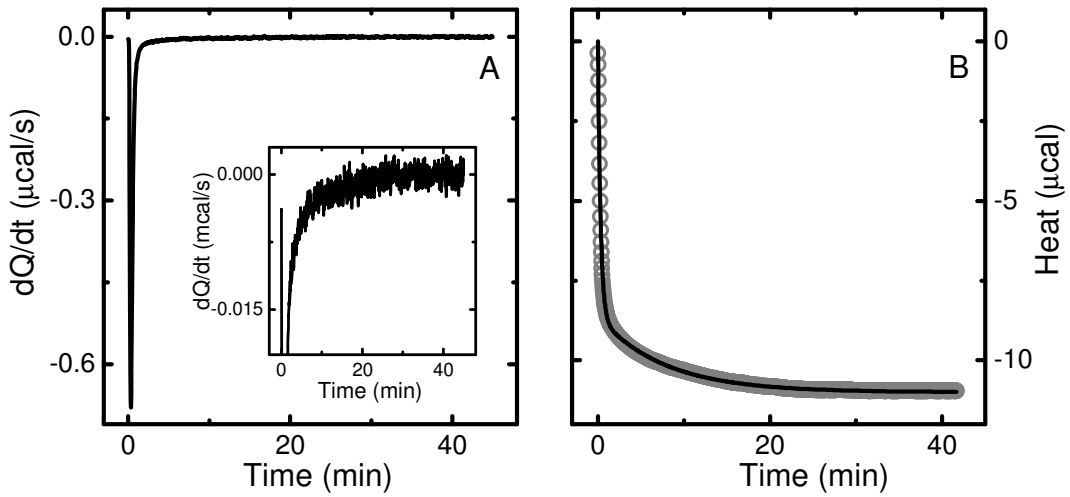

Figure II.5: Kinetic profile of the heat evolved due to the addition of POPC vesicles to an aqueous CPZ solution. Plot A: Injection of 10 µL of POPC 15 mM into CPZ 15 µM, at 37 °C, recorded for 3600 s (evidence for the slower step). Plot B: Cumulative heat in time for the partition of CPZ into POPC LUVs. The line is the best fit of eq. II.6 with the rate constants 3.1×10^{-2} and 1.3×10^{-3} s^{-1} for the fast and slow process, respectively

Kinetic Scheme II – Interaction of CPZ with the outer (out) and inner (in) leaflets of LUVs:

$$\mathrm{CPZ_W} \underset{k_-}{\overset{k_+[\mathrm{LUV}]}{\rightleftarrows}} \mathrm{CPZ_L^{out}} \overset{k_f}{\longleftrightarrow} \mathrm{CPZ_L^{in}}$$

$$\frac{\mathrm{d[CPZ]_W}}{\mathrm{d}t} = k_-[\mathrm{CPZ}]_\mathrm{L}^{\mathrm{out}} - k_+[\mathrm{LUV}][\mathrm{CPZ}]_\mathrm{W}$$

$$\frac{\mathrm{d[CPZ]_L^{out}}}{\mathrm{d}t} = k_+[\mathrm{LUV}][\mathrm{CPZ}]_\mathrm{W} - k_-[\mathrm{CPZ}]_\mathrm{L}^{\mathrm{out}} + k_f\left([\mathrm{CPZ}]_\mathrm{L}^{\mathrm{in}} - [\mathrm{CPZ}]_\mathrm{L}^{\mathrm{out}}\right) \qquad \text{eq. II.6}$$

$$\frac{\mathrm{d[CPZ]_L^{in}}}{\mathrm{d}t} = k_f\left([\mathrm{CPZ}]_\mathrm{L}^{\mathrm{out}} - [\mathrm{CPZ}]_\mathrm{L}^{\mathrm{in}}\right)$$

where k_+, k_-, and k_f are the rate constants for insertion into, desorption from, and translocation through the lipid bilayer. The heat evolved at a given time after each injection is proportional to the variation in the total amount of CPZ in the membrane (in the outer plus inner leaflets), and the rate constants may be obtained from the best fit of eq. II.6 to the experimental curve. As is evident in Figure II.5 plot A, the fast step dominates the variation of the differential heat, and this decreases the statistical weight of the best fit to the most relevant slower process. The weights of the two processes become comparable when the cumulative heat is represented, Figure II.5 plot B, and we have therefore opted for performing the best fit of the cumulative heat with the numerical integration of eq. II.6.

The results presented were obtained after the injection of 10 μL of a 15 mM POPC suspension into CPZ at 15 μM (a small concentration of POPC was already in the cell due to the injection of the recommended 4 μL), and the weight of the two steps leads to a 20% increase of CPZ in the membrane due to partitioning to the lipid in the inner leaflet, in agreement with that predicted from the value of the partition coefficient obtained using standard protocols (see Table II.1).

Table II.1: Kinetic and thermodynamic parameters for CPZ translocation in POPC and POPC:POPS 9:1 LUVs and parameters obtained for CPZ partition into those membranes taking into account partial translocation during the titration.

		Translocation			Partition		
	T (ºC)	k_f[a] (10^{-4} s^{-1})	ΔH (kJ mol^{-1})	TΔS$^{(37\,ºC)}$ (kJ mol^{-1})	K_P^{obs} (10^4)	ΔH (kJ mol^{-1})	TΔS$^{(37\,ºC)}$ (kJ mol^{-1})
POPC	25	3.9[b]	62 ± 12	- 32 ± 8	1.2 ± 0.4	- 12 ± 1	12
	37	10 ± 2			1.0 ± 0.3	- 11 ± 1	13
POPC:POPS (9:1)	25	6.6 ± 0.7	49 ± 10	- 44 ± 7	1.4 ± 0.2	- 21 ± 3	3
	37	15 ± 1			1.3 ± 0.1	- 22 ± 3	2

[a] The average values shown are from the best fit shown in Figure II.6, and the standard deviations were calculated from the three experimental measurements performed at the indicated temperature. [b] Extrapolated from the results obtained between 30 and 40 ºC, Figure II.8.

The rate constants obtained from the best fit of eq. II.6 to the cumulative heat shown in Figure II.5 plot B were 3.1×10^{-2} and 1.3×10^{-3} s^{-1} for the fast and slow processes, respectively. The fast process is due to partitioning to the outer monolayer ($k_+[\text{LUV}]+k_-$), but the characteristic rate constant obtained cannot be used to calculate the rate of insertion and desorption because the heat variation is being limited by the time response of the equipment (≈10 s). To improve the confidence in the nature of the process generating the slower heat variation, we have performed the experiment at different values of pH from 6.5 to 8.0. The reported p*K*a of CPZ inserted in lipid bilayers is equal to 8.3 (Kitamura et al., 2004), from which the fraction of ligand in the neutral form at the different values of pH may be calculated to be 0.016 at pH = 6.5, 0.05 at pH = 7, 0.11 at pH = 7.4, and 0.33 at pH = 8. This increase in the fraction of neutral form with pH is expected to accelerate significantly the rate of translocation (eq. II.7), and this was in fact observed (Figure II.6). The global rate of translocation is given by:

$$k_f = k_f^+[\text{CPZ}^+] + k_f^0[\text{CPZ}^0] \qquad \text{eq. II.7}$$

where [CPZ^+] and [CPZ^0] are the concentrations of CPZ in its cationic and neutral states, respectively, and k_f^+ and k_f^0 are their respective translocation rate constants. The concentrations of neutral and charged CPZ species are calculated from its ionization constant (K_a) and solution pH (eq. II.8).

$$[CPZ^0] = \frac{[CPZ]_T K_a}{10^{-pH} + K_a}; [CPZ^+] = [CPZ]_T - [CPZ^0] \qquad \text{eq. II.8}$$

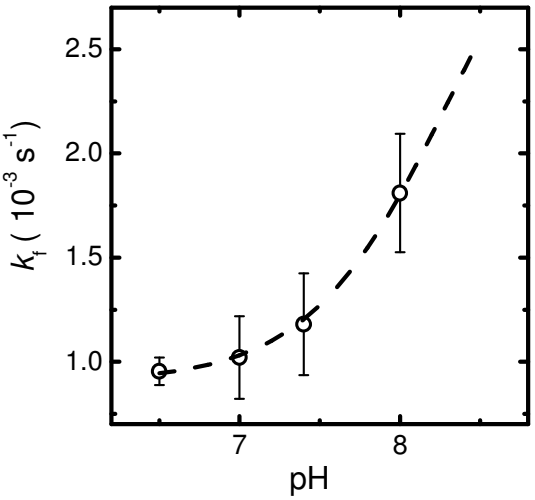

Figure II.6: Translocatin rate constants obtained for CPZ in POPC lipid bilayers at differen pH buffer solutions. The line is the best fit for the global theoretical translocation rate constant of CPZ, with pK_a = 8.3 and k_f for the neutral and cationic forms equal to 3.6×10^{-3} and 9.0×10^{-4} s^{-1}, respectively.

From the dependence of the rate of translocation with the value of pH, one can obtain the rate constant for translocation of the neutral form, k_f^0, as well as that of the cationic form, k_f^+, being 3.6×10^{-3} and 9.0×10^{-4} s^{-1}, respectively, at 37 °C. The excellent fit of the predicted dependence with pH to the observed variation gives support to the interpretation that this slow step is due to translocation of CPZ between the bilayer leaflets. The ratio between the rate constants for translocation of the neutral and charged form is equal to 4. This is smaller than anticipated based on the usually observed much faster permeation of neutral ligands as compared to charged ones (Thomae et al., 2005; Chakrabarti, 1994; Abraham, 2011). However, it should be noted that for most solutes, when the Meyer–Overton rule applies (Andreas and Peter, 2009) the rate of permeation is directly proportional to both the translocation rate and the fraction of solute associated with the outer monolayer (which is given by the partition coefficient), and, in fact, for the few

ligands where the two processes have been measured, the ratio between the rates of translocation of neutral and charged species may be even smaller than the one obtained for CPZ ($k_f^0/k_f^- = 2$ for an aromatic carboxylic acid (Thomae et al., 2005). Additionally, the translocation rate constant obtained for the neutral form is strongly dependent on the value considered for the ionization constant (e.g., if pK_a = 8.5 is assumed, the value obtained from the best fit is $k_f^+ = 4.6\times10^{-3}$ s^{-1}, leading to a ratio equal to 5).

The experiment at pH = 7.4 was performed at different temperatures, from 30 to 40 °C, to obtain the thermodynamic parameters of the translocation step. The results are shown in the next section (Figure II.8) together with data for POPC:POPS mixtures.

Translocation of CPZ in Membranes Containing POPS

The combination of uptake and release protocol was successfully used to obtain qualitative information on the translocation of CPZ in the more ordered membranes, containing cholesterol (POPC:Chol:POPS 6:3:1). The results obtained are shown in Figure II.7 and indicate that translocation of CPZ between the two leaflets is negligible during the time scale of the titration experiment, γ = 0.5, at both 25 and 37 °C. The inset shows the variation of the global fit χ^2 on the value of γ, indicating that a good global fit is obtained when considering that 40–50% of the lipid is in the outer monolayer of the LUVs. The results impose an upper limit for the rate of translocation in those membranes, which must be equal to or smaller than 4×10^{-4} s^{-1} at both temperatures.

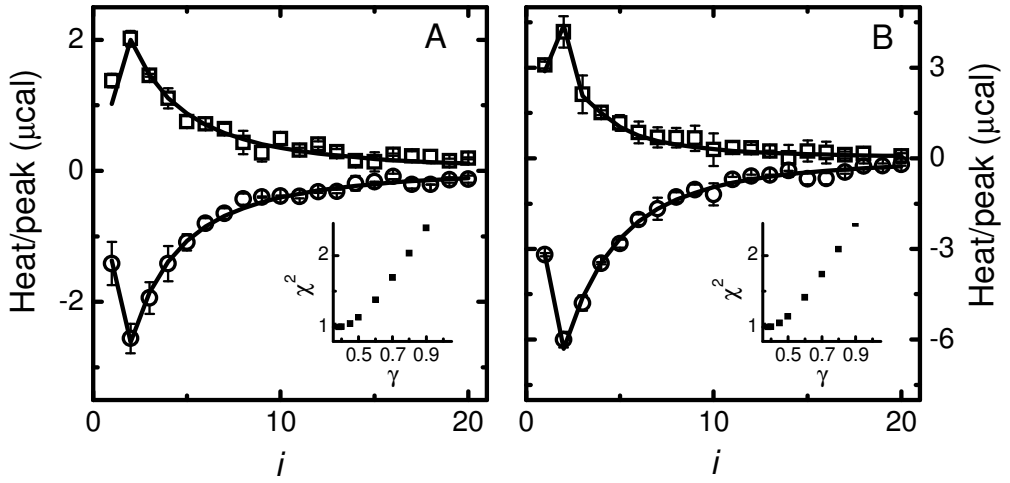

Figure II.7: Uptake (○) and release (□) experiments with membranes composed of POPC:Chol:POPS 6:3:1 at (A) 25 ºC and (B) 37 ºC. The lines are the best fit of eq. II.1-II.6 with $\gamma = 0.5$, and $K_P = 5.8 \times 10^3$, $\Delta H = -4$ kJ mol^{-1} at 25 °C and $K_P = 4.1 \times 10^3$, $\Delta H = -12$ kJ mol^{-1} at 37 °C. Insets are as in Figure II.4.

To identify the contributions from Chol (reduced membrane fluidity) and POPS (negative charge) in the smaller rate of permeation, we have also characterized the translocation of CPZ in membranes prepared from POPC with 10 mol % POPS. This was first attempted using the uptake and release protocol. However, good release titrations could not be obtained due to the presence of an unexpectedly high heat of dilution and/or heat curves that could not be well described by eq. II.1-II.5 regardless of the accessibility factor considered (results not shown). A tentative interpretation of this observation is related to the opposite charges of POPS and CPZ and the relatively high local concentrations of CPZ required for the release protocol (1 mol %). This may affect the phase behaviour of the POPC:POPS bilayer, which shows nonideal mixing even at this small fraction of charged lipid.(Huang et al., 1993). Changes in the membrane properties upon incubation with CPZ would lead to the occurrence of other processes during dilution in the release protocol, in addition to CPZ equilibration with the aqueous phase. In the uptake protocol, no evidence is encountered for unusual processes because the high local concentration of CPZ attained at the beginning of the titration is rapidly decreased as the titration proceeds due to the increase in the concentration of lipid. Effects of CPZ on the phase behaviour of charged membranes have been previously observed (Jutila, 2001).

The methodology described above for the case of POPC bilayers was therefore followed to characterize the rate of translocation of CPZ through the POPC:POPS (9:1) bilayers in the temperature range from 25 to 40 °C (Figure II.8). The rate of translocation obtained for the

charged bilayers in the liquid disordered state is slightly higher than that observed in POPC bilayers, with the best fit values being 1.5×10^{-3} and 1.0×10^{-3} s^{-1}, respectively, at 37 °C and pH = 7.4. (The rate constants for translocation shown are the observed ones corresponding to the average of the rate constants for the neutral and charged species weighted by their relative molar fractions. The expected stabilization of the cationic species at the negatively charged membrane would lead to an increased value of pK_a and a corresponding increase in the fraction of charged CPZ. This effect should have decreased the observed rate constant for translocation.) This result was at first surprising in view of the expected stabilization of the inserted state of the cationic CPZ molecule at the negative surface of the bilayer. The observed increase in the rate of translocation is most likely a result of an overcompensating effect due to the larger free volume in the charged bilayer (Manuel et al, 2008; Luna et al., 2011). Increased rates of permeation through negatively charged membranes have been observed by other authors for neutral, zwitterionic, and negatively charged ligands (Thomae et al., 2007).

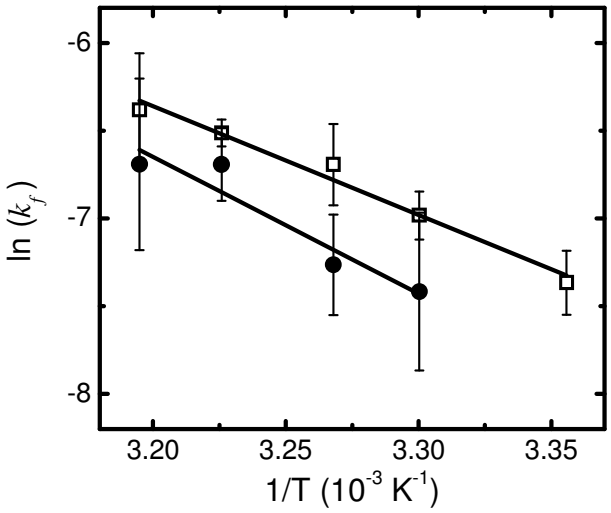

Figure II.8: Translocation rate constants for CPZ in membranes prepared from pure POPC (●) and POPC:POPS 9:1 (□). The lines are the best fit of the absolute rate theory with ΔH = 62 and 49 kJ mol^{-1} for translocation in POPC and POPC:POPS (9:1), respectively.

The experiments following the developed methodology have been repeated at different temperatures, allowing the calculation of the thermodynamic parameters associated with the formation of the transition state in translocation. The results obtained are shown in Figure II.8 and Table II.1 and indicate that the slower translocation in POPC bilayers is due to a larger enthalpy variation between the ligand in the inserted and in the transition state (it should be noted that the uncertainty associated with those parameters is very high,

due both to the large errors at each temperature and to the small temperature range studied). The entropy variation associated with the formation of the transition state in the translocation process is negative for both membranes, indicating that the bilayer is less disordered when CPZ is located in the bilayer center as compared to CPZ inserted in the leaflets. Similar results have been obtained before for ligands structurally very distinct from the membrane-forming lipids and were interpreted as evidence for the formation of defects in the membrane around the inserted ligand. The effects now observed for CPZ are far more significant than previously obtained for fatty amines and phospholipids (Cardoso et al., 2011; Moreno et al., 2006) because CPZ inserted in the bilayer has the bulky aromatic rings at the carbonyl region (Kuroda and Kitamura, 1984), creating a large defect below, in the acyl chain region of the bilayer. Smaller entropies in the translocation transition state have also been observed for bilirubin in POPC bilayers (Zucker, 1999).

When translocation is slower than equilibration between the aqueous and lipid phases, a situation encountered for CPZ in all membrane compositions studied, the permeability coefficient may be calculated from the partition coefficient and translocation rate constant (Moreno et al., 2006; Laidler et al., 1949; Zwolinski et al., 1949; Flewelling et al., 1986):

$$P = k_f \lambda K_P \qquad \text{eq. II.9}$$

where λ is required to convert the ligand concentration from volume to surface units (in the calculations, λ was equal to the radius of the solute, 3.5 Å for the case of CPZ).

The values obtained for the permeability coefficients of CPZ at 25 °C are $P_{POPC} = 1.6 \times 10^{-7}$ cm s^{-1}, $P_{POPC:POPS} = 3.2 \times 10^{-7}$ cm s^{-1}, and $P_{POPC:Chol:POPS} \leq 1 \times 10^{-7}$ cm s^{-1}, and the increase in the temperature to 37 °C leads to a 2-fold increase in the permeability coefficient for both POPC and POPC:POPS membranes. This permeability coefficient is similar to that reported for the hydrophobic ion TPP^+ (tetraphenylphosphonium), $P_{EggPC} \approx 2.0 \times 10^{-8}$ cm s^{-1} (Flewelling et al., 1986). The complete charge delocalization occurring in TPP^+ results in a much faster translocation as compared to CPZ, but this is overcompensated by a much smaller partition coefficient (Flewelling et al., 1986), leading to a similar permeation coefficient.

Permeability coefficients for CPZ across cell monolayers has been measured in vitro, being equal to 2×10^{-8} cm s^{-1}, for confluent MDCK cell monolayers at 37 °C, when measured as the rate of drug entering the receiver container (Sawada et al., 1994). Significantly larger

permeability coefficients are encountered when permeation is evaluated from the rate of drug disappearance from the donor container (Sawada et al., 1994). However, in this case, it is not transcellular permeation that is being followed but rather the rate of interaction between the drug and the cell monolayer. The permeability coefficient calculated in this work is comparable to that obtained in vitro for MDCK cell monolayers. The faster permeation coefficient obtained for the POPC bilayer is due to the larger fluidity of this model membrane as compared to the apical membrane of MDCK cells that are enriched in sphingomyelin and cholesterol (Simons et al., 1985; Simons et al., 2004).

Effect of CPZ Translocation on the Calculated Partition Coefficient

To analyze the thermograms obtained due to addition of lipid to the ligand, a value must be assumed for the accessibility factor of the lipid (and for both lipid and ligand in the case of the release protocol). In the first section of this work, we have studied the effect of ligand concentration on the observed partition coefficient at 25 °C assuming $\gamma = 0.5$, an approximation that was supported by the positive charge in CPZ and by the global fit to the results following the uptake and release protocols. Given the quantitative characterization of the translocation step using the methodology developed in this work, the value of this parameter at 25 °C may be calculated giving $k_f = 3.9 \times 10^{-4}$ s^{-1}. After the 200 s of each injection, only 8% of the equilibrium value of CPZ in the inner monolayer is attained, further supporting the assumption of slow translocation. It should be noted, however, that equilibrium between the outer and inner monolayer proceeds throughout the titration (≈3600 s), and even those small rates of translocation will influence the estimated partition coefficient.

Partial translocation may be included in the calculation of the amount of ligand associated with the bilayer by explicitly considering the outer and the inner leaflets, according to eq. II.10-II.13.

The amount of ligand in the outer monolayer at the beginning of the injection (t = 0) and at the end of injection *i* (t = δ) is given by:

$$n^{\text{out}}_{\text{CPZ\_L}}\Big|_{t=0}(i) = n^{\text{out}}_{\text{CPZ\_L}}\Big|_{t=\delta}(i-1)\left\{1+\frac{V(i)}{V_{\text{cell}}}\right\}$$

$$n^{\text{out}}_{\text{CPZ\_L}}\Big|_{t=\delta}(i) = \frac{\left\{n_{\text{CPZ\_T}}(i) - n^{\text{in}}_{\text{CPZ\_L}}\Big|_{t=\delta}(i)\right\} K_{\text{P}}\overline{V_{\text{L}}}[\text{L}]^{\text{out}}}{1+K_{\text{P}}\overline{V_{\text{L}}}[\text{L}]^{\text{out}}} \qquad \text{eq. II.10}$$

and the amount of ligand in the inner monolayer at the beginning and end of the injection is given by:

$$n^{\text{in}}_{\text{CPZ\_L}}\Big|_{t=0}(i) = n^{\text{in}}_{\text{CPZ\_L}}\Big|_{t=\delta}(i-1)\left\{1+\frac{V(i)}{V_{\text{cell}}}\right\}$$

$$n^{\text{in}}_{\text{CPZ\_L}}\Big|_{t=\delta}(i) = n^{\text{in}}_{\text{CPZ\_L}}\Big|_{t=\infty}(i)+\left\{n^{\text{in}}_{\text{CPZ\_L}}\Big|_{t=0}(i)-n^{\text{in}}_{\text{CPZ\_L}}\Big|_{t=\infty}(i)\right\}e^{-\beta\delta} \qquad \text{eq. II.11}$$

$$\text{with} \quad n^{\text{in}}_{\text{CPZ\_L}}\Big|_{t=\infty}(i) = n_{\text{CPZ\_T}}(i)\times\frac{K_{\text{P}}\overline{V_{\text{L}}}[\text{L}]^{\text{in}}}{1+K_{\text{P}}\overline{V_{\text{L}}}[\text{L}]^{\text{out}}+K_{\text{P}}\overline{V_{\text{L}}}[\text{L}]^{\text{in}}}$$

where the characteristic rate constant, β, is given by:

$$\beta = k_{\text{f}}\,\frac{K_{\text{P}}\overline{V_{\text{L}}}[\text{L}]^{\text{in}}}{1+K_{\text{P}}\overline{V_{\text{L}}}[\text{L}]^{\text{out}}+K_{\text{P}}\overline{V_{\text{L}}}[\text{L}]^{\text{in}}} \qquad \text{eq. II.12}$$

The moles of ligand that have partitioned to the membrane during injection *i* (responsible for the heat generated in that titration step) is given by eq. II.13:

$$\Delta n_{\text{CPZ\_L}}(i) = \left\{n^{\text{out}}_{\text{CPZ\_L}}\Big|_{t=\delta}(i)+n^{\text{in}}_{\text{CPZ\_L}}\Big|_{t=\delta}(i)\right\}-\left\{n^{\text{out}}_{\text{CPZ\_L}}\Big|_{t=0}(i)+n^{\text{in}}_{\text{CPZ\_L}}\Big|_{t=0}(i)\right\} \qquad \text{eq. II.13}$$

Under the experimental conditions of this work, low ligand concentrations, and 100 nm LUVs, the amount of lipid in the inner and outer leaflet is the same ($[\text{L}]^{\text{out}} = [\text{L}]^{\text{in}} = [\text{L}]/2$), and the observed partition coefficient may be used in the above equation, being equal for both monolayers. The time between injections was 200 s, and this interval was considered for the calculation of the heat per injection (δ = 200 s).

With the above equations, it is possible to evaluate the effect of the rate of translocation on the calculated parameters. For titrations performed at 25 °C, the inclusion of partial translocation in the model did not significantly affect the values obtained for both $K_{\text{P}}^{\text{obs}}$ and ΔH as compared to those obtained without translocation. The values shown in Table II.1 (using the observed accessibility factor) and in Table II.2 (imposing γ = 0.5) are slightly different from those indicated in the first section of this work because they included all titrations performed that lead to a lipid:CPZ_L ratio above 25 at the first 10 μL injection

using $[CPZ]_T$ from 5 to 15 μM and a lipid concentration in the syringe from 5 to 15 mM (over 10 titrations at each temperature), while in the previous section only the titrations with 2.5 and 5 μM CPZ and 5 mM POPC were considered. The less restrictive rule used throughout the work generated a small decrease in the value of K_P^{obs} obtained.

Table II.2: Equilibrium parameters obtained for the partition of CPZ to the different membranes studied using a simple partition model and after correction for the electrostatic effects.

		Simple Model			Corrected for electrostatic interactions		
	T (ºC)	K_P^{obs} (10^4)	ΔH (kJ mol^{-1})	TΔS (kJ mol^{-1})	K_P (10^4)	ΔH (kJ mol^{-1})	TΔS (kJ mol^{-1})
POPC	25	1.3 ± 0.1	- 15 ± 2	9	1.5 ± 0.4	- 13 ± 1	11
	37	1.4 ± 0.2	- 14 ± 1	10	1.4 ± 0.3	- 13 ± 1	12
POPC:POPS (9:1)	25	1.5 ± 0.3	- 23 ± 3	1	1.0 ± 0.3	- 21 ± 3	1
	37	1.3 ± 0.3	- 28 ± 6	- 4	0.9 ± 0.2	- 27 ± 3	- 3
POPC:Chol:POPS (6:3:1)	25	0.68 ± 0.03	- 5 ± 1	17	0.61 ± 0.03	- 4 ± 1	18
	37	0.63 ± 0.08	- 14 ± 2	8	0.41 ± 0.04	- 12 ± 2	10

[a] The accessibility factor considered was 0.5 (corresponding to slow CPZ translocation).

The values obtained for the partition parameters at 37 °C are somewhat more sensitive to the model used due to the occurrence of significant translocation during the titration. Figure II.9 shows the best fit of the extreme situations (γ = 0.5 and 1) to a titration profile calculated with the average values of the parameters for CPZ interaction with POPC bilayers at 37 °C ($k_f = 1.0 \times 10^{-3}$ s^{-1}, $K_P^{obs} = 1.0 \times 10^4$, and ΔH = − 11 kJ mol^{-1}). The two extreme situations lead exactly to the same shape for the titration curve although with different parameters (K_P^{obs} is reduced to one-half when fast translocation is considered). There is a clear misfit of the extreme models to the last part of the titration, although it should be noted that when experimental noise is added the distinction between the models could not be done on the basis of a better fit. The deviations observed result from the significant additional heat evolved between 15 and 50 min (injections 5−15) due to translocation of CPZ (with a characteristic time, $\tau_f = 1/k_f$, equal to 17min) inserted into the outer monolayer in the first injections (over 75% CPZ is associated with the bilayer after injection 6).

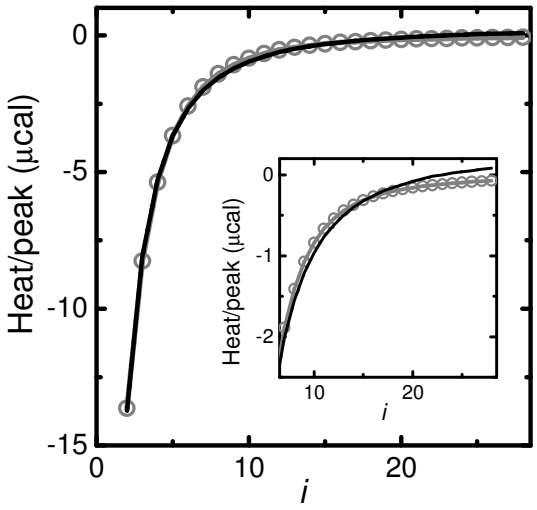

Figure II.9: Effect of translocation on the shape of the titration curve. The best fit of a typical titration of 15 μM CPZ with 15 mM POPC at 37 °C is shown in gray (○), and the best fit with very slow and very fast translocation is show in black. The inset shows a closer view of the end of titration to highlight the misfit. The gray curve was obtained with the average values for the parameters (Table I.1): $k_f = 1.0 \times 10^{-3}$ s^{-1}, $K_P^{obs} = 1.0 \times 10^4$, and $\Delta H = -11$ kJ mol^{-1}. The best fit of the two extreme conditions has exactly the same shape but different values for the parameters: $k_f = 0$ s^{-1}, $K_P^{obs} = 9.6 \times 10^3$, and $\Delta H = -13$ kJ mol^{-1} (black line) and $k_f = 3.0 \times 10^{-2}$ s^{-1}, $K_P^{obs} = 4.8 \times 10^3$, and $\Delta H = -13$ kJ mol^{-1} (black line).

In the first section of this work, we report a small but significant increase in the intrinsic partition coefficient of CPZ to POPC membranes at lipid:CPZ molar ratios smaller than 10, Figure II.3 plot A. This increase was interpreted as an overcorrection of the electrostatic effects using the Gouy−Chapman theory. The increase observed in K_P may also result from variations in the rate of CPZ translocation at those high local concentrations, an increase in the rate of translocation leading to an accessibility factor larger than the assumed value of 0.5. In fact, the rate of translocation of 50 μM CPZ when titrated with 5 mM POPC (leading to L:CPZ_L equal to 6 after the first 10 μL injection) was sufficiently fast to be measured at 25 °C using the methodology developed in this work and is equal to 2.0×10^{-3} s^{-1} (5 times faster than obtained for smaller local concentrations of CPZ). This result supports the qualitative observation of increased lipid scrambling in the presence of relatively high CPZ concentrations (Ahyayauch et al., 2010; Rosso et al., 1988; Schrier et al., 1992).

The titrations performed with POPC and with POPC:POPS (9:1), at a lipid to ligand ratio above 25 in the first 10 μL injection, were analyzed with eq. II.10-II.13 taking into account the observed value for the translocation rate constant. The parameters obtained are shown in Table II.1.

A small decrease in K_P^{obs} is observed when the temperature is increased from 25 to 37°C for the association of CPZ with both membranes, as predicted for an exothermic process. The thermodynamic parameters obtained indicate that partitioning to the POPC membrane has significant contributions from both enthalpy and entropy, while interaction with the negatively charged membrane is dominated by the enthalpic term.

The value of K_P^{obs} obtained for partitioning to the negatively charged membrane is only slightly higher than that for partitioning to the POPC membrane. This result was unexpected due to the electrostatic interaction between CPZ and the negatively charged membrane, but is in agreement with the reported small increase observed in EggPC:EggPS 9:1 membranes (Takegami et al., 2005). The thermodynamic parameters obtained in this work allow an interpretation of this result. Relatively small increase in the Gibbs free energy associated with partition of CPZ to the charged membranes is due to a decrease in the entropy contribution that almost balances the more favourable enthalpy contribution observed in the negatively charged membrane. Given that an increase in entropy is expected when CPZ partitions to the membrane, due to the hydrophobic effect, this result points toward a reduction of the entropy of the POPC:POPS membrane upon partition of CPZ. This corroborates CPZ perturbation of the (already nonideal) mixing of the two lipids and with the problems encountered with the titrations performed according to the release protocol. From the temperature variation observed for the partition coefficient, the van't Hoff enthalpy may be calculated to be −12 and −5 kJ mol^{-1} for the POPC and POPC:POPS membranes, respectively. The disagreement between the van't Hoff and the calorimetric enthalpy obtained for the charged membrane further supports the occurrence of additional processes in this membrane upon partition of CPZ. The interaction between the head groups of phosphatidyl serine lipids is relatively strong due to the formation of hydrogen bonds, but the electrostatic repulsion between the negatively charged lipids prevents their phase separation in the mixed membranes (Huang et al., 1993) Changes in the electrostatic potential of the bilayer may affect their phase behaviour. We speculate that the cationic ligand CPZ induces POPS clustering (and eventually phase separation) in the POPC:POPS 9:1 membrane.

The comparison between the affinities of CPZ for both membranes is more easily done after deconvolution of the observed partition coefficient into the electrostatic and hydrophobic contributions. This may be done through the computation of the intrinsic partition coefficient (K_P), via eq. II.4 and II.5, and will be performed in the next section

together with the results obtained for the additional membrane composition studied (POPC:Chol:POPS 6:3:1).

Effect of Lipid Composition in the Interaction of CPZ with Lipid Bilayers

Table II.2 summarizes the parameters obtained for the interaction of CPZ with all membranes studied. The best fit of the simple model (eq. II.1-II.3) provides the observed partition coefficient, K_P^{obs}, and enthalpy variation allowing the comparison between the different membranes in terms of the effective amount of CPZ that associates with them at the experimental conditions used (lipid:CPZ_L ≥ 25 at the first titration step). In this model, the interaction is interpreted globally, without distinction between the contributions from hydrophobic and electrostatic interactions. To compare charged and neutral membranes, it is preferable to separate the two types of interactions, and this may be done through the calculation of the intrinsic partition coefficient, K_P, where the electrostatic interactions have been taken into account explicitly using the Gouy–Chapman theory (eq. II.4 and II.5). It is not possible to consider partial translocation (according to the model developed in this work) and correction for electrostatic effects due to the different values of the effective partition coefficient and rate of translocation that would be required for the inner and outer leaflet. The required model to account for this situation is too complex, and with too many unknown variables, to be of practical utility. For all membranes and temperatures studied, the approximation of slow translocation was always closer to the observed behaviour, and therefore the parameters shown in Table II.2 after correction for the electrostatic effects have all been calculated assuming $\gamma = 0.5$.

The comparison of the partition coefficient obtained from the two models for CPZ interaction with the zwitterionic POPC membrane indicates that even with the small concentrations of CPZ used (5–15 μM), the charge imposed by CPZ in the membrane is still significant. The POPC:CPZ_L ratios varied from ≈ 30 to over 100 at the end of the titration being typically around 50 at 50% ligand titrated. At this local concentration of CPZ, the calculated surface potential is 9 mV, originating a reduction in the observed partition coefficient of nearly 20%, according to eq. II.4.

The electrostatic contributions in the case of membranes containing POPS are of two types: (i) electrostatic attraction between the negatively charged membrane and the cationic CPZ,

and (ii) change in the membrane charge due to the presence of CPZ. The two effects have been taken into account in the model by using both CPZ and POPS charges in eq. II.5. In the absence of CPZ, the calculated surface potential of the membranes with 10% POPS is equal to −26 mV, and for the typical ratios at 50% titration the surface potential is reduced to −21 mV, both conditions leading to an attractive electrostatic interaction between CPZ and the membrane surface. The ζ potentials of POPC:POPS (9:1) liposomes with and without CPZ were also measured and were in qualitative agreement with those calculated for the surface potential using the Gouy−Chapman theory (see Material and Methods). The exclusion of this electrostatic interaction leads to a reduction in the calculated intrinsic partition coefficient (K_P) that is smaller than the observed partition (K_P^{obs}) for those negatively charged membranes (Table II.2).

Comparing the intrinsic partition coefficients obtained for POPC and POPC:POPS, the hydrophobic contribution to solvation of CPZ by the lipid bilayer is smaller for the charged membrane. This suggests a more superficial location for CPZ when associated with negatively charged membranes (Agasosler et al., 2001).

Cholesterol insertion in the membrane leads to a reduction in both the partition coefficient and the interaction enthalpy. Although the characterization of CPZ partition to POPC:Chol 7:3 membranes by ITC was attempted, the heat change involved was too small. This corroborates the results obtained for the interaction of other ligands with POPC:Chol membranes (McIntosh et al., 2001; Estronca et al., 2007) and highlights the poor salvation properties of those ordered membranes. The addition of POPS to the bilayer increases the heat change involved in the interaction, allowing its characterization by ITC, due to the electrostatic interaction between CPZ and the negatively charged membrane. The comparison between the results obtained with POPC:POPS and POPC:Chol:POPS indicates a decrease in the partition coefficient to nearly one-half due to the addition of cholesterol. This result is in excellent agreement with published results for the effect of 30% cholesterol in EggPC membranes (Takegami et al., 1999). The temperature variation of the interaction enthalpy with membranes containing 10% POPS and 30% cholesterol is even more accentuated than that observed for POPC:POPS 9:1. This result reinforces the interpretation that, at low temperatures, POPS and POPC do not mix well in the presence of CPZ and indicates that this effect is accentuated by the presence of cholesterol in the membrane.

Conclusions

In this chapter, we have developed methodology, which allows the quantitative characterization of the translocation of ligands through lipid bilayers using the ITC technique. This complements the available protocols for describing qualitatively this process (Tsamaloukas et al., 2007). The rate of translocation of CPZ through the membranes in the liquid disorder phase has been measured: 3.9×10^{-4} and 6.6×10^{-4} s^{-1} for POPC and POPC:POPS 9:1, respectively, at 25 °C and nearly twice as large at 37 °C. Together with the partition coefficient measured, this allows the calculation of the permeability coefficient, which is equal to 2.0×10^{-7} cm s^{-1} for POPC, 3.9×10^{-7} cm s^{-1} for POPC:POPS 9:1, and smaller than 5.0×10^{-8} cm s^{-1} for POPC:Chol:POPS 6:3:1 membranes at 37 °C. The values obtained are similar to that reported for other hydrophobic cations (Flewelling et al., 1986) and to that observed in vitro for permeation through MDCK cell monolayers (Sawada et al., 1994). Local concentrations of CPZ in the POPC membrane above 10 mol % lead to an increase in the rate of CPZ translocation, which may be explained by the increased lipid scrambling (Ahyayauch et al., 2010; Rosso et al., 1988; Schrier et al., 1992) and may be of relevance to the observed suppression of multi drug resistance (Wadkins et al., 1993; Michalak et al., 2006; Hendrich et al., 2003) by high CPZ concentrations.

The introduction of negative charge in the membrane leads only to a small increase in the observed partition coefficient (1.3×10^4 and 1.5×10^4 for POPC and POPC:POPS 9:1, respectively). This is due to the much smaller entropy variation observed for partition to the negatively charged membrane that almost counterbalance the more favourable enthalpy variation due to the electrostatic interaction between CPZ and the membrane. This and other unexpected observations and results obtained for the membranes containing POPS suggest that CPZ may be inducing some changes in the phase behaviour of the membranes, eventually leading to POPS clustering or phase separation, even at the low local concentrations used in this work.

The addition of cholesterol to the POPC bilayer reduces the affinity of CPZ to the membrane, which becomes essentially driven by entropy and therefore inaccessible by ITC. The addition of POPS to the membrane increases the interaction enthalpy and allowed the characterization of the partition of CPZ to POPC:Chol:POPS 6:3:1 membranes. The partition coefficient obtained was reduced by 50% due to the presence of cholesterol and the consequent ordering of the lipid bilayer. The translocation of CPZ through those

membranes was too slow to be measured using the available methodology, and only an upper limit may be established, $k_f \leq 4 \times 10^{-4}$ s^{-1}.

References

Abraham, M. H. (2011) The permeation of neutral molecules, ions and ionic species through membranes: brain permeation as an example. J. Pharm. Sci. 2011, 100, 1690−1701

Agasosler, A. V., Tungodden, L. M., Cejka, D., Bakstad, E., Sydnes, L. K. and Holmsen, H. (2001) Chorpromazine-induced increase in dipalmitoylphosphatidylserine surface area in monolayers at room temperature. *Biochemical Pharmacology*, 61, 817−825

Ahyayauch, H., Bennouna, M., Alonso, A. and Goni, F. M. (2010) Detergent effects on membranes at subsolubilizing concentrations: transmembrane lipid motion, bilayer permeabilization, and vesicle lysis/reassembly are independent phenomena. *Langmuir*, 26, 7307−7313

Attwood, D., Boitard, E., Dubes, J. P. and Tachoire, H. (1992) Apparent molar enthalpies of amphiphilic drugs in aqueous solution. Journal of Physical Chemistry, 96, 11018-11021

Attwood, D., Waigh, R., Blundell, R., Bloor, D., Thevand, A., Boitard, E., Dubes, J. P. and Tachoire, H. (1994) ^{1}H and ^{13}C NMR studies of the self-association of chlorpromazine hydrochloride in aqueous solution. Magnetic Resonance in Chemistry, 32, 468-472

Attwood, D. (1995) The mode of association of amphiphilic drugs in aqueous solution. *Advances in Colloid and Interface Science*, 55, 271−303

Beschiaschvili, G. and Seelig, J. (1992) Peptide binding to lipid bilayers. Nonclassical hydrophobic effect and membrane-induced p*K* shift. *Biochemistry*, 31, 10044-10053

Cardoso, R. M. S., Martins, P. A. T., Gomes, F., Doktorovova, S., Vaz, W. L. C. and Moreno, M. J. (2011) Chain-length dependence of insertion, desorption and translocation of a homologous series of 7-nitrobenz-2-3-diazol-4-yl-labeled aliphatic amines in membranes. *Journal of Physical Chemistry B*, 115, 10098−10108

Chakrabarti, A. C. (1994) Permeability of membranes to amino-acids and modified amino-acids – Mechanisms involved in translocation. *Amino Acids*, 6, 213-229

do Canto, A., Carvalho, A. J. P., Ramalho, J. and Loura, L. M. S. (2011) Molecular dynamics simulations of T-20 HIV fusion inhibitor interacting with model membranes. *Biophysical Chemistry*, 159, 275-286

Estronca, L. M. B. B., Moreno, M. J. and Vaz, W. L. C. (2007) Kinetics and thermodynamics of the association of dehydroergosterol with lipid bilayer membranes. *Biophysical Journal*, 93, 4244–4253

Flewelling, R. F. and Hubbell, W. L. (1986) Hydrophobic ion interactions with membranes. Thermodynamic analysis of tetraphenylphosphonium binding to vesicles. *Biophysical Journal*, 49, 531–540

Hanpft, R. and Mohr, K. (1985) Influence of cationic amphiphilic drugs on the phase transition temperature of phospholipids with different polar headgroups. *Biochimica et Biophysica Acta*, 814, 156–162

Heerklotz, H. H., Binder, H. and Epand, R. M. (1999) A "release" protocol for isothermal titration calorimetry. *Biophysical Journal*, 76, 2606–2613

Heerklotz, H. (2004) The microcalorimetry of lipid membranes. *Journal of Physics: Condensed Matter*, 16, R441–R467

Heerklotz, H. (2008) Interactions of surfactants with lipid membranes. *Quarterly Reviews of Biophysics*, 41, 205–264

Hendrich, A. B., Wesolowska, O., Pola, A., Motohashi, N., Molnar, J. and Michalak, K. (2003) Neither lipophilicity nor membrane-perturbing potency of phenothiazine maleates correlate with the ability to inhibit P-glycoprotein transport activity. *Molecular Membrane Biology*, 20, 53-60

Hidalgo, A. A., Caetano, W., Tabak, M. and Oliveira, O. N. (2004) Interaction of two phenothiazine derivatives with phospholipid monolayers. *Biophysical Chemistry*, 109, 85–104

Hornby, A. P. and Cullis, P. R. (1981) Influence of local and neutral anesthetics on the polymorphic phase preferences of egg-yolk phosphatidylethanolamine. *Biochimica et Biophysica Acta*, 647, 285-292

Huang, J. Y., Swanson, J. E., Dibble, A. R. G., Hinderliter, A. K. and Feigenson, G. W. (1993) Nonideal mixing of phosphatidylserine and phosphatidylcholine in the fluid lamellar phase. *Biophysical Journal*, 64, 413-425

Jutila, A., Soderlund, T., Pakkanen, A. L., Huttunen, M. and Kinnunen, P. K. J. (2001) Comparison of the effects of clozapine, chlorpromazine and haloperidol on membrane lateral heterogeneity. *Chemistry and Physics of Lipids*, 112, 151-163

Keller, S., Heerklotz, H., Jahnke, N. and Blume, A. (2006) Thermodynamics of lipid membranes solubilisation by sodium dodecyl sulphate. *Biophysical Journal*, 90, 4509-4521

Kitamura, K., Takenaka, M., Yoshida, S., Ito, M., Nakamura, Y. and Hozumi, K. (1991) Determination of dissociation constants of sparingly soluble phenothiazine derivatives by second.derivative spectrophotometry. *Analytica Chimica Acta*, 242, 131-135

Kitamura, K., Imayoshi, N., Goto, T., Shiro, H., Mano, T. and Nakai, Y. (1995) Second derivative spectrophotometric determination of partition coefficients of chlorpromazine and promazine between lecithin bilayer vesicles and water. *Analytica Chimica. Acta*, 304, 101-106

Kitamura, K., Goto, T. and Kitade, T. (1998) Second derivative spectrophotometric determination of partition coefficients of phenothiazine derivatives between human erythrocyte ghost membranes and water. *Talanta*, 46, 1433-1438

Kitamura, K., Takegami, S., Kobayashi, T., Makihara, K., Kotani, C., Kitade, T., Moriguchi, M., Inoue, Y., Hashimoto, T. and Takeuchi, M. (2004) Dissociation constants of phenothiazine drugs incorporated in phosphatidylcholine bilayer of small unilamellar vesicles as determined by carbon-13 nuclear magnetic resonance spectrometric titration. *Biochimica et Biophysica Acta*, 1661, 61-67

Krivanek, R., Okoro, L. and Winter, R. (2008) Effect of cholesterol and ergosterol on the compressibility and volume fluctuations of phospholipid-sterol bilayers in the critical point region: a molecular acoustic and calorimetric study. *Biophysical Journal*, 94, 3538–3548.

Kuroda, Y. and; Kitamura, K. (1984) Intra- and intermolecular ^{1}H-^{1}H nuclear overhauser effect studies on the interactions of chlorpromazine with lecithin vesicles. *Journal of the American Chemical Society*, 106, 1-6

Jing, P., Rodgers, P. J. and Amemiya, S. (2009) High lipophilicity of perfluoroalkyl carboxylate and sulfonate: implications for their membrane permeability. *Journal of the American Chemical Society*, 131, 2290-2296

Jones, M. N. (1995) The surface-properties of phospholipid liposome systems and their characterization. *Advances in Colloid Interface Science*, 54, 93-128

Kramer, S. D., Lombardi, D., Primorac, A., Thomae, A. V. And Wunderli-Allenspach, H. (2009) Lipid-bilayer permeation of drug-like compounds. *Chemistry and Biodiversity*, 6, 1900-1916

McIntosh, T. J., Vidal, A. and Simon, S. A. (2001) The energetics of binding of a signal peptide to lipid bilayers: the role of bilayer properties. *Biochemical Society Transactions*, 29, 594-598

Missner, A. and Pohl, P. (2009) 110 years of the Meyer-Overton rule: predicting membrane permeability of gases and other small compounds. ChemPhysChem, 10, 1405-1414

Laidler, K. J. and Shuler, K. E. (1949) The kinetics of membrane processes. 1. The mechanism and the kinetic laws for diffusion through membranes. *Journal of Chemical Physics*, 17, 851-855

Luna, C., Stroka, K. M., Bermudez, H. and Aranda-Espinoza, H. (2011) Thermodynamics of monolayers formed by mixtures of phosphatidylcholine/phosphatidylserine. *Colloids and Surfaces B: Biointerfaces*, 85, 293-300

Luxnat, M. and Galla, H. J. (1986) Partition of chlorpromazine into lipid bilayer membranes: the effect of membrane structure and composition. *Biochimica et Biophysica Acta*, 856, 274–282

Manuel, M. and Martins, J. (2008) Partitioning of 1-pyrenesulfonate into zwitterionic/anionic fluid phospholipid bilayers. *Chemistry and Physics of Lipids*, 154, 79-86;

Matos, C., Lima, J. L. C., Reis, S., Lopes, A. and Bastos, M. (2004) Interaction of antiinflammatory drugs with EPC liposomes: Calorimetric study in a broad concentration range. *Biophysical Journal*, 86, 946–954

Michalak, K., Wesolowska, O., Motohashi, N., Molnar, J. and Hendrich, A. B. (2006) Interactions of phenothiazines with lipid bilayer and their role in multidrug resistance reversal. *Current Drug Targets*, 7, 1095–1105

Moreno, M. J., Estronca, L. M. B. B. and Vaz, W. L. C. (2006) Translocation of phospholipids and dithionite permability in liquid-ordered and liquid-disordered membranes. *Biophysical Journal*, 91, 873-881

Moreno, M. J., Bastos, M. and Velazquez-Campoy, A. (2010) Partition of amphiphilic molecules to lipid bilayers by isothermal titration calorimetry. *Analytical Biochemistry*, 399, 44-47

Murray, D., Arbuzova, A., Hangyas-Mihalyne, G., Gambhir, A., Ben-Tal, N., Honig, B. and McLaughlin, S. (1999) Electrostatic properties of membranes containing acidic lipids and adsorbed basic peptides: theory and experiment. *Biophysical Journal*, 77, 3176-3188

Rosso, J., Zachowski, A. and Devaux, P. F. (1988) Influence of chlorpromazine on the tranverse mobility of phospholipids in the human erythrocyte membrane: relation to shape changes. *Biochimica et Biophysica Acta*, 942, 271-279

Sampaio, J. L., Moreno, M. J. and Vaz, W. L. C. (2005) Kinetics and thermodynamics of association of a fluorescent lysophospholipid derivative with lipid bilayers in liquid-ordered and liquid-disordered phases. *Biophysical Journal*, 88, 4064-4071

Sawada, G. A., Ho, N. F. H., Williams, L. R., Barsuhn, C. L. and Raub, T. J. (1994) Transcellular permeability of chlorpromazine demonstrating the roles of protein-binding and membrane partitioning. *Pharmaceutical Research*, 11, 665-673

Sawada, G. A., Barsuhn, C. L., Lutzke, B. S., Houghton, M. E., Padbury, G. E., Ho, N. F. H. and Raub, T. J. (1999) Increased lipophilicity and subsequent cell partitioning decrease passive transcellular diffusion of novel, highly lipophilic antioxidants. *Journal of Pharmacology and Experimental Therapeutics*, 288, 1317-1326

Schrier, S. L., Zachowski, A. and Devaux, P. F. (1992) Mechanisms of amphipath-induced stomatocytosis in human erythrocytes. *Blood*, 79, 782-786

Shapovalov, V. L. and Brezesinski, G. (2006) Breakdown of the Gouy-Chapman model for highly charged Langmuir monolayers. *Journal of Physical Chemistry B*, 110, 10032-10040

Simons, K. and Fuller, S. D. (1985) Cell-surface polarity in epithelia. *Annual Review of Cell Biology*, 1, 243-288

Simons, K. and Vaz, W. L. C. (2004) Model Systems, lipid rafts and cell membranes. *Annual Review of Biophysics and Biomolecular Structure*, 33, 269-295

Takegami, S., Kitamura, K., Kitade, T., Hasegawa, K. and Nishihira, A. (1999) Effects of particle size and cholesterol content on the partition coefficients of chlorpromazine and triflupromazine between phosphatidylcholine-cholesterol bilayers of unilamellar vesicles and water studied by second-derivative spectrophotometry. *Journal of Colloid and Interface Science*, 220, 81−87

Takegami, S., Kitamura, K., Kitade, T., Kitagawa, A. and Kawamura, K. (2003) Thermodynamics of partitioning of phenothiazine drugs between phosphatidylcholine bilayer vesicles and water studied by second-derivative spectrophotometry. *Chemical and Pharmaceutical Bulletin*, 51, 1056-1059

Takegami, S., Kitamura, K., Kitade, T., Takashima, M., Ito, M., Nakagawa, E., Sone, M., Sumitani, R. and Yasuda, Y. (2005) Effect of phosphatodylserine and phosphatidylethanolamine content on partitioning of triflupromazine and chlorpromazine between phosphatidylcholine-aminophospholipid bilayer vesicles and water studied by second-derivative spectrophotometry. *Chemical and Pharmaceutical Bulletin*, 53, 147−150

Tan, A. M., Ziegler, A., Steinbauer, B. and Seelig, J. (2002) Thermodynamics of sodium dodecylsulphate partitioning into lipid membranes. *Biophysical Journal*, 83, 1547-1556

Tatulian, S. A. (1987) Binding of alkaline-earth metal-cations and some anions to phosphatidylcholine liposomes. *European Journal of Biochemistry*, 170, 413-420

Thomae, A. V., Wunderli-Allenspach, H. and Kramer, S. D. (2005) Permeation of aromatic carboxylic acids across lipid bilayers: the pH-partition hypothesis revisited. *Biophysical Journal*, 89, 1802-1811

Thomae, A. V., Koch, T., Panse, C., Wunderli-Allenspach, H. and Kramer, S. D. (2007) Comparing the lipid membrane affinity and permeation of drug-like acids: the intriguing effects of cholesterol and charged lipids. *Pharmaceutical Research*, 24, 1457-1472

Torrie, G. M. and Valleau, J. P. (1982) Electrical double layers. 4. Limitations of the Gouy-Chapman theory. *Journal of Physical Chemistry*, 86, 3251−3257

Tsamaloukas, A. D., Keller, S. and Heerklotz, H. (2007) Uptake and release protocol for assessing membrane binding and permeation by way of isothermal titration calorimetry. *Nature Protocols*, 2, 695-704

Wadkins, R. M. and Houghton, P. J. (1993) The role of drug-lipid interactions in the biological activity of modulators of multi-drug resistance. *Biochimica et Biophysica Acta*, 1153, 225-236

Wajnberg, E., Tabak, M., Nussenzveig, P. A., Lopes, C. M. B. and Louro, S. R. W. (1988) pH dependent phase transition of chlorpromazine micellar solutions in the physiological range. *Biochimica et Biophysica Acta*, 944, 185-190

Welti, R., Mullikin, L. J., Yoshimura, T. and Helmkamp, G. M. (1984) Partition of amphiphilic molecules into phospholipid vesicles and human erythrocyte ghosts: measurements by ultraviolet difference spectroscopy. *Biochemistry*, 23, 6086-6091

Wiener, M. C. and White, S. H. (1992) Structure of a fluid dioleoylphosphatidylcholine bilayer determinedby joint refinement of x-ray and neutron diffraction data. *Biophysical Journal*, 61, 428–433

Zucker, S. D., Goessling, W. and Hoppin, A. G. (1999) Unconjugated bilirubin exhibits spontaneous diffusion through model lipid bilayers and native hepatocyte membranes. *Journal of Biological Chemistry*, 274, 10852-10862

Zwolinski, B. J., Eyring, H. and Reese, C. E. (1949) Diffusion and membrane permeability. *Journal of Physical and Colloid Chemistry*, 53, 1426-1453

Chapter III

Chlorpromazine interaction with representative lipid membranes of the blood brain barrier endothelium

Introduction

As described in Chapter I, the lipid distribution in biological membranes is asymmetric between the inner and outer monolayers. This lipid asymmetry is generated by the asymmetric synthesis and insertion of lipids in the membranes and maintained by ATP dependent systems. One of the most relevant lipid asymmetries in eukaryotic cell membranes is the enrichment of sphingolipids, as well as depletion of phosphatidylethanolamine and the negatively charged phosphatidylserine and phosphatidylinositol, in the extracellular leaflet (Fisher, 1976, Rothman and Lenard, 1977; Op den Kamp, 1979; Devaux, 1992; Lehninger et al., 1997; Marrink et al, 2007).

The lipid asymmetry in the erythrocyte was the first biological membrane characterized, by Bretscher (1972), which proposed that phosphatidylethanolamine and phosphatidylserine are mainly in the cytoplasmic monolayer of the bilayer and phosphatidylcholine and sphingomyelin comprise the external monolayer.

Cholesterol distribution is still controversial (Devaux and Morris, 2004; Daleke, 2007): some authors defend it is enriched in the extracellular leaflet of plasma membranes due to its high affinity for sphingolipids (vanMeer, 2009) but it has been reported to be evenly present in both leaflets (Bloj and Zilversmit, 1976; Wydro, 2007). The fast translocation of Chol imposes that its distribution between both monolayers is close to equilibrium.

Lipid-lipid immiscibility in the plane of the bilayer, leads to microscopic lipid domains within membranes, defined as small regions with distinct physical properties and composition. These distinct membrane domains are called “rafts” enriched in certain lipids, cholesterol and proteins (Simons and Vaz, 2004).

Another kind of asymmetry comprises the differences in composition between the apical and the basolateral membranes from polarized cells (epithelial and endothelial).

To mimetize membranes composing the endothelial cells that constitute tight epithelia such as the BBB, the lipid mixtures choosen were POPC:SpM:Chol (1:1:1) for the external leaflet and POPC:Chol:POPE:POPS (4:3:2:1) for the internal leaflet.

Ternary phase diagram for POPC:SpM:Chol

Three components mixtures containing cholesterol, one phospholipid having a relatively high Tm and another phospholipid having a relatively low Tm, are widely used as model for the

outer leaflet of animal cell membranes, as they contain representative compounds from each of the three major lipid groups (Feigenson, 2006).

Since they embody the essential features of the lipid component of raft-containing membranes, ternary mixtures of SpM, POPC and Chol have drawn a lot of attention during the last decade and the determination of phase diagrams of POPC:SpM:Chol ternary systems has been a topic of major interest. At some proportions of the constituent lipids, those membranes have coexistence of two liquid phases – a liquid-ordered phase (enriched in SpM) and a liquid-disordered phase (de Almeida et al., 2003; Veatch and Keller, 2005; Pokorni et al., 2006; Ionova et al., 2012). Because the high-melting lipid component is a sphingolipid and the low-melting lipid component is a sn-2 unsaturated phosphatidylcholine, it closely resembles a natural membrane lipid composition and has come to be considered the canonical raft–lipid mixture (Marsh, 2009).

The first temptative phase diagram for this ternary mixture was published by de Almeida and co-workers (2003) (Figure III.1) being followed by others (Veatch and Keller, 2005; Ionova et al., 2012) (See Figure III.2). All studies confirmed the coexistence of liquid-disordered (L_α) and liquid-ordered (L_o) phases at some lipid compositions although significant disagreement exists regarding the placement of phase boundaries. The phase diagrams show a three phase triangle ($L_\alpha + L_o + L_\beta$) and a region of fluid-fluid ($L_\alpha + L_o$) coexistence, in addition to two regions of gel-fluid coexistence ($L_\alpha + L_\beta$ and $L_o + L_\beta$) that extend to the axes for the binary mixtures. It should be noted that the coexistence of three phases has never been demonstrated directly: the three-phase triangle is indirectly inferred on thermodynamic grounds.

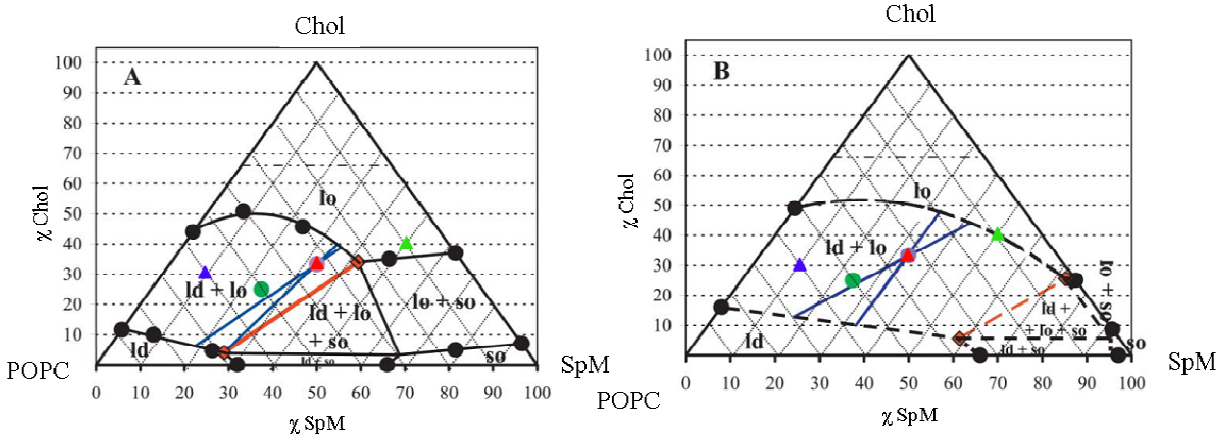

Figure III.1: Phase diagram for ternary mixtures of POPC, SpM and Chol, at (A) 23 ºC and (B) 37 ºC. The red, blue and green triangles mark the 1:1:1, 6:1:3 and 1:5:4 compositions studied during the work done for this manuscript. According to de Almeida et al. (2003) the red (quasi) tie-line describes the l_o/l_d composition at the right of which there is also s_o phase, the blue tie-lines are the interval for the possible tie-line that contain the 1:1:1 composition and the green circle marks the 1:2:1 composition. Image adapted from de Almeida et al. (2003).

The discrepancies between these phase diagrams for the same ternary mixture, at the same temperature, may be attributed, on one hand, to the different experimental methods that are used to determine the phase boundaries, and, on the other hand, to uncertainties in inference of the three-phase region. The most significant qualitative differences between them is that the region of fluid-fluid coexistence ($L_\alpha + L_o$) extends out to the binary mixture POPC:Chol in the phase diagram from de Almeida et al. (2003) but not on the following studies. Another important discrepancy is related with the maximal fraction of cholesterol in this coexistence region which is around 0.5 in the first study but doesn't go above 0.3 on the phase diagrams from Veatch et al. (2005) and Ionova et al. (2012).

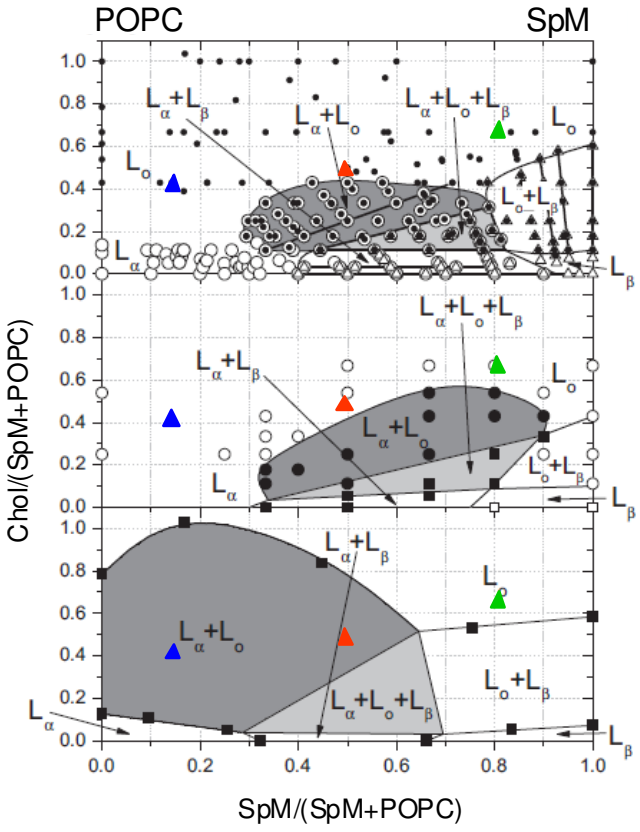

Figure III.2: Phase diagrams for the ternary mixtures of POPC, SpM and Chol at 23 ºC, with rectilinear coordinates: the abscissa is the mole fraction of PSM solely with respect to phospholipid and the ordinate is the mole ratio of cholesterol to total phospholipid. The region of two coexisting fluid phases is shaded grey and that of three-phase coexistence is shaded light grey. The red, blue and green triangles mark the 1:1:1, 6:1:3 and 1:5:4 compositions. Top: Data obtained with spin-label EPR, from Ionova et al. (2012) Middle: Data obtained with fluorescence microscopy of giant vesicles, from Veatch and Keller (2005) Bottom: Data obtained with fluorescence polarization of diphenylhexatriene and fluorescence life-times of *trans*-parinaric acid, from de Almeida et al. (2003). Image adapted from Ionova et al. (2012).

The coexistence of L_α-L_o in binary mixtures of POPC and Chol, indicated in the phase diagram from de Almeida et al. (2003), is not universally accepted and has been contested by

various laboratories (Filippov et al., 2003; Greenwood et al., 2006; Estronca et al., 2007; Veatch and Keller, 2005; Konyakhina et al., 2011; Ionova et al., 2012). Evidence for L_α-L_o coexistence in this binary mixture, at 23 °C and above, is indirect, resting upon theoretically expected linear dependences for the fluorescence polarization of diphenyl hexatriene and the mean fluorescence lifetime of trans-parinaric acid on the mole fraction of cholesterol in a two-phase region (de Almeida et al., 2003) and also on the fluorescence polarization and biphasic distribution of fluorescence lifetimes for trans-parinaric acid (Mateo et al., 1995). Fluid-fluid phase separation in POPC:Chol mixtures might not have been detected in the work of Veatch and Keller (2005), because the domains may be too small for light microscopy. This size limitation does not apply, however, to spin-label EPR studies used by Ionova et al. (2012). Indeed, L_α-L_o phase coexistence has been detected by spin-label EPR in binary mixtures of SpM and cholesterol (Collado et al., 2005), where none is seen by fluorescence microscopy. The formation of 2D micelles in the plane of the membrane, has been alternatively proposed for POPC:Chol binary mixtures (Estronca et al., 2007), with Chol representing the 2D core with the POPC molecules oriented such that the saturated acyl chain faces the sterol and the unsaturated point towards the outer part of the 2D micelle. Since the components of the putative micelles would be in rapid equilibrium with the bulk lipid phase of the bilayers, this would be a case of microscopic heterogeneity, thermodynamically quite distinct from a phase separation.

In the phase diagrams described by Veatch and Keller (2005) and Ionova et al. (2012) (Figure III.2, top and middle) the position of the L_α-L_o phase coexistence and of the three phase triangle is in good agreement and the major difference between these two phase diagrams is the placement of the boundaries defining the L_o-L_β phase coexistence. However, in the work done by Veatch and Keller (2005) the L_o-L_β phase boundaries were inferred rather than identified by fluorescence microscopy.

Results and Discussion

Partition into membranes representative of the outer monolayer

With the objective of determining the partition of CPZ into membranes representative of the outer monolayer of the endothelium, we studied the interaction of CPZ with POPC membranes containing sphingomyelin and cholesterol with the molar proportions 1:1:1. Experiments were performed by injecting aliquots of Pc:SpM:Chol (1:1:1) (from now on

named PcSC 111) at 45 mM into buffer containing 30 μM CPZ. Given the presence of SpM, a small rate of translocation is anticipated (Sampaio et al., 2005; Moreno et al., 2006), and therefore the accessibility factor was assumed to be 0.5. The results obtained are shown in Figure III.3.

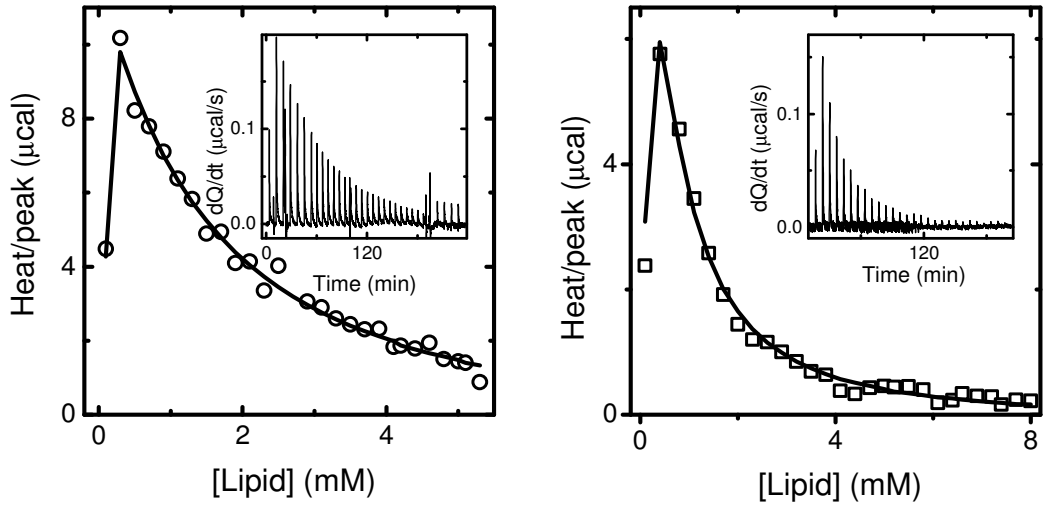

Figure III.3: Typical titration curves obtained for the titration of CPZ at 30 μM with membranes composed of POPC:SpM:Chol (1:1:1) at 45 mM for (A) 25 ºC and (B) 37 ºC. Experimental thermograms are shown in the Insets. The lines are the best fit obtained with eqs II.1-II.5 (See Chapter II) with $\gamma = 0.5$ and $K_P = 8 \times 10^2$, $\Delta H = 15$ kJ mol^{-1}, at 25 ºC and $K_P = 1.3 \times 10^3$, $\Delta H = 4$ kJ mol^{-1}, at 37 ^{o}C.

At both temperatures, the partition of CPZ into the lipid vesicles is an endothermic process. Accordingly, a small increase in K_P is observed when the temperature is increased from 25 to 37 °C. In the previous chapter we reported that partition of CPZ into POPC:Chol:POPS (6:3:1) membranes was accompanied by a negative enthalpy variation, although less negative than for partition into the liquid-disordered POPC:POPS (9:1) bilayer. The higher conformational order of the lipids in this membrane leads to a more deficient solvation ability that results in a positive enthalpy variation (partition is only driven by the hydrophobic effect). The intrinsic K_P for this lipid composition is significantly smaller than for any of the lipid mixtures studied in Chapter II, being at least one order of magnitude smaller than the intrinsic K_P for POPC lipid bilayers (1.5×10^4 at 25 ºC and 1.4×10^4 at 37 ºC).

The available phase diagrams are not in agreement regarding the phase composition of this lipid mixture (PcSC 111), (Figures III.1 and III.2). The first reported phase diagram propose coexistence of l_o and l_d phases while the data from the most recent publications indicates a single l_o phase although near the upper limit of l_o and l_d phase coexistence. In an attempt to solve this controversy and understand the contribution of each phase to the overall parameters

observed we have characterized the interaction of CPZ with membranes at lipid compositions expected for each of the coexistent phases according to the phase diagram of de Almeida et al. 2003.

The proportions chosen for the l_d or l_o compositions were POPC:SpM:Chol (6:1:3) and POPC:SpM:Chol (1:5:4), respectively (from now on designated PcSC 631 and PSC 154). All phase diagrams available indicate that the lipid composition enriched in SpM (PcSC 154) is in the l_o phase at both temperatures (Figures III.1 and III.2). The lipid bilayer enriched in POPC (PcSC 613) is expected to be in the liquid crystalline l_d phase according to the phase diagrams presented by Veatch and Keller (2005) and Ionova et al. (2012). From the phase diagram proposed by Almeida et al. (2003), this lipid mixture is expected to have phase coexistence with a larger proportion of l_d phase.

The results obtained for the lipid mixture PcSC 613 are displayed in Figure III.4 and Table III.1. For the lipid ratio PcSC 154 quantitative titrations were not possible using ITC due to the small partition coefficient. With the highest lipid concentration used, 50 mM, at the end of the 28 injections the titration was only slightly deviated from the linear part of the curve introducing large uncertainties in both the partition coefficient and the ΔH obtained. However, it is possible to obtain some information from the dependence of the squared residues and ΔH to given values of K_P^{obs}. The enthalpy variation was positive and very large and K_P^{obs} is about one order of magnitude smaller than for the other lipid mixtures assessed (See Figure III.5) indicating that the partition of CPZ into membranes of PcSC 154 is solely a result of the hydrophobic effect.

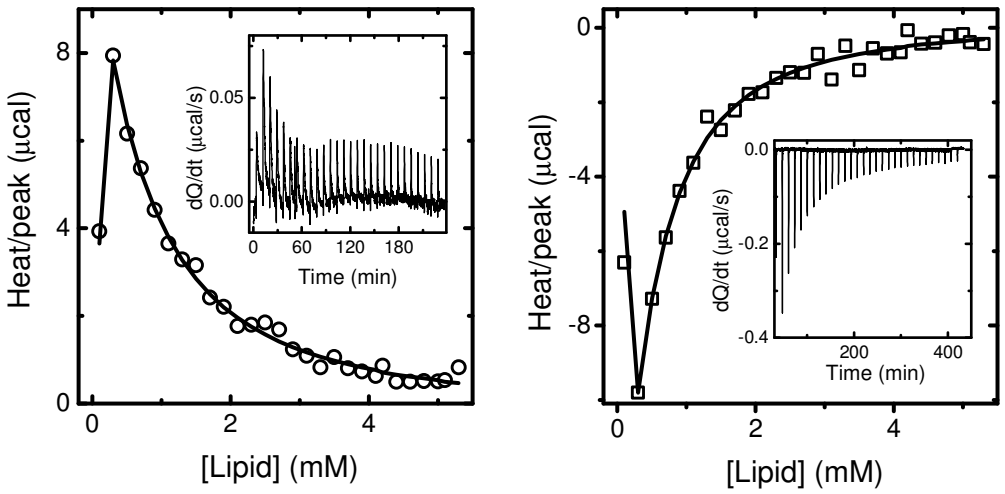

Figure III.4: Typical titration curve obtained for membranes composed of POPC:SpM:Chol (6:1:3) 30 mM with CPZ 30 µM at (A) 25 ºC and (B) 37 ºC. Experimental thermograms in the Insets. The lines are the best fit obtained with eqs II.1-II.5 (see chapter II) with γ = 0.5 and K_P = 2.4 × 10^3, ΔH = 4 kJ mol^{-1}, at 25 ºC and K_P = 2.7 × 10^3 and ΔH = - 8 kJ mol^{-1}, at 37 ºC.

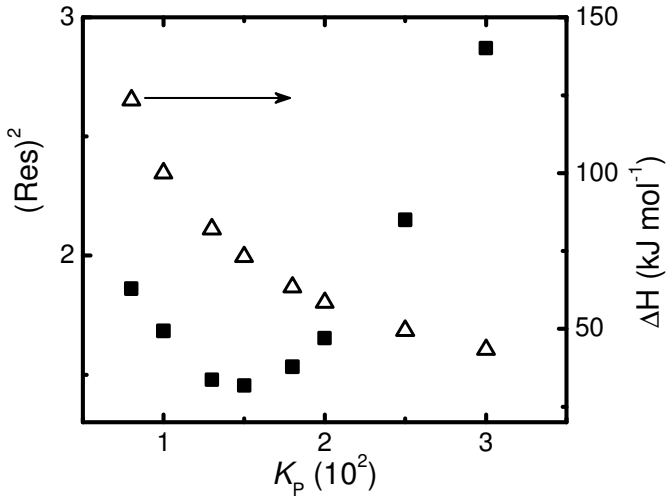

Figure III.5: Dependence of the square deviation between the best fit to eq. II.1-II.5 (chapter II) and the experimental results and ΔH as a function of K_P^{obs}, for the titration of CPZ 30 µM with membranes composed of POPC:SpM:Chol (1:5:4) 30 mM.

Table III.1: Equilibrium parameters obtained for the partition of CPZ to membranes composed of POPC:SpM:Chol in different ratios, using a simple partition model and after correction for the electrostatic effects.

	T (ºC)	K_P (10^3)	ΔH (kJ mol^{-1})	$T\Delta S$ (kJ mol^{-1})	ΔG (kJ mol^{-1})
POPC:SpM:Chol (6:1:3)	25	2.4 ± 0.5	5 ± 1	23	- 19
	37	2.7 ± 0.2	- 8 ± 1	12	- 20
POPC:SpM:Chol (1:1:1)	25	0.8 ± 0.1	15 ± 3	31	- 16
	37	1.3 ± 0.4	4 ± 1	23	- 19
POPC:SpM:Chol (1:5:4)	25	< 0.15	70	82	- 12

From the results shown in Table III.1 it is evident the weak solvation properties of the membranes, especially at low temperatures, which is compensated by a higher entropic contribution for the partition. At 37 ºC, for the mixture with higher content in POPC (PcSC 631), ΔH is negative indicating the establishment of favourable interactions between CPZ and the membrane. In chapter II it was seen that for membranes composed of pure POPC, in a liquid crystalline (l_d) state, ΔH was also negative. We can attribute the positive enthalpy to be a direct consequence of the more ordered membrane were the presence of the solute creates a defect, this is in agreement with the results obtained for the partition of amphiphilic molecules for SpM:Chol (6:4) bilayers that were characterized by a positive van't Hoff enthalpy variation (Abreu et al., 2004; Sampaio et al., 2005; Estronca et al, 2007).

For the mixture PcSC 631, mostly or completely in the l_d phase, the value of K_P is larger than the one observed for the other membranes shown in Table III.1 and increases with temperature as expected from the positive ΔH at 25 ºC. This enthalpy variation indicates a significant conformational order in the membrane and suggests the presence of l_d-l_o phase coexistence. The trend observed on the enthalpy variation as a function of temperature is consistent with a larger fraction of membrane in the l_d phase at higher temperatures, as expected from the phase diagram shown in Figure III.1.

As anticipated, the solvation properties of the membranes composed of PcSC 111 are intermediate between PcSC 631 and PcSC 154. However, a quantitative interpretation taking into account the fraction of phases present is not possible since none of the phase diagrams proposed has well defined tie-lines in the l_d + l_o coexistence regions. Some additional information may be obtained from the time dependent profile of the heat evolved due to association of CPZ with the lipid bilayers and this will be discussed in chapter IV.

Partition into membranes representative of the inner monolayer

The inner monolayer of epithelial cells is considered to be enriched in PE and contain a significant amount of charged lipids. To mimetize this membranes we have used the lipid mixture POPC:Chol:POPE:POPS (4:3:2:1), from now on designated by PcCPePs 4321.

Titrations were performed as described in Material and Methods, injecting aliquots of PcCPePs 4321 30 mM into 30 μM CPZ in buffer. The accessibility factor was assumed to be 0.5 since, at 30 % Chol, bilayers are sufficiently ordered to prevent fast translocation (see Chapter II). The results obtained are shown in Figure III.6 and Table III.2.

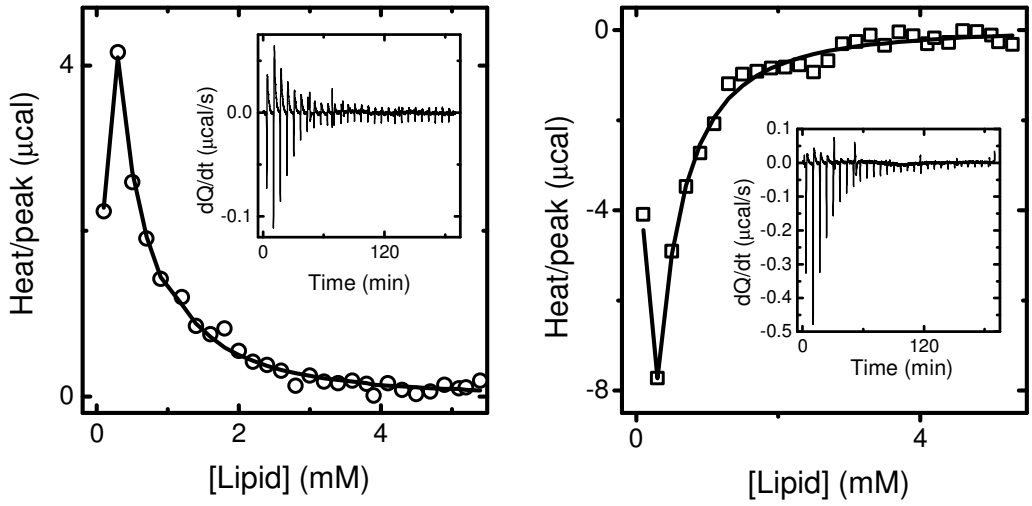

Figure III.6: Typical titration curves obtained for membranes composed of POPC:Chol:POPE:POPS (4:3:2:1) 30 mM with CPZ 30µM at (A) 25 ºC and (B) 37 ºC. Insets show the experimental thermograms. The lines are the best fit obtained with eqs II.1-II.5 (see chapter II) with $K_P = 1.8 \times 10^3$ and $\Delta H = 3$ kJ mol^{-1}, at 25 ºC and $K_P = 1.5 \times 10^3$ and $\Delta H = -5$ kJ mol^{-1} at 37 ºC.

The observed partition coefficient is considerably higher than the intrinsic K_P due to the effect of the electrical attraction between the negative charge in the membrane and the positively charged CPZ. The value of ΔH does not change significantly upon correction for the electrostatic effect but is accompanied by a significant decrease in entropy indicating that POPS makes the membrane less available for the insertion of CPZ as was already observed in chapter II for PcCPs 631 membranes. The partition of CPZ into membranes containing POPS is mainly driven by electrostatic attraction.

The value obtained for the intrinsic partition coefficient of CPZ with PcCPePs membranes at 37 ºC, is not significantly different from that at 25 ºC, but ΔH becomes negative which, as discussed above, could be explained by a more disordered state of the bilayer at higher temperatures. We note that large heat variations are associated with interaction of CPZ with those membranes but both an endothermic and an exothermic process are taking place resulting in a small overall enthalpy variation (Figure III.6). This is particularly relevant at 25 ºC. The deconvolution of both heat contributions will be done in the next section.

To identify and evaluate the contribution from POPE, we also studied the partition of CPZ into membranes composed of POPC:Chol:POPE (5:3:2) (PcCPe 532). Titrations were performed in the same way as with the lipid mixtures PcCPePS 4321 and the results obtained are summarized in Table III.2. As observed for the PcCPePs membranes, the thermograms show the presence of two processes associated with the interaction of CPZ with those

membranes, an exothermic and an endothermic one, this being particularly evident at 25 ^{o}C, Figure III.7 inset of plot A.

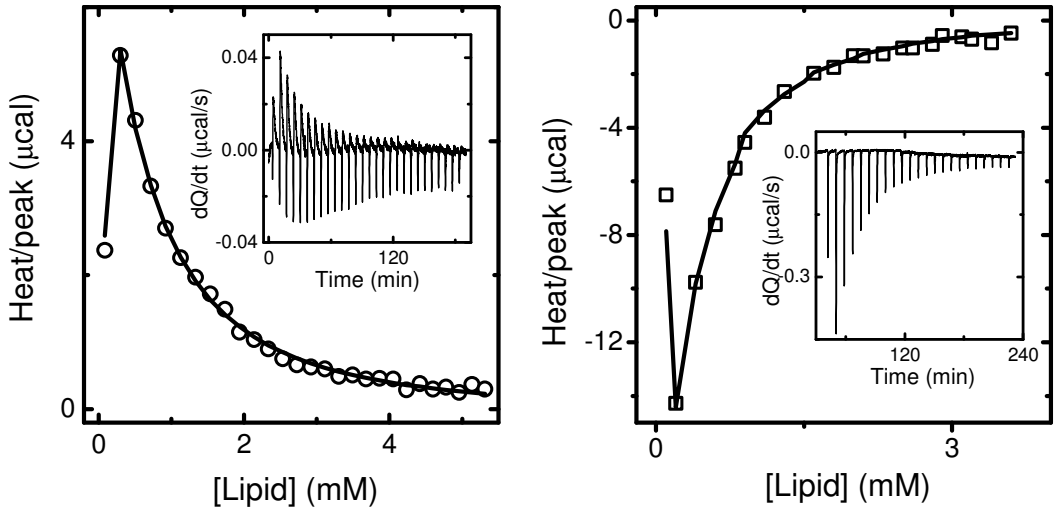

Figure III.7: Typical titration curve obtained for membranes composed of POPC:Chol:POPE (5:3:2) 30 mM with CPZ 30µM at (A) 25 ºC and (B) 37 ºC. Inserts show the experimental thermograms. The lines are the best fit obtained with eqs II.1-II.5 (see chapter II) with $K_P = 2.1 \times 10^3$ and $\Delta H = 4$ kJ mol^{-1}, at 25 ºC and $K_P = 1.7 \times 10^3$ and $\Delta H = -1$ kJ mol^{-1}, at 37 ºC.

Table III.2: Equilibrium parameters obtained for the partition of CPZ to membranes composed of POPC:Chol:POPE (5:3:2) and containing 10 % of the charged lipid POPS, using a simple partition model and after correction for the electrostatic effects.

		Simple model				Corrected for the electrostatic interactions			
	T (ºC)	K_P^{obs} (10^3)	ΔH (kJ mol^{-1})	TΔS (kJ mol^{-1})	ΔG (kJ mol^{-1})	K_P (10^3)	ΔH (kJ mol^{-1})	TΔS (kJ mol^{-1})	ΔG (kJ mol^{-1})
PcCPePs 4321	25	3.8 ± 0.6	3 ± 1	23	- 20	3.6 ± 0.5	3 ± 1	23	- 20
	37	3.3 ± 0.3	- 5 ± 1	16	- 21	2.9 ± 0.3	- 4 ± 1	16	- 19
PcCPe 532	25	1.7 ± 0.4	5 ± 2	24	- 18	2.1 ± 0.6	4 ± 1	23	- 19
	37	1.3 ± 0.5	- 1 ± 1	18	- 19	1.7 ± 0.2	- 1 ± 1	20	- 21

The intrinsic K_P for PcCPe 532 at both temperatures is significantly larger than K_P^{obs} unlike what happens for mixtures with 10 % POPS indicating that the effect of the charge imposed by CPZ in the membrane upon partition is considerable, even though the ratio of L:CPZ$_{bound}$ was always kept above 25 lipid molecules per bound CPZ.

The value of the K_P^{obs} is much larger for PcCPePs 4321 membranes but the intrinsic K_P is not significantly different for both lipid mixtures. This indicates that the larger partition

coefficient observed for membranes containing POPS is mostly a consequence of the electrostatic attraction between the negative charged serine and the positive charge in CPZ.

The partition is lower at higher temperature although the positive enthalpy variation at 25 ^{o}C would lead to an increase in the partition coefficient with the increase in temperature. This contradictory behaviour was already seen for the lipid mixture PcCPs 631 (see Chapter II) and the quaternary mixture PcCPePs 4321 and was interpreted as ~~an~~ indicative of some structural alterations induced in the membrane upon partition of CPZ. If the membrane has already a tendency for phase separation, the insertion of CPZ into the bilayer may promote this phase separation.

POPE is a phospholipid with a smaller head group compared to POPC, not being very suitable to form planar bilayers alone (Gennis, 1989). Additionally, the presence of 30 % Chol has an ordering effect on the acyl chains of POPE, despite less pronounced than for the PC equivalent (Gennis, 1989). The phase diagram proposed by Paré and Lafleur (1998) for the lipid mixture POPE:Chol doesn't show any region with coexistent $l_d + l_o$. Also Marinov and Dufourc (1996) reports that a lipid mixture of POPE:Chol (7:3) reflects intra and intermolecular motions of the liquid-ordered lamellar phase. The defects produced by the presence of POPE in the bilayer may conduce to a phase separation which seems to be the case happening for these two lipid mixtures, more pronounced when the temperature is lower, and resulting in positive ΔH for the partition of CPZ into the lipid bilayers.

In light of the reported above, the results obtained in this work for the PE containing membranes point towards the presence of phase coexistence. The results indicate that the most ordered phase is dominant at 25 ºC, resulting in a positive ΔH for the partition of CPZ into the lipid bilayers, with the opposite situation obtained at 37 ºC and resulting in a negative ΔH.

Comparing the results obtained for the lipid compositions model of the external and internal leaflets of the membrane, we can observe that the partition into the internal leaflet is about five times that for the external leaflet at 25 ºC but at 37 ºC is only two and a half times higher. Partition into the external leaflet is only a consequence of the hydrophobic effect while for the internal leaflet, at 37 ºC, the partition is also favoured by enthalpy.

Deconvolution of the endothermic and exothermic contribution

Two components are present at both temperatures in the heat evolved upon interaction of CPZ with the membranes containing POPE and with PcSC 613 (an endothermic and an exothermic)

as is evident in the thermograms show in Figures III.4, III.6 and III.7. We have analysed the temporal evolution of the heat evolved to gain insight into the nature of the two processes involved.

The two contributions to the heat evolved were deconvoluted with the sum of two exponential functions (eq. III.1 and Figure III.8). This corresponds to the assumption that two processes occur in parallel and independently, with different characteristic times, and that the heat measured is the sum from both processes. In eq. III.1 $q_{(t)}$ is the heat evolved at t (time elapsed since the beginning of injection), which is the result from the heat evolved from both processes ($q^1_{(t)}$ and $q^2_{(t)}$), A_x is the amplitude and β_x is the kinetic constant for process x (x=1 or 2), and τ is the time at which a given fraction of lipid was injected. The injection was done at a rate of 0.5 µL *per* s and the time resolution was 2 s, this corresponds to t_i=20 s for the injection of 10 µL of lipid and the step increment on τ was 2 s.

$$q_{(t)} = q^1_{(t)} + q^2_{(t)} \; ; \quad q^x_{(t)} = \sum_{\tau=0}^{\tau=t_i} A_x e^{-\beta_x (t-\tau)} \qquad \text{eq. III.1}$$

The heat evolved from each process after a given titration step, q^1 and q^2, was obtained from the integration of the respective $q^x_{(t)}$. The dependence of q^x with the lipid concentration was analysed independently using the simple partition model described in Chapter II. Two partition coefficients (K^1_P and K^2_P) and two enthalpy variations (ΔH^1 and ΔH^2), were therefore obtained for each lipid mixture and temperatures.

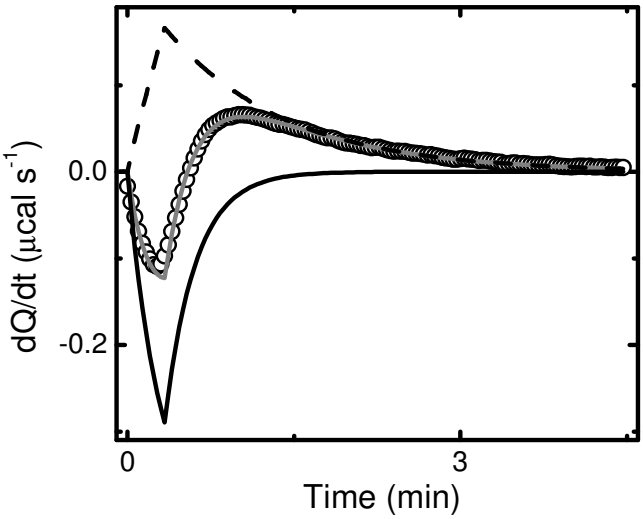

Figure III.8: Time profile of the heat evolved after addition of 10 µL of PcCPePs 4321 30 mM liposomes to 30 µM CPZ in buffer (□). The grey line is the best fit of eq. III.1 with two characteristic rate constants from two independent processes (black lines, straight and dashed).

Figure III.9 shows the two titration curves obtained after deconvolution of the each titration step into two processes for the titration of PCPePs 4321 30 mM with 30 µM CPZ, as an example. The inset shows the global titration curve with the experimental data directly obtained with the Origin software (see Figure III.6 A) and the sum of the heat from both processes obtained after deconvolution. The heat associated with the faster process (q^1) has a large uncertainty associated because the majority is evolved during the injection of lipid where the description of the thermogram by equation III.1 is less accurate. We have therefore obtained q^1 from the subtraction of q^2 to the experimental total heat associated with the respective titration step.

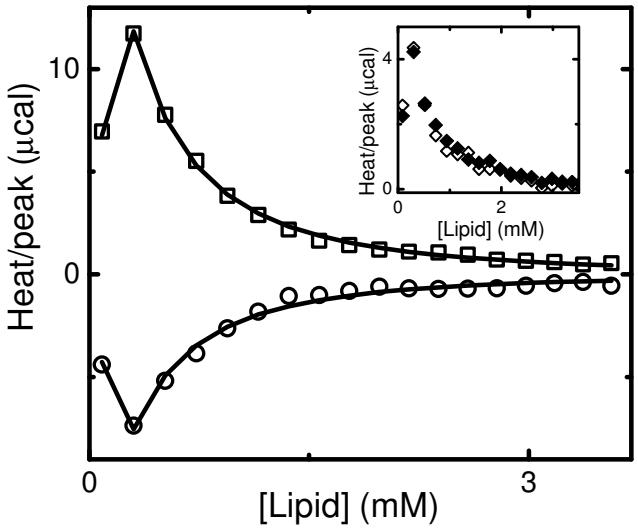

Figure III.9: Titration curve obtained for membranes composed of POPC:Chol:POPE:POPS (4:3:2:1) 30 mM with CPZ 30µM at 25 ºC after deconvolution of the experimental peaks into the exothermic and endothermic components. The lines are the best fit obtained with eq. II.1-II.5 (see chapter II) with $K_P^1 = 2.3 \times 10^3$ and $\Delta H^1 = -5$ kJ mol^{-1}, and $K_P^2 = 3.0 \times 10^3$ and $\Delta H^2 = 8$ kJ mol^{-1}. The Inset shows the global titration curve with the experimental points in full squares and the open squares corresponding to the sum of both components.

In the best fit of equations II.1 to II.5 to q^1 and q^2, it is necessary to define the lipid and CPZ concentrations available for each process. The lipid concentration assumed affects the partition coefficient obtained while the total concentration of CPZ affects the enthalpy variation. The unavailability of a detailed phase diagram for those lipid mixtures precludes a rational establishment of the volume fraction of each phase. A volume fraction of 0.5 was therefore *ad hoc* attributed to each phase. The values obtained for K_P towards a given phase (Table III.3) are therefore overestimated (underestimated) if the volume fraction of that phase is larger (smaller) than 0.5. We have also assumed that half of the total CPZ is available to equilibrate with each phase.

Table III.3: Equilibrium parameters obtained after deconvolution of the double peaks found for the lipid mixtures POPC:Chol:POPE (5:3:2) and POPC:Chol:POPE:POPS (4:3:2:1).

		Exothermic interaction		Endothermic interaction	
	T (ºC)	$K_P^1 (10^3)$	ΔH^1 (kJ mol^{-1})	$K_P^2 (10^3)$	ΔH^2 (kJ mol^{-1})
POPC:Chol:POPE:POPS	25	2.3 ± 0.7	- 12 ± 1	3.0 ± 0.4	14 ± 1
(4:3:2:1)	37	3.3 ± 0.4	- 26 ± 2	3.4 ± 0.5	16 ± 2
POPC:Chol:POPE (5:3:2)	25	0.8 ± 0.1	- 19 ± 2	1.4 ± 0.2	17 ± 3
	37	0.9 ± 0.1	- 31 ± 2	1.6 ± 0.1	17 ± 1

Discarding the possibility of Overshooting

The presence of peaks with negative and positive components in the thermogram is not *per se* a proof of the occurrence of two processes in the interaction of CPZ with the lipid bilayers. One possibility that must be discarded, prior to the attribution of any physical meaning regarding the interaction, is the eventual overshooting on the ITC feedback system.

When the ITC equipment senses variations in the temperature inside the sample cell (compared with the reference cell) it responds by adding more energy to heat the cell if the temperature has dropped or removing the heat input if the temperature has raised. The operator can choose the feedback gain to be high or low, i.e., the equipment to be faster or slower in response to the temperature variation. In addition, higher values selected for the reference power will result in larger variations in the heat supplied by the equipment as a response to temperature variations in the sample cell. These different options will result in distinct time profiles for heat evolved in each injection peak.

If small heat variations are expected and a reference power is set to high, the equipment will respond stronger to maintain the reference power selected and an overshooting process can occur. This problem may be minimized with the selection of a smaller reference power.

Another important parameter is the feedback gain selected. If no gain is selected, the temperature in the sample compartment will slowly approach that of the reference as the heat is supplied to or dissipated from the sample cell. This setup is usually not selected as it results in very broad peaks reducing the sensitivity and requiring very large intervals between injections. If the feedback gain is set to high, the compensation in temperature variations in the sample compartment occurs fast (large heat *per* s resulting in improved sensitivity and faster experiments) but it may generate overshooting if the heat involved is small.

We have changed the equipment conditions for the same experiment, injecting POPC:Chol:POPE:POPS (4:3:2:1) 30 mM into 30 μM CPZ in buffer, and the time dependence of the heat evolved is shown in figure III.10.

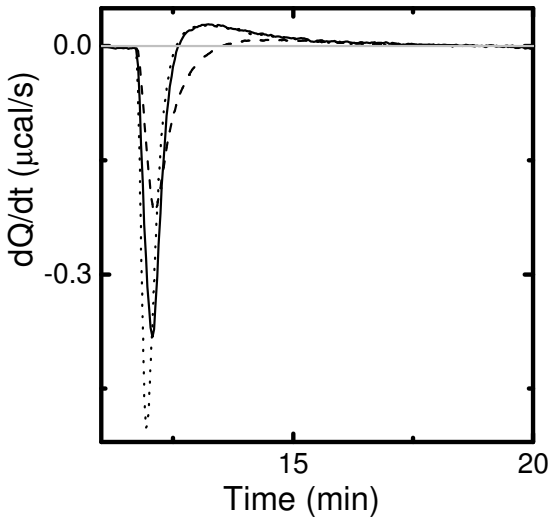

Figure III.10: Thermogram profile of an injection peak of POPC:Chol:POPE:POPS (4:3:2:1) 30 mM into 30 µM CPZ with different equipment conditions: feedback gain high and reference power 10 µcal s^{-1} (straight line), feedback gain low and reference power 10 µcal s^{-1} (dashed line) and feedback gain high with a reference power 2 µcal s^{-1}(dot line).

For the reference power 10 µcal s^{-1}, the same used throughout the work, we have two distinct heat profiles when changing the feedback gain from high to low. With the low feedback gain the signal from the fast exothermic process broadens and consequently, the endothermic component can only be observed at longer times. It is however evident that the signal goes to positive values and accompanies the signal from the high feedback gain in the final part of the curve. When the reference power was set to 2 µcal s^{-1}, with a high feedback gain, the time response of the equipment is faster resulting in a sharper exothermic peak while the slower exothermic component is unaffected.

It should be noted that after deconvolution according to equation III.1, the integrated heat from the exothermic and endothermic components is the same for all above setup conditions: q = - 6 µcal; q^1 = - 15 µcal and q^2 = 9 µcal. This allowed us to conclude that two simultaneous processes with opposite heat variations are occurring.

We have interpreted the two processes as interaction of CPZ with distinct phases in the lipid bilayer. This was supported by the fact that the interaction with membranes in the liquid disordered phase is fast and has a negative ΔH (see Chapter II) being slower and with a positive ΔH for membranes in the liquid ordered phase (e.g. PcSC 154).

Conclusions

In this chapter, we have determined the partition of CPZ into representative membranes of the outer and inner monolayers of the endothelial cells. We have used the lipid compositions POPC:SpM:Chol (1:1:1) and POPC:Chol:POPE:POPS (4:3:2:1) for the membranes of the outer and inner monolayers, respectively. We have found that the CPZ partition into the internal leaflet is about five times higher than that for the external leaflet, 3.8×10^3 and 8×10^2, at 25 ºC and about two and a half times higher, 3.3×10^3 and 1.3×10^3, at 37 ºC. The partition into the outer monolayer is mainly driven by the hydrophobic effect but a favourable enthalpic contribution is obtained for interaction with the inner monolayer.

The lipid mixture representative of the outer monolayer is expected to present coexistence of liquid-disordered and liquid-ordered phases, at both temperatures studied, according to the phase diagram described by Almeida et al. (2003). The two additional phase diagrams reported for this lipid composition were only obtained at 23 ^{o}C and indicate that this mixture is mainly or exclusively in the liquid-ordered phase. The thermograms obtained for the interaction of CPZ with this lipid mixture show a single endothermic component which supports the existence of a single liquid-ordered phase.

In an attempt to further elucidate this controversy we have characterized the interaction of CPZ with two additional lipid compositions, one enriched in POPC (PcSC 613) and another enriched in SpM (PcSC 154). We found that for the lipid mixture PcSC 613 the partition is higher (2.4×10^3 at 25 ºC and 2.7×10^3 at 37 ºC) while it is much lower for the PcSC 154 ($< 1.5 \times 10^2$). Additionally, the process is driven by enthalpy for PcSC 613 membranes and is mainly driven by the hydrophobic effect for PcSC 154, with a positive enthalpy variation. The thermograms obtained for the interaction of CPZ with membranes enriched in SpM were characterized by a single endothermic component while those obtained for interaction with the membranes enriched in POPC showed an exothermic and an endothermic component at 25 ^{o}C and a single exothermic component at 37 ^{o}C. Those results indicate that at the lipid composition PcSC 154 the membrane is in the liquid-ordered phase (in agreement with all phase diagrams available for this lipid mixture) and that it is near the phase boundary for the lipid composition PcSC 613. This phase behaviour is not in full agreement with none of the proposed phase diagrams, being closer to the one obtained through the interaction of delta-lysin with those ternary mixtures by Pokorny et al. (2006). The phase diagram described by these authors was obtained with porcine brain Sphingomyelin while all the others described above and the present work were done using egg Sphingomielin

In the case of the lipid mixture representative of the inner monolayer, we observed that the heat profile for the injection peaks presents both exothermic and endothermic contributions, unlike what happened in the case of the partition into POPC:Chol:POPS (6:3:1) where only an exothermic process was observed (Chapter II). To evaluate the influence of the 20 % POPE we have also studied the partition of CPZ into membranes composed of POPC:Chol:POPE (5:3:2). The results showed also the presence of two processes occurring. Furthermore, the dependence of K_P with temperature provides evidence that the presence of POPE induces structural changes in the membrane possibly enhanced by the insertion of CPZ into the lipid bilayers.

Altogether, the results obtained for the interaction of CPZ with those lipid compositions indicate that the interaction with membranes in the liquid-disordered state is fast and exothermic while interaction with membranes in the liquid-ordered state is slow and endothermic, the presence of two components in the thermogram being evidence for the presence of phase coexistence. The time dependence of the heat evolved upon interaction with membranes in the liquid-ordered phase will be analyzed in the next chapter to obtain information regarding the microscopic rate constants for the interaction.

References

Abreu, M. S. C., Moreno, M. J. and Vaz, W. L. C. (2004) Kinetics and thermodynamics of association of a phospholipid derivative with lipid bilayers in liquid-disordered and liquid-ordered phases. Biophysical Journal, 87, 353-365

Bloj, B. and Zilversmit, D. B. (1976) Asymmetry and transposition rates of phosphatidylcholine in rat erythrocyte ghosts. *Biochemistry*, 15, 1277-

Bretsche, M. S. (1972) Phosphatidylethanolamine – diferential labelling in intact cells and cell ghosts of human erythrocytes by a membrane impermeable reagent. *Journal of Molecular Biology*, 71, 523-

Collado, M. I., Goñi, F. M., Alonso, A. And Marsh D. (2005) Domain formation in sphingonyelin/cholesterol mixed membranes studied by spin-label electron spin resonance spectroscopy. *Biochemistry*, 44, 4911-4918

Daleke, D. L. (2007) Phospholipid flippases. *The Journal of Biological Chemistry*, 282, 821-825

de Almeida, R. F. M., Fedorov, A. and Prieto, M. (2003) Sphyngomyelin/phosphatidylcholine/cholesterol phase diagram: boundaries and composition of lipid rafts. *Biophysical Journal*, 85, 2406-2416

Devaux, P. F. (1992) Protein involvement in transmembrane lipid asymmetry, *Annual Review of Biophysics and Biomolecular Structure*, 21, 417-439

Devaux, P. F. and Morris, R. (2004) Transmembrane asymmetry and lateral domains in biological membranes. *Traffic*, 5, 241-246

Estronca, L. M. B. B., Moreno, M. J. and Vaz, W. L. C. (2007) Kinetics and thermodynamics of the association of dehydroergosterol with lipid bilayer membranes. *Biophysical Journal*, 93, 4244–4253

Feigenson, G. W. (2006) Phase behaviour of lipid mixtures. *Nature Chemical Biology*, 2,

Filippov, A., Oradd, G. and Lindblom, G. (2003) The effect of cholesterol on the lateral diffusion of phospholipids in oriented bilayers. *Biophysical Journal*, 84, 3079-3086

Fisher, K. A. (1976) Analysis of membrane halves: cholesterol. *Proceedings of the Natural Academy of Sciences USA*, 73, 173-177

Gennis, R.B. (1989) Biomembranes: Molecular Structure and Function, New York, Springer-Verlag.

Greenwood, A. I., Tristam-Nagle, S. and Nagle, J. F. (2006) Partial molecular volumes of lipids and cholesterol. *Chemistry and Physics of Lipids*, 143, 1-10

Ionova, I. V., Liyshits, V. A. and Marsh, D. (2012) Phase diagram of ternary cholesterol/palmitoylsphingomyelin/palmitoyloleoyl-phosphatidylcholine mixtures: spin-label EPR study of lipid-raft Formation. *Biophysical Journal*, 102, 1856-1865

Konyakhina, T. M., Goh, S. L., Amazon, J., Heberle, F. F., Wu, J. and Feigenson, G. W. (2011) Control of a Nanoscopic-to-Macroscopic Transition: Modulated Phases in Four-Component DSPC/DOPC/POPC/Chol Giant Unilamellar Vesicles. *Biophysical Journal*, 101, L8-L10

Lehninger, A.L., Nelson, D.L. and Cox, M.M. (1997) *Principles of Biochemistry*. (2nd ed.) U. S.: Worth Publishers Inc.

Marinov, R. and Dufourc, E. J. (1996) Thermotropism and hydration properties of POPE and POPE-cholesterol systems as revealed by solid state ^{2}H and ^{31}P-NMR. *European Biophysics Journal*, 24, 423-431

Marrink, S. J., de Vries, A. H., Harroun, T. A., Katsaras, J. and Wassal, S. R. (2008) Cholesterol shows preference for the interior of polyunsaturated lipid membranes. *Journal of the American Chemical Society*, 130, 10-11

Marsh, D. (2009) Cholesterl-induced fluid membrane domains: A compendium of lipid-raft ternaty phase diagrams. *Biochimica et Biophysica Acta*, 1788, 2114-2123

Mateo, C. R., Acuña, A. U. And Brochon, J. C. (1995) Liquid-crystalline phases of cholesterol/lipid bilayers as revealed by the fluorescence of trans-parinaric acid. *Biophysical Journal*, 68, 978-987.

Moreno, M. J., Estronca, L. M. B. B. and Vaz, W. L. C. (2006) Translocation of phospholipids and dithionite permability in liquid-ordered and liquid-disordered membranes. *Biophysical Journal*, 91, 873-881

Op den Kamp, J. A. F. (1979) Lipid asymmetry in membranes. *Annual Review of Biochemistry*, 48, 47-71

Paré, C. and Lafleur, M. (1998) Polymorphism of POPE/cholesterol system: a ^{2}H nuclear magnetic resonance and infrared spectroscopic investigation. *Biophysical Journal*, 74, 899-890

Pokorny, A., Yandek. L. E., Elegbede, A. I., Hiderliter, A. and Almeida, P. F. F. (2006) Temperature and composition dependence of the interaction of δ-Lysin with ternary mixtures of sphingomyelin/cholesterol/POPC. *Biophysical Journal*, 91, 2184-2197

Rothman, J. E. and Lenard, J. (1977) Membrane asymmetry. *Science*, 195, 743-753

Sampaio, J. L., Moreno, M. J. and Vaz, W. L. C. (2005) Kinetics and thermodynamics of association of a fluorescent lysophospholipid derivative with lipid bilayers in liquid-ordered and liquid-disordered phases. *Biophysical Journal*, 88, 4064-4071

Simons, K. and Vaz, W. L. C. (2004) Model Systems, lipid rafts and cell membranes. *Annual Review of Biophysics and Biomolecular Structure*, 33, 269-295

van Meer, G., Voelker, D. R. and Feigenson, G. W. (2008) Membrane lipids: where they are and how they behave. *Nature Reviews*, 9, 112-124

Veatch, S. L. and Keller, S. L. (2005) Miscibility phase diagrams of giant vesicles containing sphyngomyelin. *Physical Review Letters*, 94, 148101

Wydro, P. and Haük-Wydro, K. (2007) Thermodynamic description of the interactions between lipids in ternary Langmuir monolayers: the study of cholesterol distribution in membranes. *Journal of Physical Chemistry B*, 111, 2495-2502

Chapter IV

Kinetics of the interaction of CPZ with membranes in the liquid ordered state

Introduction

Most pharmacological agents active in the central nervous system (CNS) must permeate the blood-brain barrier (BBB) by passive transport in order to achieve their target. It is therefore of extreme pharmaceutical and medical importance to quantitatively understand the mechanisms and rate of the passive transport of these agents across the BBB.

In most of the work done previously to describe the permeation through a cell monolayer, the emphasis has been placed on the equilibrium partition to the lipid bilayers (Deamer et al, 1999). Overton's rule assumes equilibrium for the partition of molecules between the aqueous media and the lipid bilayer and considers the diffusion through the membrane as the rate limiting step. However, the rate of interaction of small molecules with membranes may be relatively slow, especially for very hydrophobic amphiphiles and membranes in the liquid ordered phase (Abreu et al., 2004; Sampaio et al., 2005; Estronca, et al., 2007), and this step may have a strong influence on the rate of passive permeation. This is particularly relevant because the supply of drugs from the blood into the endothelial cells is a steady state process and the amount of active agent that associates with the endothelium depends on the relative rate of interaction and the duration of the contact between the blood and the capillaries during each blood passage. The rate of insertion and desorption (k_+ and k_-) are therefore relevant parameters, together with the translocation rate constant (k_f), that control the effective rate of passive permeation.

The lack of quantitative information regarding the kinetics of the interaction of amphiphilic molecules with lipid bilayers, and the biological and pharmacological relevance of this subject, prompted our group towards a detailed study of the processes involved in the permeation through lipid bilayers (Abreu et al, 2004; Sampaio et al, 2005; Moreno et al, 2006; Estronca et al, 2007, Cardoso, et al., 2011). We were able to characterize all three steps involved in the interaction of amphiphiles with lipid bilayers in the liquid-disordered state for an homologous series of fluorescent molecules (NBD-C_n; n=8 to 16) (Cardoso et al., 2011) and the interaction of fluorescent phospholipid derivatives with bilayers in the liquid-disordered and liquid-ordered state (Abreu et al., 2004; Sampaio et al., 2005; Moreno et al., 2006). Those results were used to develop a mechanistic model for the permeation of a cell monolayer (Filipe, 2009 and unpublished work) that allowed the establishment of rules between the rate of the individual processes and the overall rate of permeation. It was clearly observed that Overton's rule was only observed for amphiphiles with a high hydrophilic/hydrophobic ratio (where translocation was the rate limiting step),

the opposite behaviour being observed for more hydrophobic amphiphiles. This behaviour was due to the slow interaction between the amphiphiles and the ordered membrane of the apical portion of endothelial cells (modelled by the lipid mixture SpM:Chol (6:4), in the l_o phase) that become the rate limiting step in the overall process.

Kinetic Scheme

To fully characterize the interaction of amphiphiles with lipid bilayers, the rate constants of insertion and desorption, which defines the equilibrium association constant or the related partition coefficient, and the translocation rate constant must be known.

The kinetic scheme for the interaction of an amphiphile with lipid bilayers is represented as:

$$A + L_v \underset{k_-}{\overset{k_+}{\rightleftarrows}} AL_v^{out} \underset{k_f}{\overset{k_f}{\rightleftarrows}} AL_v^{in}$$

$$K_L = \frac{k_+}{k_-} = \frac{[AL_v^{out}]}{[A][L_v]}$$

And is described by the differential equations:

$$\frac{d[AL_v^{out}]}{dt} = k_+[A][L_v] + k_f[AL_v^{in}] - (k_- + k_f)[AL_v^{out}]$$
$$\frac{d[AL_v^{in}]}{dt} = k_f\left([AL_v^{out}] - [AL_v^{in}]\right) \qquad \text{eq. IV.1}$$

where A represents the amphiphile and L_v the lipid bilayer. The amphiphilic molecule may insert in the outer monolayer of the bilayer, with a rate constant for the insertion (k_+), originating AL_v^{out} . The inserted molecule may then desorb from the bilayer with a characteristic rate constant (k_-) or translocate to the inner leaflet of the bilayer with a characteristic rate constant (k_f) (see also chapter II).

If the translocation rate constant is slow enough, the amount of amphiphile accumulated in the inner monolayer (AL_v^{in}) during the equilibration between the aqueous phase and the outer monolayer is negligible and the process is well described by a differential equation of the form:

$$\frac{d[x]}{dt} = -\beta([x] + b) \qquad \text{eq. IV.2}$$

which, by integration, leads to an equation of the type

$$[x]_t = [x]_{(\infty)} + \left([x]_{(0)} - [x]_{(\infty)}\right) e^{-\beta t} \qquad \text{eq. IV.3}$$

Under those conditions, the transfer rate constant (β) is related with the microscopic rate constants of insertion and desorption by equation:

$$\beta = k_- + k_+ [L_v] \qquad \text{eq. IV.4}$$

allowing the calculation of both k_+ and k_- from the linear dependence of the transfer rate constant with the liposome concentration.

This model has been used before by this research group to characterize the interaction of fluorescent amphiphiles with lipid bilayers in the liquid-ordered or in the liquid-disordered state (Estronca et al., 2007; Abreu et al., 2004; Sampaio et al., 2005). It was shown that the insertion in the lipid bilayer is not diffusion controlled, being slower for membranes in the liquid-ordered phase (1.3×10^5 M^{-1} s^{-1} for DHE, 1.8×10^5 M^{-1} s^{-1} for NBD-DMPE and 1.7×10^9 M^{-1} s^{-1} for NBD-lysoMPE, in S:C 6:4 at 37 ^oC) than in the liquid-disordered phase (5.1×10^7 M^{-1} s^{-1} for DHE, 2.3×10^6 M^{-1} s^{-1} for NBD-DMPE and 3.4×10^{10} M^{-1} s^{-1} for NBD-lysoMPE, in POPC at 37 ^oC).

In this chapter we will quantitatively analyze the kinetics of the slow component observed in the temporal profile of the heat evolved due to interaction of CPZ with membranes enriched in cholesterol, previous chapter.

Results and Discussion

The slow step observed in the transfer of CPZ between the aqueous media and the membranes will be quantitatively analyzed for the lipid compositions: POPC:SpM:Chol (1:1:1) (PcSC111), POPC:SpM:Chol (6:1:3) (PcSC 613), POPC:Chol:POPE:POPS (4:3:2:1) (PcCPePs 4321) and POPC:Chol:POPE (5:3:2) (PcCPe 532).

In Figure IV.1, the time profile of the heat evolved, after the addition of 10 μL of liposome solution to an aqueous solution of CPZ, is presented for all the above lipid compositions as well as for POPC.

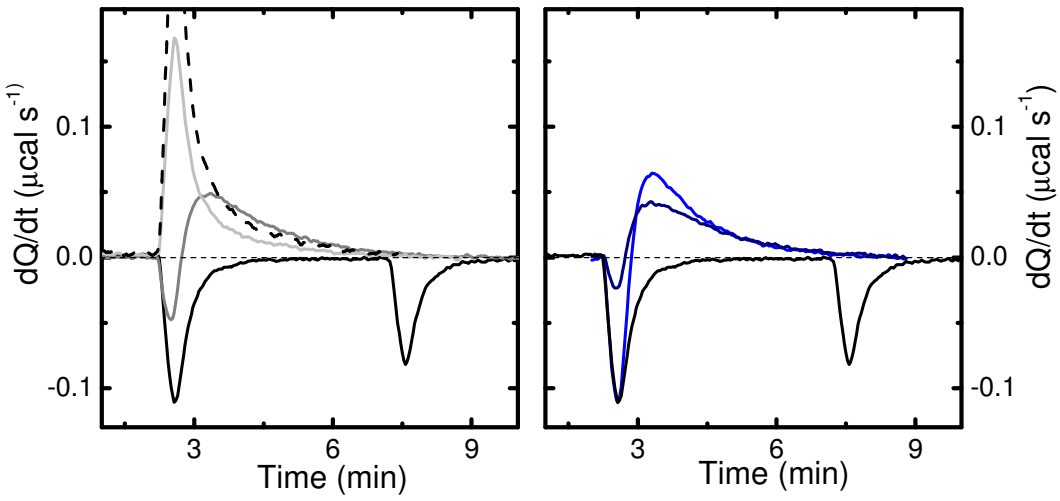

Figure IV.1: Time profile for the heat evolved after the addition of 10 µL of a liposome solution to an aqueous solution of CPZ for the case of liposomes prepared from pure POPC (solid black), SpM:Chol (6:4) (dashed black), POPC:SpM:Chol (1:1:1) (light grey), POPC:SpM:Chol (6:1:3) (dark grey), POPC:Chol:POPE:POPS (4:3:2:1) (light blue) and POPC:Chol:POPE (5:3:2) (dark blue).

One first observation is that the recovery of the baseline is faster for membranes prepared from POPC (in black). Another striking observation is that for some lipid mixtures the time profile of the heat evolved has two components: an exothermic component with a time dependence similar to that observed for pure POPC membranes, and a slower endothermic component. In the previous chapter we have attributed this endothermic component to partition of CPZ into bilayers in a more ordered state. In this chapter we will analyze the kinetics of this component in an attempt to obtain the rate constants for the interaction of CPZ with lipid bilayers in the l_o phase.

In chapter II we have already observed a second (much) slower component in the recovery of the baseline that was attributed to translocation of CPZ through the l_d POPC membranes. In the case of the lipid mixtures studied in this chapter, this slower step cannot be due to translocation for three reasons: *i*) The amplitude of the signal for the slowest component is, in some cases, higher than half of the total heat evolved; *ii*) for most lipid mixtures, the signal of the heat evolved in the slowest component is opposite to that of the faster one (the additional heat evolved due to translocation into the inner monolayer is due to the partition of more amphiphiles into the outer monolayer and must therefore have the same thermodynamic parameters); *iii*) when translocation is occurring it is possible to determine the amplitude variation of the signal attributed to translocation for all the titration curve and in the case of the lipid mixtures studied in this chapter that is not the case.

When the heat evolved due to partition of CPZ into POPC bilayers is analyzed in the time scale where most variation is occurring (200 s) we find a mono-exponential behaviour with a characteristic transfer rate constant of 0.06 s^{-1}, equation III.1 (See chapter III) and figure IV.2. This rate constant is similar to the specified time response of the equipment and it is therefore not possible to obtain the rate constants for the interaction of CPZ with this membrane. The time profile of the heat evolved due to interaction of CPZ with membranes of SpM:Chol (6:4) was also well described by a mono-exponential, but in this case the characteristic rate constant was much smaller (0.01 s^{-1}) (Figure IV.2). This lipid composition is expected to be in a single liquid-ordered phase according to all phase diagrams published for SpM:Chol mixtures.

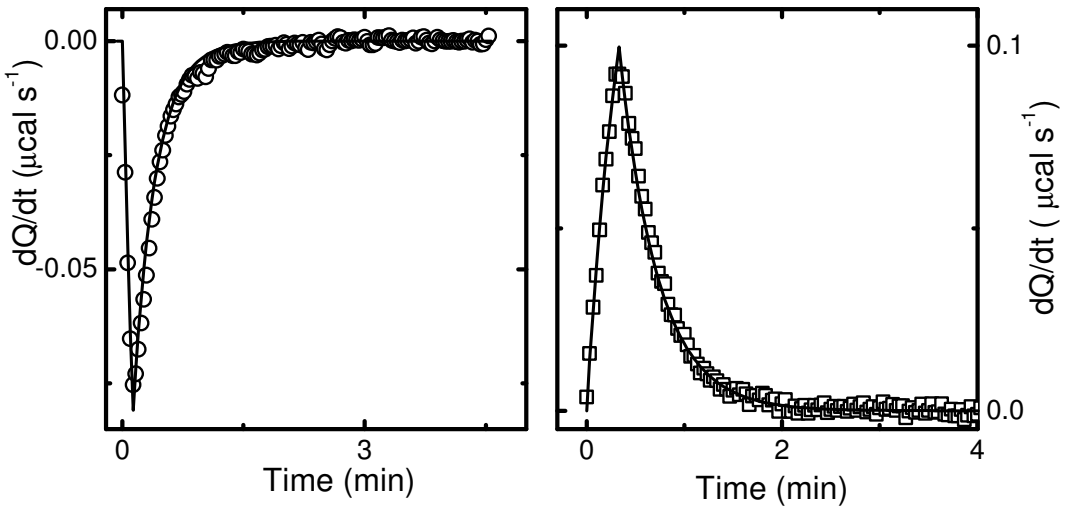

Figure IV.2: Time profile of heat evolved after the addition of 10 µL of a liposome solution prepared from pure POPC (left) and SpM:Chol (6:4) (right) to an aqueous solution of CPZ. The lines are the best fit to eq. III.1 with β = 0.07 s^{-1} and β = 0.01 s^{-1} for POPC and SpM:Chol 6:4, respectively.

In contrast to what was observed for pure POPC and for SpM:Chol (6:4) bilayers, the temporal evolution of the heat profile observed for most other lipid compositions studied was bi-exponential strongly suggesting the presence of two coexisting phases. The results were analyzed with equation IV.6; the characteristic rate constant for the fast step was similar to that observed for POPC bilayers (limited by the time response of the equipment) and a significantly slower step was observed with a rate constant at the first 10 µL of lipid addition equal to 0.015, 0.012, 0.015 and 0.012 s^{-1} for PcSC 111, PcSC 613, PcCPePs 4321 and PcCPe 532, respectively, at 37 ºC.

In an attempt to give physical meaning to the slow component of the heat profile, we have analyzed the dependence of its characteristic rate constant with the concentration of liposomes, equation IV.4. If this step is due to the direct interaction of CPZ in the aqueous phase with the lipid bilayers, the rate constants for insertion and desorption may be obtained from the slope and intercept respectively. The results obtained are shown in figures IV.3 to IV.6 and summarized in table IV.1.

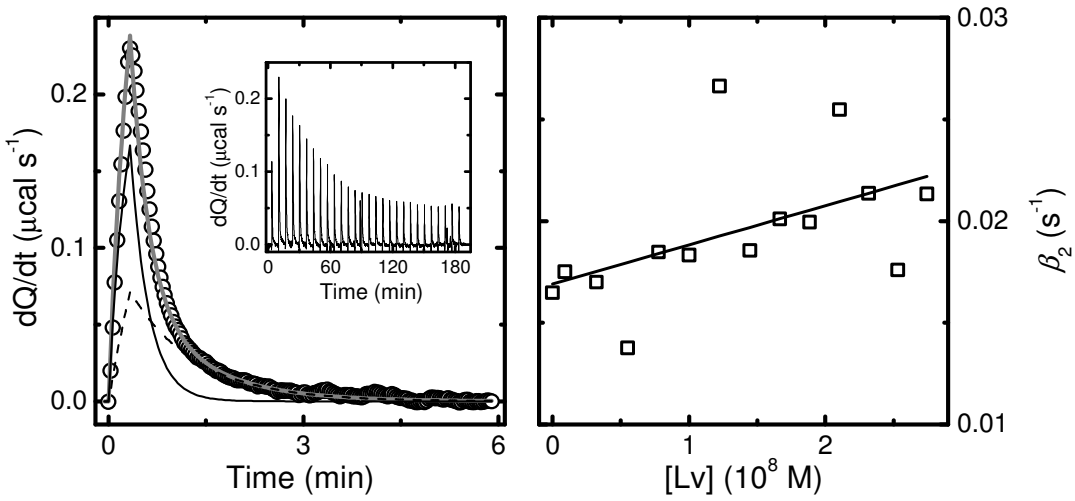

Figure IV.3: Left: Time profile of heat evolved after addition of 10 μL POPC:SpM:Chol (1:1:1) 50 mM to an aqueous solution of CPZ. The grey line is the fit to the experimental data with eq. IV.6, at 25 ºC. Right: Transfer rate constant for the slowest step as a function of LUV concentration. The line is the best fit of eq. IV.4 with $k_+ = 1.9 \times 10^5$ M^{-1}s^{-1} and $k_- = 1.7 \times 10^{-2}$ s^{-1}.

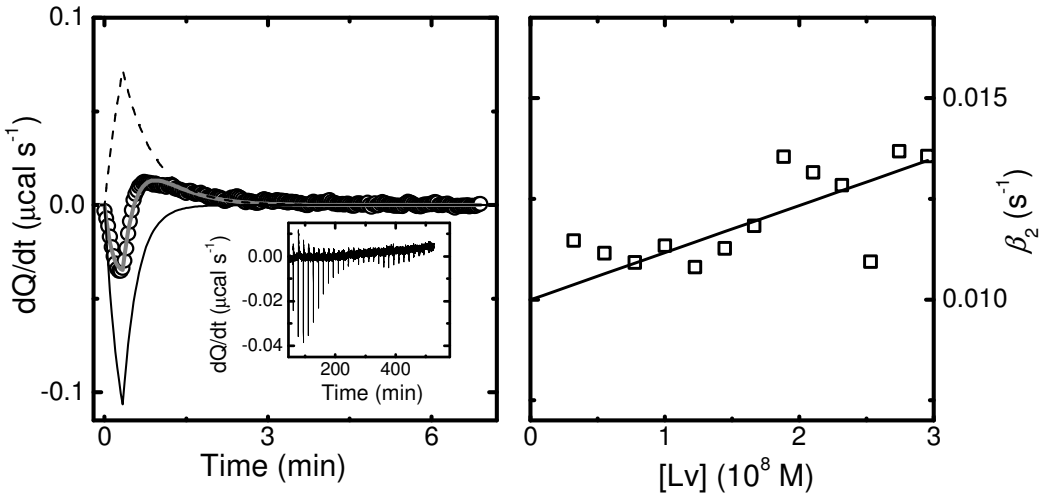

Figure IV.4: Left: Time profile of heat evolved after addition of 10 μL POPC:SpM:Chol (6:1:3) 30 mM to an aqueous solution of CPZ. The grey line is the fit to the experimental data with eq. III.1, at 25 ºC. Right: Transfer rate constant for the slowest step as a function of LUV concentration. The line is the best fit of eq. IV:4 with $k_+ = 1.2 \times 10^5$ M^{-1}s^{-1} and $k_- = 1.0 \times 10^{-2}$ s^{-1}.

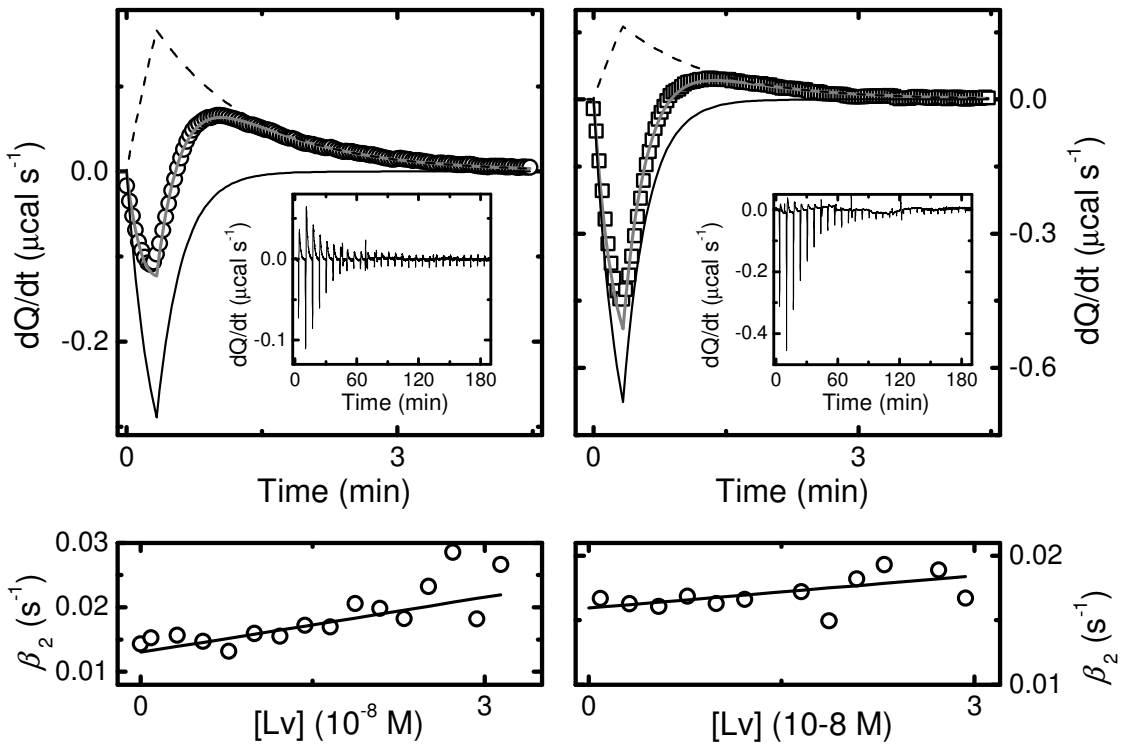

Figure IV.5: Top: Time profile of heat evolved after addition of 10 µL POPC:Chol:POPE:POPS (4:3:2:1) 30 mM to an aqueous solution of CPZ. The grey line is the fit to the experimental data with eq. IV.6, at 25 ºC (left) and 37 ºC (right). Down: Transfer rate constant for the slowest step as a function of LUV concentration, at 25 ºC (left) and 37 ºC (right). The line is the best fit of eq. IV.4 (See Kinetic Model) with $k_+ = 3.7 \times 10^5$ $M^{-1}s^{-1}$ and $k_- = 1.3 \times 10^{-2}$ s^{-1} at 25 ºC and $k_+ = 2.0 \times 10^5$ $M^{-1}s^{-1}$ and $k_- = 1.6 \times 10^{-2}$ s^{-1} at 37 ºC.

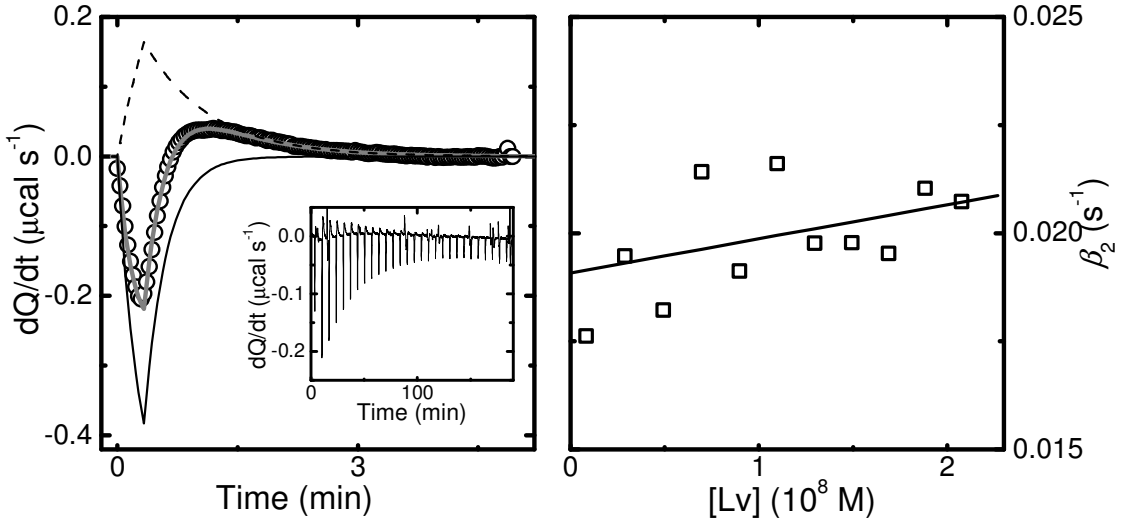

Figure IV.6: Left: Time profile of heat evolved after addition of 10 µL POPC:Chol:POPE (5:3:2) 30 mM to an aqueous solution of CPZ, at 25 ºC. The grey line is the fit to the experimental data with eq. IV.6. Right: Transfer rate constant for the slowest step as a function of LUV concentration. The line is the best fit of eq. IV.4 with $k_+ = 1.2 \times 10^5$ $M^{-1}s^{-1}$ and $k_- = 1.0 \times 10^{-2}$ s^{-1}.

For bilayers composed of PSC 111 and PSC 613, at 37 ºC, the experimental data was well fitted with eq. III.1. The characteristic rate constant, β, obtained was 0.04 s^{-1} and 0.07 s^{-1} for PSC 111 and PSC 613, respectively (Figure IV.7). From this kinetic analysis one could infer that the membranes composed of PSC 111 and PSC 613 are in a single phase, at 37 ºC, in agreement with the phase diagrams described by Veatch and Keller (2005) and Ionova et al. (2012).

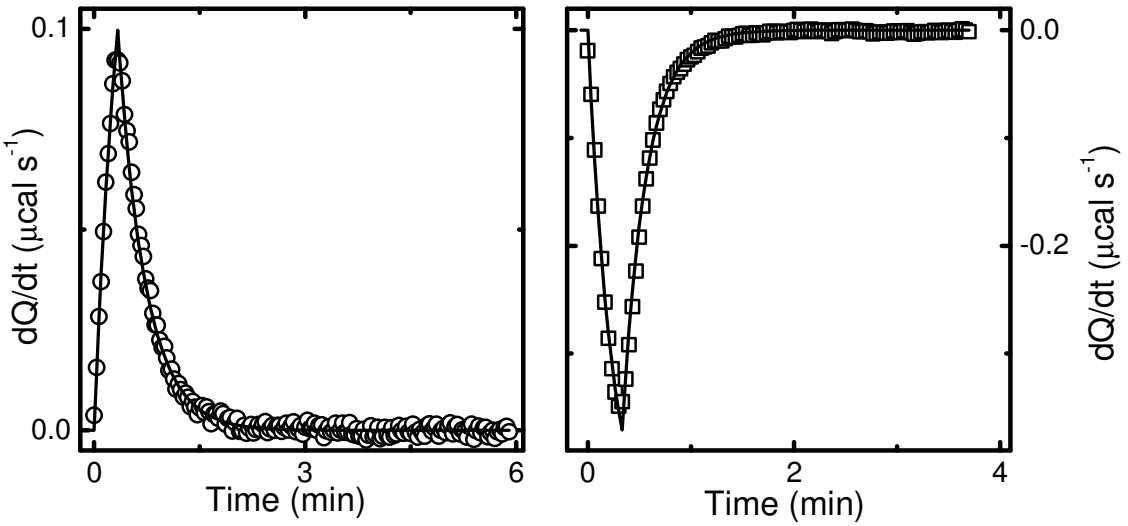

Figure IV.7: Time profile of heat evolved after the addition of 10 µL of a liposome solution 30 mM to an aqueous solution of CPZ 10 µM, at 37 ºC for the case of POPC:SpM:Chol (1:1:1) (left) and POPC:SpM:Chol (6:1:3) (right). The lines are the best fit to eq. III.1 with β = 0.04 s^{-1} for PSC 111 and β = 0.07 s^{-1} for PSC 613.

Table IV.1: Values for the characteristic rate constant obtained with eq. III.1 and for the k_+ and k_- of eq. IV.4 found for the interaction of CPZ with membranes composed of the lipid mixtures in study.

	T (ºC)	k_+ (10^5 M^{-1} s^{-1})	k_- (10^{-2} s^{-1})	β (s^{-1})
POPC:SpM:Chol (1:1:1)	25	1.9 ± 0.5	1.7 ± 0.1	
	37			0.04
POPC:SpM:Chol (6:1:3)	25	1.2 ± 0.4	1.0 ± 0.1	
	37			> 0.06
POPC:Chol:POPE:POPS (4:3:2:1)	25	3.7 ± 0.7	1.3 ± 0.1	
	37	2.0 ± 0.5	1.6 ± 0.1	
POPC:Chol:POPE (5:3:2)	25	1.2 ± 0.3	1.0 ± 0.1	
	37	0.9 ± 0.3	1.6 ± 0.1	
SpM:Chol (6:4)	25			
	37			0.01
POPC	25			
	37			> 0.06

The order of magnitude for the slope of the characteristic transfer rate constant as a function of the concentration of LUVs (insertion rate constant according to equation IV.4), at 25 ºC, is in accordance with the value of k_+ found for the interaction of dehydroergosterol (DHE) with bilayers in the l_o phase, composed of SC 64 (Estronca et al., 2007). The intercept (desorption rate constant according to the model presented) is three orders of magnitude larger than that of DHE from membranes in the l_o phase indicating a weaker interaction, as expected from the much smaller partition coefficient of CPZ (1.5×10^2 as compared with 1.2×10^6 for DHE). Those results give confidence on the adequacy of the model presented. However, the dependence of the putative rate constants with temperature is not the expected, being for example k_+ slower at 37 ºC than at 25 ºC for PCPePs 4321 membranes. Additionally, the similar values obtained for the dependence of the characteristic transfer rate constant in all lipid mixtures were unexpected.

From the results obtained and from the data published for the insertion and desorption rate constants for other molecules, it is tempting to assume that the slope and intercept of eq. IV.4 can be attributed to the insertion (k_+) and desorption (k_-) rate constants for the interaction of CPZ with the l_o phase of the lipid bilayers in study. However, the current data available is not enough to fully support this interpretation. The heat evolved is certainly a consequence of the interaction of CPZ with the lipid bilayers in the l_o phase but the simple model presented may be insufficient for the kinetic description of the process.

One important limitation of the model used to analyze the results is the assumption that the two processes are independent. In the presence of phase coexistence the amphiphile may be interacting first with the less ordered phase and then slowly equilibrating with the more ordered one. This complexity was included in a more realistic model (results not shown) but it was not explored due to the high number of unknown parameters required.

To strengthen our hypothesis, and give physical meaning to the temporal dependence of the heat evolved, it is mandatory to characterize the interaction of CPZ with membranes showing phase coexistence and for which the phase diagram is well characterized. One possible system are lipid bilayers of DMPC:Chol bilayers (Almeida et al., 1992) that present regions of known lipid composition in the l_d, l_o or coexistent l_d + l_o phases, at accessible temperatures. The tie lines in the region of phase coexistence are also know for this system, being possible to characterize the interaction of the amphiphile with the two pure phases and in the presence of well defined volume fractions of each when coexisting in the bilayer.

Conclusions

The interaction of CPZ with membranes in the liquid ordered phase, or with coexistence of liquid-disordered and liquid ordered phases, shows a characteristic time constant significantly smaller that the time response of the calorimeter. Additionally, the time profile of the heat evolved was mono-exponential for membranes in a single phase and bi-exponential for most membranes expected to present phase coexistence.

The dependence of the characteristic rate constant of the slow process with the total concentration of liposomes in solution was analyzed and a linear relation was encountered for most mixtures. A simple model was developed to interpret those results, assuming that the two processes were independent, and the rate constants for insertion/desorption into/from the lipid bilayers in the liquid ordered phase were estimated. The rate constants obtained are compatible with those found previously for the interaction of the fluorescent sterol (DHE) with membranes in the liquid-ordered phase, CPZ showing a similar insertion rate constant (comparable cross sections for both amphiphiles) and a much faster desorption rate constant (much weaker interaction of CPZ with the membranes).

The interpretation of the results obtained is complicated by the fact that the phase diagram for the lipid mixtures used is not known or not well defined. Those results are therefore preliminary and must be confirmed through the characterization of the interaction of CPZ with membranes showing coexistence of liquid-ordered and liquid-disordered phases with a well defined phase diagram, such as mixtures of DMPC and cholesterol.

References

Abreu, M. S. C., Moreno, M. J. and Vaz, W. L. C. (2004) Kinetics and thermodynamics of association of a phospholipid derivative with lipid bilayers in liquid-disordered and liquid-ordered phases. *Biophysical Journal*, 87, 353-365

Almeida, P. F. F., Vaz, W. L. C. and Thompson, T. E. (1992) Lateral diffusion in the liquid-phases of dimyristoylphosphatidylcholine cholesterol lipid bilayers: a free volume analysis. *Biochemistry*, 31, 6739-6747

Cardoso, R. M. S., Martins, P. A. T., Gomes, F., Doktorovova, S., Vaz, W. L. C. and Moreno, M. J. (2011) Chain-length dependence of insertion, desorption and translocation of a homologous series of 7-nitrobenz-2-3-diazol-4-yl-labeled aliphatic amines in membranes. *Journal of Physical Chemistry B*, 115, 10098−10108

Deamer, D.W., Kleinzeller, A. and Fambrough, D.M. (Eds.) (1999) *Membrane Permeability 100 Years since Ernest Overton.* Current Topics in Membranes. SanDiego, USA: Academic Press.

Estronca, L. M. B. B., Moreno, M. J. and Vaz, W. L. C. (2007) Kinetics and thermodynamics of the association of dehydroergosterol with lipid bilayer membranes. *Biophysical Journal*, 93, 4244–4253

Filipe, H. A. L. (2009) *Quantitative modelling of passive permeation through the blood brain barrier.* Master thesis. Coimbra: Faculdade de Ciências e Tecnologia – Universidade de Coimbra.

Moreno, M. J., Estronca, L. M. B. B. and Vaz, W. L. C. (2006) Translocation of phospholipids and dithionite permability in liquid-ordered and liquid-disordered membranes. *Biophysical Journal*, 91, 873-881

Sampaio, J. L., Moreno, M. J. and Vaz, W. L. C. (2005) Kinetics and thermodynamics of association of a fluorescent lysophospholipid derivative with lipid bilayers in liquid-ordered and liquid-disordered phases. *Biophysical Journal*, 88, 4064-4071

Veatch, S. L. and Keller, S. L. (2005) Miscibility phase diagrams of giant vesicles containing sphyngomyelin. *Physical Review Letters*, 94, 148101

Chapter V

Conclusions

In this work we have studied the interaction of a pharmacologically active drug, CPZ, with membranes of different lipid compositions, using isothermal titration calorimetry. The objective of this study was to understand the individual processes involved in the passive permeation of a cell monolayer, such as the endothelium that composes the blood brain barrier.

We have developed methodology to obtain information on the kinetic parameters of interaction of CPZ with lipid bilayers using ITC, a technique traditionally used to obtain only the thermodynamic parameters. The full characterization of the kinetic parameters for the interaction of small molecules with membranes is limited to a very small number of fluorescent molecules (Cardoso et al., 2011; Massey et al., 1997; Thomas et al., 2002; Zhang et al., 1996). The possibility of characterization of both kinetic and thermodynamic parameters using ITC is a major achievement as it allows the study of the interaction of pharmacologically active molecules with lipid bilayers.

The quantitative characterization of the translocation step was accomplished for membranes where this process occurs within the timescale available by this technique. For membranes in the liquid disordered phase, the translocation rate constants were measured: being 3.9×10^{-4} and 6.6×10^{-4} s^{-1} for POPC and POPC:POPS 9:1, respectively, at 25 °C and nearly twice as large at 37 °C, chapter II. This parameter, together with the partition coefficient, allowed the determination of the permeability coefficient, which is equal to 2.0×10^{-7} cm s^{-1} for POPC, 3.9×10^{-7} cm s^{-1} for POPC:POPS 9:1, and smaller than 5.0×10^{-8} cm s^{-1} for POPC:Chol:POPS 6:3:1 membranes at 37 °C. The rate of translocation for the membrane enriched in cholesterol was found to be smaller than 4×10^{-4} s^{-1} and cannot be quantitatively accessed using this technique.

In the currently accepted model for passive permeation through lipid bilayers, the Overton's rule, it is assumed that diffusion through the bilayer (translocation for the case of amphiphiles) is the rate limiting process. In spite of that, the rate of this process is usually unknown and a simple dependence on the size of the diffusing molecule is assumed. Additionally, the partition coefficient to the lipid bilayer is assumed to be proportional to its partition coefficient between water and organic solvents such as octanol (or distribution at a given value of pH for the case of weak acids or bases). Not surprisingly, the correlation with the observed permeation through biological membranes is poor. The working hypothesis behind this work is that in most cases the small predictive value of this approach is due to the fact that the organic solvent does not capture the solvation properties

of the lipid bilayers and that the rate of translocation is not directly dependent on the size of the amphiphile.

The lipid composition of biological membranes is complex and not homogeneous through the different cell membranes and monolayers for a given membrane. In endothelial and epithelial cells there is additionally lateral heterogeneity with the apical and basolateral portions of the membrane presenting very distinct lipid compositions (Fisher, 1976; Rothman and Lenard, 1977; Op den Kamp, 1979). To understand the effect of each compositional difference, and rationalize the interaction of CPZ with the different membranes, we have characterized the interaction of CPZ with lipid bilayers of different lipid composition and increasing complexity from a simple pure POPC membrane towards the quaternary mixture that models the cytoplasmic side of the plasma membrane of endothelial cells.

The effect of introducing negatively charged lipids in the membrane was studied with bilayers of POPC:Chol 9:1, and the consequences of cholesterol addition were studied using POPC:Chol:POPS 6:3:1. The presence of 10 % negatively charged lipid does not affect significantly the observed partition coefficient (1.0×10^4 and 1.3×10^4 for POPC and POPC:POPS 9:1 respectively, at 37 ^{o}C) although the interaction enthalpy become more favourable (- 11 and - 22 kJ/mol for POPC and POPC:POPS 9:1 respectively, at 37 ^{o}C) due to the electrostatic interaction established between CPZ (a cation at pH=7.4) and the negatively charged membrane. The addition of 30 % Chol to the POPC bilayers containing 10 % POPS reduces the partition coefficient by 50 % due to the poor solvation ability of the more ordered lipid bilayer ($K_P = 0.63 \times 10^4$ and ΔH = -14 kJ/mol, at 37 ^{o}C).

The equilibrium parameters for the interaction of CPZ with those membranes were also studied at 25 ºC. The temperature dependence obtained for the parameters in membranes containing POPS was unexpected and pointed towards the induction of significant structural rearrangements in the membrane due to the presence of CPZ (most particularly in the membranes containing cholesterol).

We have also characterized the interaction of CPZ with lipid bilayers representative of the outer and inner monolayers of the apical portion of endothelial cells, Chapter III. The affinity of CPZ for those membranes is significantly smaller that that observed for pure POPC bilayers being smaller for the membranes enriched in sphingomyelin ($K_P = 3.3 \times 10^3$, ΔH = - 5 kJ/mol for POPC:Chol:POPE:POPS 4:3:2:1 (modelling the cytoplasmic leaflet)

and $K_P = 1.3 \times 10^3$, $\Delta H = 4$ kJ/mol for POPC:SpM:Chol 1:1:1 (modelling the exoplasmic leaflet), at 37 ºC).

It is generally accepted that membranes prepared from POPC:SpM:Chol at the molar proportions 1:1:1 present coexistence of l_o and l_d phases (Almeida et al., 2003; Veatch and Keller, 2005). To understand the effect of the phase coexistence we have also characterized membranes with the expected lipid composition of the coexistent l_o and l_d phases (at the boundaries of the phase coexistence region). The choice of the lipid compositions was complicated by the inexistence of well defined tie lines and by the different phase coexistence regions reported in the literature for this ternary mixture (Almeida et al., 2003; Veatch and Keller, 2005; Ionova et al., 2012). We have selected POPC:SpM:Chol 1:5:4 and POPC:SpM:Chol 6:1:3 for the lipid compositions representative of the l_d and l_o coexisting phases. The partition coefficient to the SpM enriched membrane was very small and only an upper limit could be obtained ($K_P < 1.5 \times 10^2$). This partition was only driven by entropy (hydrophobic effect and disordering of the lipid bilayer due to the presence of CPZ) with a very positive ΔH. At 37 ^oC, the interaction of CPZ with the lipid bilayer representative of the coexisting l_d phase was significantly more efficient ($K_P = 2.7 \times 10^3$) and with a favourable enthalpy contribution ($\Delta H = -8$ kJ/mol). The parameters obtained for the interaction of CPZ with POPC:SpM:Chol 1:1:1 bilayers were intermediate between those obtained for the supposedly coexisting l_d and l_o phases but a quantitative interpretation could not be done.

The time profile of the heat evolved due to the interaction of CPZ with the lipid bilayers representative of the exoplasmic and cytoplasmic leaflet of endothelial cells was complex showing an exothermic and an endothermic contribution. This was particularly evident for the quaternary mixture of POPC:Chol:POPE:POPS (4:3:2:1) at 25 ^oC. We have analyze the weight from both contributions, assuming that they are being originated from two independent processes, and calculated the partition coefficient and the enthalpy variation for the interaction of CPZ with the lipid bilayer due to each of the two processes. The enthalpy variations obtained were compatible with the coexistence of l_d and l_o phases, with the interaction with lipid bilayers in the l_d phase being favoured by enthalpy while with lipid bilayers in the l_o phase it is accompanied by a positive variation in the enthalpy of the system. We could not perform a quantitative interpretation of the results obtained (partition coefficient and interaction enthalpy) because the available information in the literature does not allow the calculation of the volume fraction of each phase.

On all lipid bilayers showing an endothermic and an exothermic process, the exothermic interaction was always faster than the endothermic one. In addition, for simple lipid mixtures without phase coexistence, only a contribution was observed being fast and exothermic for membranes in the liquid-disordered phase and slow and endothermic for lipid bilayers in the liquid-ordered phase. The complex heat profiles obtained for the membranes with POPS and/or POPE strongly suggest that those membranes are not homogeneous at the temperatures studied.

Finally, an attempt was made to evaluate the kinetics of the interaction of CPZ with membranes in the liquid ordered phase or with coexistent $l_d + l_o$ phases, using ITC. For this purpose, we obtained the characteristic rate constant associated with the slow component of the heat change as a function of time for each titration step. The kinetic parameters for the interaction of CPZ with the membranes in the liquid-ordered phase, insertion and desorption rate constants, were tentatively obtained from the dependence of the characteristic rate constant with the concentration of LUVs. The values obtained were in agreement with those reported for the interaction of a sterol derivative with membranes in the liquid ordered phase (Estronca et al., 2007). However, we refrain from doing a detailed quantitative interpretation of the results obtained because the phase diagram of those lipid mixtures is not known in sufficient detail. The partition of CPZ into membranes showing coexistence of $l_d + l_o$ phases, and with a well defined phase diagram, is required to support and help in the development of the kinetic models required. The results obtained are nevertheless very promising as they indicate that the rate constants for interaction of amphiphiles with lipid bilayers in the liquid-ordered state may all be obtained using ITC. This will allow the characterization of the interaction between pharmaceutically active agents and the membrane barriers in biological systems opening the way to obtain predictive rules between the structure of the drug and its bioavailability.

References

de Almeida, R. F. M., Fedorov, A. and Prieto, M. (2003) Sphyngomyelin/phosphatidylcholine/cholesterol phase diagram: boundaries and composition of lipid rafts. *Biophysical Journal*, 85, 2406-2416

Cardoso, R. M. S., Martins, P. A. T., Gomes, F., Doktorovova, S., Vaz, W. L. C. and Moreno, M. J. (2011) Chain-length dependence of insertion, desorption and translocation of a homologous series of 7-nitrobenz-2-3-diazol-4-yl-labeled

aliphatic amines in membranes. *Journal of Physical Chemistry B*, 115, 10098–10108

Estronca, L. M. B. B., Moreno, M. J. and Vaz, W. L. C. (2007) Kinetics and thermodynamics of the association of dehydroergosterol with lipid bilayer membranes. *Biophysical Journal*, 93, 4244–4253

Fisher, K. A. (1976) Analysis of membrane halves: cholesterol. *Proceedings of the Natural Academy of Sciences USA*, 73, 173-177

Massey, J. B., Bick, D. H. and Pownall, H. J. (1997) Spontaneous transfer of monoacyl amphiphiles between lipid and protein surfaces. *Biophysical Journal*, 72, 1732-1743

Op den Kamp, J. A. F. (1979) Lipid asymmetry in membranes. *Annual Review of Biochemistry*, 48, 47-71

Rothman, J. E. and Lenard, J. (1977) Membrane asymmetry. *Science*, 195, 743-753

Thomas, R. M., Baici, A., Werder, M., Schulthess, G. and Hauser, H. (2002) Kinetics and mechanism of long-chain fatty acid transport into phosphatidylcholine vesicles from various donor systems. *Biochemistry*, 41, 1591-1601

Veatch, S. L. and Keller, S. L. (2005) Miscibility phase diagrams of giant vesicles containing sphyngomyelin. *Physical Review Letters*, 94, 148101

Zhang, F. L., Kamp, F. and Hamilton, J. A. (1996) Dissociation of long and very long chain fatty acids from phospholipid bilayers. *Biochemistry*, 35, 16055-16060

Chapter VI

Material and Methods

Chemical compounds

All aqueous solutions were made using distilled water (Aquatron A4000), further purified in a system containing particles and charcoal filters and UV irradiation. The purity of water was evaluated through conductivity analysis and kept below 0.5 μS. The pH was controlled using Hepes buffer 10 mM pH = 7.4 containing 0.15 M NaCl, 1 mM EDTA and 0.02 % (m/v) NaN_3. CPZ and all other reagents used were from Sigma-Aldrich Química (Sintra, Portugal). The non-aqueous solvents used were spectroscopic grade (Uvasol® Merck or Sigma).

The phospholipids POPC, POPS, POPE and egg-yolk SpM, cholesterol and the labelled NBD-DMPE were all obtained from Avanti Polar Lipids (Alabaster, AL, USA).

The fluorescent amphiphile NBD-C_{16} was synthesized as described by Cardoso et al. (2010). Briefly, the amine was dissolved in dry chloroform and excess sodium carbonate was added. NBD-Cl, dissolved in a minimal amount of dry chloroform was added drop wise with constant stirring. The reaction was allowed to occur for two hours, at room temperature in the dark, and the reaction mixture was purified using Si60 preparative TLC plates and $CHCl_3$:MeOH:CH_3COOH 80:20:1 as eluent. The product was extracted with chloroform and further purified by preparative liquid chromatography using the stationary phase RP18 and acetonitrile:water 75:25 as eluent. The concentration of the fluorescent amine was determined by measuring its absorbance at ~460 nm, using an extinction coefficient of 2.1×10^4 M^{-1} cm^{-1}, in methanol.

Preparation of solutions

Lipid stocks were prepared weighting the estimated amount of powder and dissolved in azeotropic mixture of chloroform:methanol 87:12. The stock solutions were kept at – 20 ºC. The concentration was determined using the methods described below for phosphate (in the case of phospholipids) and cholesterol quantifications.

CPZ solutions were prepared directly in buffer and their concentrations were determined by measuring the absorbance at 310 nm using an extinction coefficient of 3260 M^{-1} cm^{-1} in aqueous solution.

Preparation of Large Unilamellar Vesicles

Aqueous suspensions of lipids were prepared by evaporating a solution of the desired lipid or premixed lipid mixture in the azeotropic mixture of chloroform:methanol (87:13, v/v) by blowing dry nitrogen over the heated solution (blowing hot air over the external surface of the tube) and then leaving the residue in a vacuum desiccator for at least 8h at room temperature. The solvent-free residue was hydrated with the aqueous buffered solution. The hydrated lipid was subjected to several cycles of gentle vortex/incubation for at least 1 h, to produce a suspension of multilamelar vesicles, which was then extruded in a water-jacketed extruder (Lipex Biomembranes, Vancouver, British Columbia, Canada) using a minimum of 10 passes, through two stacked polycarbonate filters (Nucleopore) with a pore diameter of 0.1 μm (Hope et al., 1985). The hydration and extrusion steps were performed at a temperature that was at least 10 ºC higher than the transition temperature of the phospholipid with the highest phase transition temperature. The same procedure was followed for vesicles containing CPZ or NBD-DMPE, except that an appropriate volume of a stock solution of CPZ 5 mM or NBD-DMPE 0.1 mM in chloroform:methanol (87:13, v/v) was added to the lipids and thoroughly mixed prior to vesicle preparation. The LUVs suspensions were, afterwards, diluted to the desired concentrations with the aqueous buffer.

Phosphate Quantification

During the preparation of LUV there are some critical steps influencing the exact amount of lipid present in the assays, namely the weighting of dry lipid and the extrusion of MLVs through the polycarbonate filters. For the quantitative analysis made throughout this project the knowledge of the exact amounts of lipid present is essential.

The final phospholipid concentrations in the LUV were determined using a modified version of the Bartlett phosphate assay (Bartlett, 1959).

A calibration curve was generated using a standard solution of inorganic phosphate between 0 and 0.3 μmol (K_2HPO_4). The samples of phospholipid suspensions whose concentrations were to be determined were appropriately diluted so that the final concentration would fall into the calibration curve and aliquots of these diluted suspensions were used in the assay. The total volume of calibration standards and phospholipids suspensions was adjusted to 300 μL with distilled deionized water. To these tubes, 700 μL of perchloric acid at 70 % (v/v) was added before heating to 190 ºC in a block heater,

covered with glass marbles to avoid splattering of hot acid, until completely color loss for a maximum of two hours. Solutions were allowed to slowly cool to room temperature, after which 2 mL of ammonium molybdate 1 % (w/v) and 2 mL of ascorbic acid 4 % (w/v) were added. Final solutions were incubated at 37 ºC for 1 to 2 hours and the absorbance was measured at λ=700 nm.

Cholesterol Quantification

The final cholesterol concentration was determined using the Lieberman–Burchard method as described by Taylor and co-workers (1978).

A calibration curve was generated using a standard solution of cholesterol and pipetting the appropriate volumes containing between 0 and 0.5 μmol. The samples were appropriately diluted so that the final concentration would fall into the calibration curve. The total volume of calibration standards and phospholipids suspensions was adjusted to 100 μL with isopropanol. To all solutions 3 mL of glacial acetic acid:acetic anhydride:sulfuric acid 35:55:10 (v/v/v) (prepared on ice and stabilized with 1% sodium sulfate) were added and the final solutions were incubated ate 37 ºC for 20 minutes, after which the absorbance was read at λ = 625 nm.

Characterization of the LUVs

Determination of size and zeta potential

The average size of the LUVs at 25 ºC and their zeta potential were measured on a Malvern Nano ZS (Malvern Instruments, Malvern, UK).

The measurements of LUV size were performed at a total lipid concentration of 1 mM using samples extruded at 1−10 mM through 100 nm pore size filters. A typical result obtained is given in Figure VI.1, for POPC LUVs.

Results

		Size (d.n...	% Volume	Width (d.n...
Z-Average (d.nm): 115.5	Peak 1:	112.6	100.0	27.67
PdI: 0.041	Peak 2:	0.000	0.0	0.000
Intercept: 0.968	Peak 3:	0.000	0.0	0.000
Result quality Good				

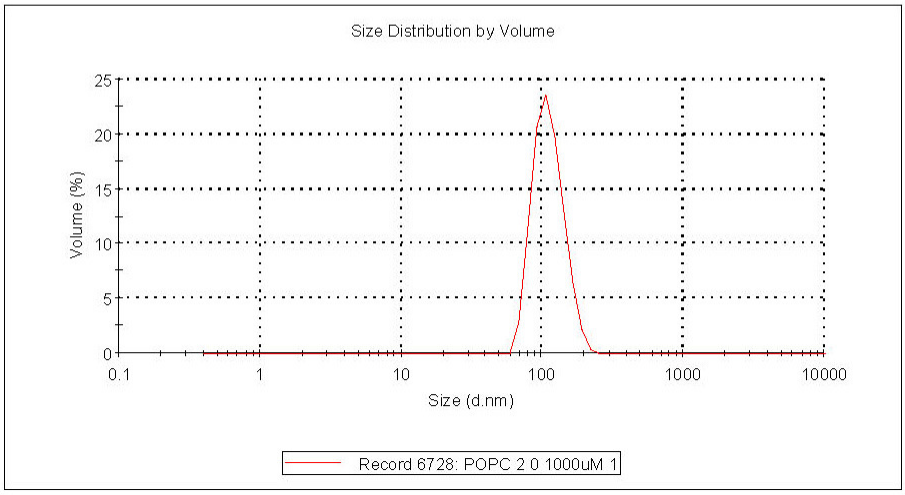

Figure VI.1: Typical results obtained for the size distribution of a sample prepared by extrusion of POPC MLVs through two stacked polycarbonate filters. The average diameter considered for this sample was given by the volume distribution of peak 1, 112.6 nm. Ten independent POPC samples have been characterized leading to an average diameter of 106 ± 7 nm.

For LUVs prepared from pure POPC, the samples were monodisperse with an average diameter of 96 to 117 nm, when evaluated from the size distribution by volume, leading to an average diameter of 106 ± 7 nm. Some samples were also characterized for the other lipid compositions used in this work, and the average diameter obtained was 101 nm for POPC:POPS 9:1 LUVs and 117 nm for POPC:Chol:POPS 6:3:1.

The mobility of the LUVs containing 10% POPS was measured at a total lipid concentration of 2 mM and the ζ potential was calculated using eq. VI.1, which is valid at all values of ionic strength used (Jones, 1995).

$$\zeta = \frac{\eta u}{\varepsilon_0 \varepsilon_r} \qquad \text{eq. VI.1}$$

The values used for the viscosity (η) and dielectric constant (ε_r) of the aqueous solutions are given in Table VI.1, together with the results obtained.

For LUVs containing CPZ at concentrations from 2 to 10 molar %, the value of the ζ potential was also calculated for the lipid compositions POPC and POPC:POPS 9:1 at a

total lipid concentration of 2 and 4 mM, respectively. For some compositions, ζ was too small to be accurately measured at the ionic strength used, and it was measured in aqueous buffer at the same pH but with different concentrations of NaCl. For these compositions, ζ at 150 mM NaCl was calculated from the results obtained at smaller ionic strengths, assuming the same dependence observed for the mixtures mentioned above.

Table VI.1: Results obtained for the Zeta potential of typical liposomes used.

[NaCl] (mM)		0	10	25	50	80	150
η (mPa s) / ε_r [a]		0.890/80.2	0.896/80.2	0.905/80.2	0.918/80.4	0.933/80.0	0.970/78.7
Lipid	CPZ:Lipid	ξ (mV)					
PC:PS 9:1	-	- 39.0 ± 1.6	- 35.4 ± 0.8	- 28.7 ± 1.1	- 23.8 ± 1.4	- 20.4 ± 1.5	- 17.3 ± 0.8
	1:50						- 16.2 ± 0.5
	1:25						- 11.3 ± 0.6
	1:10	- 6.36 ± 2.0					- 4 ± 2
PC:Chol:PS 6:3:1	-						- 23.8 ± 0.9
POPC	1:50	4.3 ± 0.9			2.1 ± 0.7		1.6 ± 0.8 [b]
	1:20	10.2 ± 0.7	13.0 ± 0.6	10.8 ± 1.3	8.0 ± 0.7	7.5 ± 0.5	5.9 ± 0.8
	1:10						9.4 ± 1.0

[a] the viscosity of the NaCl aqueous solutions assumed were taken from Ozbek and the dielectric constant from Nortemann (1997). [b] predicted from the values measured at 0 and 50 mM NaCl assuming the same dependence with the ionic strength as that observed for the samples with CPZ:POPC 1:20.

Determination of multilamellarity

Multilamellarity in the LUVs was evaluated from the relative weight of the different steps in the reduction of NBD-C_{16} or NBD-DMPE, at a molar concentration of 0.1%, by dithionite added to the aqueous solution outside the LUVs, on a thermostated stopped-flow fluorimeter (Hi-Tech model SF-61) (Cardoso, et al., 2011; Moreno et al., 2006). Typical results obtained are shown in Figure VI.2.

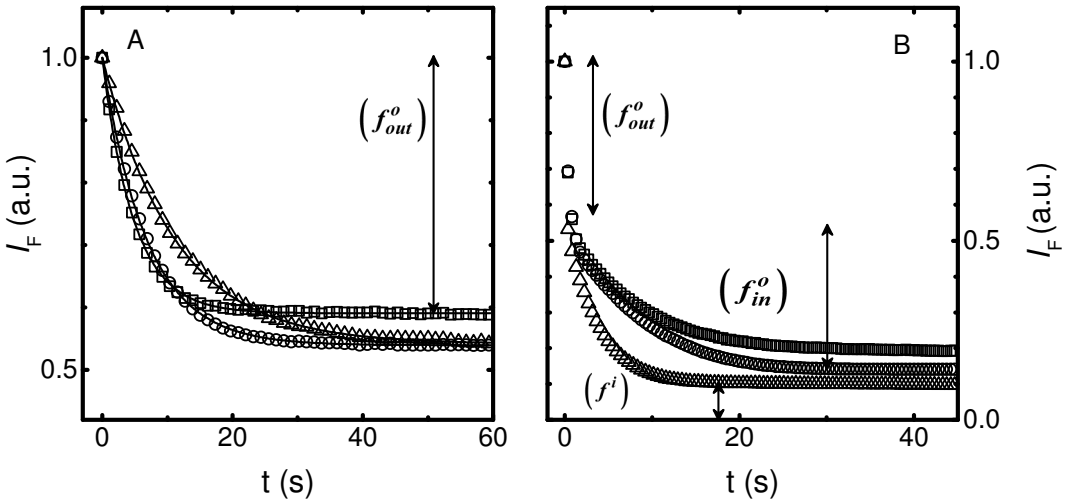

Figure VI.2: Typical results obtained for the distribution of the lipid by the outer (f^o_{out}) and inner (f^o_{in}) monolayers of the outer bilayer and by the inner f^i bilayers for LUVs prepared from POPC (□), POPC:POPS 9:1 (○) and POPC:Chol:POPS 6:3:1 (△) containing 0.1 molar % of NBD-DMPE (Plot A) or NBD-C_{16} (Plot B). The fraction of lipid in inner bilayers may be calculated from the results obtained for NBD-DMPE f^i = 1 - 2 f^o_{out}, leading to 18, 8 and 9 % for POPC, POPC:POPS and POPC:Chol:POPS, respectively. The reduction of NBD-C_{16} by dithionite directly gives the fraction of lipid in inner bilayers being 19, 14 and 10 % for POPC, POPC:POPS and POPC:Chol:POPS, respectively.

The reduction of NBD-DMPE by dithionite is a well established method to evaluate the fraction of lipid in the outer monolayer (f^o_{out}) (McIntyre and Sleight, 1991; Balch et al., 1994; Pautot et al., 2003; Moreno et al., 2006). This fraction is equal to the fraction of lipid in the inner monolayer of the outer bilayer (f^o_{in}) for 100 nm LUVs, from which the fraction of lipid in inner bilayers could be calculated ($f^i = 1-(f^o_{out} + f^o_{in})$). This method could not, however, be followed to characterize the large majority of samples used throughout this work because NBD-DMPE must be added together with the lipid and its presence could influence the interaction of CPZ with the LUVs. To overcome this difficulty we followed the reduction of NBD-C_{16} by dithionite added to the aqueous solution outside the LUVs (Cardoso et al., 2011). NBD-C_{16} may be added after the preparation of the LUVs and this method was used for the characterization of some of the samples. An aliquot of this fluorescent amphiphile was added from a stock solution in methanol (final methanol concentration smaller than 0.5%) at a molar concentration of 0.1 % and the samples were allowed to equilibrate overnight. The decrease in NBD-C_{16} fluorescence due to reaction with dithionite showed three distinct regimes: *i*) a very fast process due to reaction with NBD-C_{16} exposed to the aqueous solution outside the LUVs

(f_{out}^{o}) , *ii*) a slower step due to reaction with NBD-C_{16} initially in the inner monolayer of the outer bilayer (f_{in}^{o}) after its translocation to the outer monolayer and *iii*) a much slower process that corresponds to reduction of NBD-C_{16} initially in inner bilayers from which the fraction of lipid in the inner bilayer of multilamellar LUVs (f^{i}) could be directly calculated. The fraction of lipid in inner bilayers obtained by both methods was similar being 9 ± 2 % for LUVs with the lipid composition POPC:Chol:POPS 6:3:1, 12 ± 4 % for POPC:POPS 9:1 and 18 ± 5 % for POPC LUVs.

Biocalorimetry

Calorimetry directly measures the heat associated with a given process, which, at constant pressure, is equal to the enthalpy change in that process, ΔH. Due to sensitivity and accuracy reasons, the calorimeters used to characterize binding processes, such as the ones we are interested in, belong to the category of titration calorimeters with dynamic power compensation, operating at constant temperature.

Isothermal Titration Calorimetry

Isothermal titration calorimetry (ITC) is a technique used to measure the heat exchange associated with molecular interactions, at constant temperature. It is most often used as a direct method to characterize the binding to proteins including the thermodynamic characterization associated with this binding (Perozzo et al. 2004; Freyer and Lewis, 2008), as first described in 1965 by Christensen and co-workers.

Since 1989, when the first commercial titration calorimeter was made available, ITC is routinely used to directly characterize the thermodynamics of biological interactions. It is a well established technique in ligand binding studies, mainly between small molecules and proteins (Velazquez-Campoy, 2006), but has been less used in the characterization of the interaction of solutes with lipid membranes, which is the focus of this dissertation. This is mostly a consequence of the fact that the data analysis procedures are less well established and not commercially available (Moreno et al. 2010). In the last 15 years Heerklotz and co-workers have contributed with valuable work on the study of ligand binding to lipid membranes, using ITC, as can be consulted in the papers published by this group from 1999, 2000, 2001, 2004, 2006, 2007 and 2008.

A schematic representation of an isothermal titration calorimeter is presented in Figure VI.3. The instrument has two identical cells (sample and reference) composed of a highly efficient thermal conducting material, surrounded by an adiabatic chamber. A syringe is used to titrate the ligand into the sample cell containing the binding agent. A sequence of injections is programmed and the solution inside the syringe is injected periodically into the sample cell. A feedback control system supplies thermal power continuously to maintain the same temperature in both reference and sample cells. Any event taking place in the sample cell, usually accompanied by heat release or absorption, will change the temperature in that cell and the feedback control system will modulate the power supply in order to minimize such temperature imbalance (Velazquez-Campoy, 2005).

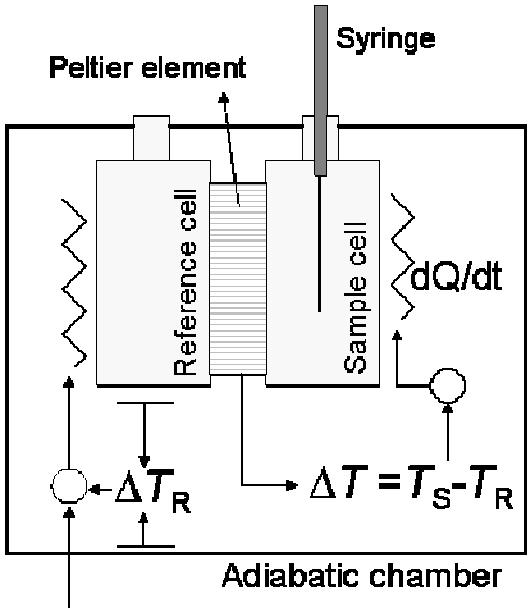

Figure VI.3: Schematic representation of an isothermal titration calorimeter.

The value of the association (or partition) constant governs the equilibrium, i.e. the partition between the different species, free and bound. The change in composition inside the sample cell, after each injection, triggers the binding reaction and the rearrangement of the population leading to the binding form of reactants. The system will pass through different equilibrium states, differing in composition, as the sequence of injections proceeds. The heat associated with each injection is proportional to the fraction of bound ligand and is calculated by integrating the area under the deflection of the signal measured (amount of heat per unit of time provided to maintain both cells, sample and reference, at the same temperature).

Applying non-linear regression and using the appropriate modeling data analysis procedure, it is possible to estimate the association constant or binding affinity and the binding enthalpy with a single experiment.

For ligand protein interactions the usual protocol is to titrate the protein (in the sample cell) with the ligand to be studied (in the syringe). With lipid bilayers the protocol must be different since we are dealing with a high plasticity binding agent, without well defined binding sites and that changes its structure significantly ,sometimes irreversibly, with the presence of high concentrations of ligands. Therefore, if we titrate the lipid bilayer in the sample cell with the ligand highly concentrated in the syringe, high local concentrations of ligand in the lipid bilayer are attained, inducing strong deviations from the ideal behaviour (Moreno et al., 2010).

ITC is unique in that it is capable of measuring simultaneously the association constant (K_a) and the enthalpy change upon binding (ΔH). Therefore, it is possible a complete thermodynamic characterization of the binding process, that is, the evaluation of the main thermodynamic parameters associated with the binding process, using basic thermodynamic relationships (eq. VI.2) to calculate changes in entropy (ΔS) and Gibbs Free Energy (ΔG) (Velazquez-Campoy and Freire, 2005; Holdgate and Ward, 2005).

$$\Delta G^\circ = -RT \ln K_a$$
$$\Delta G^\circ = \Delta H^\circ - T\Delta S^\circ \qquad \text{eq. VI.2}$$

ITC has other advantages over some of the techniques used for the study of complex interaction such as the ease of use and cost. It does not require any fluorescent probes or radioactive labels, chemical modification or immobilization of the biomolecules as the study is made in solution (Edink et al., 2010; Ladbury et al., 2010) and does not have any limitation associated with the transparency of the solution, molecular weight, temperature or pH. Nonetheless, low sensitivity, low throughput and large sample requirement have been pointed out as major drawbacks of this technique (Liang, 2008; Zhou et al., 2008).

The last decades have been fruitful in the development of new ITC instruments with increased sensitivity, allowing the use of this technique in the characterization of some nonpolar ligands with lipid bilayers (Bjelic and Jelesarov, 2008). These interactions are in many cases driven by the hydrophobic effect and small heats are expected to be evolved during the titration. The sensitivity of modern ITC instruments allows the accurate measurement of heats as small as 20 ncal *per* s and, therefore, permits the reduction of the

ligand concentration down to values that have, traditionally, only been accessible by fluorescence methods. This allows the direct and accurate characterization of the interaction of amphiphilic molecules with unperturbed lipid bilayers (Moreno et al., 2010).

Protocol:

Titrations were performed on a VP-ITC instrument from MicroCal (Northampton, MA) with a reaction cell volume of 1410.9 μL, at 25 and 37 °C. The injection speed was 0.5 μL s^{-1}, stirring speed was 459 rpm, and the reference power was 10 μcal s^{-1} (2 in μcal s^{-1} some experiments). As recommended by the manufacturer, a first injection of 4 μL was performed before the experiment was considered to start, to account for diffusion from/into the syringe during the equilibration period, but the injected amount was taken into consideration in the calculations. The titration proceeded with additions of 10 μL per injection. Amphiphilic ligands like CPZ may adsorb to some equipment parts, in particular to the filling syringe, reducing the amount of ligand available. To overcome this difficulty, after cleaning thoroughly with water, the equipment cell was rinsed with a solution with the same composition as the solution used in the experiment before filling with the required titration solution. All solutions were previously degassed for 15 min. Two protocols for the ITC experiments were used in this work: (i) uptake, in which liposomes were injected into a CPZ solution in the cell, and (ii) release, in which a liposome solution containing CPZ was injected into the buffer containing cell. The purpose of the uptake and release protocols was to obtain thermodynamic parameters for the reaction as well as a qualitative evaluation of the translocation rate constant (Tsamaloukas et al., 2007; Heerklotz et al., 1999). The thermograms were integrated using the data analysis software Origin 7.0 as modified by MicroCal to deal with ITC experiments, and the resulting differential titration curves were fitted with the appropriate equations using Microsoft Excel and the Add-In Solver. The concentrations in the cell were calculated taking into account the volume that overflows the cell due to the addition of solution from the syringe considering that overflow is faster than mixing, meaning that the composition of the solution leaving the cell is the equilibrium composition before the addition (Freire et al., 2009; Velazquez-Campoy et al., 2005; Velazquez-Campoy et al., 2006).

The appropriate models are explained within each chapter for an easier reading and discussion of the results.

References

Balch, C.; Morris, R.; Brooks, E. and Sleight, R. G. (1994) The use of N-(7-nitrobenz-2-oxa-1,3-diazole-4-yl)-labelled lipids in determining transmembrane lipid distribution. *Chemistry and Physics of Lipids*, 70, 205-212

Bartlett, G. R. (1959) Phosphorus assay in column chromatography. *The Journal of Biological Chemistry*, 234, 466–468

Bjelic, S. and Jelesarov, I. (2008) A survey of the year 2007 literature on applications of isothermal titration calorimetry. *Journal of Molecular Recognition*, 21, 289–311.

Cardoso, R. M. S.; Martins, P. A. T.; Gomes, F.; Doktorovova, S.; Vaz, W. L. C. and Moreno, M. J. (2011) Chain-Length Dependence of Insertion, Desorption, and Translocation of a Homologous Series of 7-Nitrobenz-2-oxa-1,3-diazol-4-yl-Labeled Aliphatic Amines in Membranes. *The Journal of Physical Chemistry B*, 115, 10098–10108

Christensen, J. J.; Izatt, R. M.; Eatough, D. Thermodynamics of metal cyanide coordination. V. Log K, ΔHo, and ΔS values for the Hg2 + -cn-system. Inorg. Chem. 1965, 4, 1278–1280

Edink, E.; Jansen, C. and Leurs, R. (2010) The heat is on: Thermodynamic analysis in fragment-based drug discovery. *Drug Discovery Today: Technologies*, 7, 189–201

Freire, E.; Schon, A. and Velazquez-Campoy, A. (2009) Isothermal titration calorimetry: general formalism using binding polynomials. *Methods in Enzymology: Biothermodynamics*, 455, 127–155

Freyer, M. W.; Lewis, E. A. Isothermal titration calorimetry: Experimental design, data analysis, and probing macromolecule/ligand binding and kinetic interactions. Methods Cell Biol. 2008, 84, 79–113

Heerklotz, H.; Binder, H. and Epand, R. M. (1999) A "release" protocol for isothermal titration calormetry. *Biophysical Journal*, 76, 2606–2613

Heerklotz, H. (2001) Membrane stress and permeabilization induced by asymmetric incorporation of compounds. *Biophysical Journal,* 81, 184–195

Heerklotz, H. and Seelig, J. (2000) Titration calorimetry of surfactant-membrane partitioning and membrane solubilisation. *Biochimica et. Biophysica Acta*, 1508, 69–85

Heerklotz, H. and Seelig, J. (2007) Leakage and lysis of lipid membranes induced by the lipopeptide surfactin. *European Biophysics Journal With Biophysics Letters,* 36, 305–314

Heerklotz, H. (2008) Interactions of surfactants with lipid membranes. *Quarterly Reviews of Biophysics*, 41, 205–264

Heerklotz, H. (2004) The microcalorimetry of lipid membranes. *Journal of Physics: Condensed Matter*, 16, R441–R467

Holdgate, G. A.; Ward, W. H. J. (2005) Measurement of binding thermodynamics in drug discovery. *Drug Discovery Today*, 22, 1543–1550

Hope, M. J.; Bally, M. B.; Webb, G. and Cullis, P. R. (1985) Production of large unilamellar vesicles by a rapid extrusion procedure. Characterization of size distribution, trapped volume and ability to maintain a membrane potential. *Biochimica et Biophysica Acta*, 812, 55-65.

Jones, M. N. (1995) The surface properties of phospholipid liposome systems and theys characterization. *Advances in Colloid and Interface Science*, 54, 93−128

Keller, S.; Heerklotz, H.; Jahnke, N. and Blume, A. (2006) Thermodynamics of lipid membrane solubilization by sodium dodecyl sulphate. *Biophysical Journal*, 90, 4509–4521

Keller, S.; Heerklotz, H. and Blume, A. (2006) Monitoring lipid membrane translocation of sodium dodecyl sulfate by isothermal titration calorimetry. *Journal of the American Chemical Society*, 128, 1279–1286.

Ladbury, J. E.; Klebe, G. and Freire, E. (2010) Adding calorimetric data to decision making in lead discovery: A hot tip. *Nature Reviews Drug Discovery*, 9, 23–27

Liang, Y. (2008) Application of isothermal titration calorimetry in protein science. *Acta Biochimica Biophysica Sinica*, 40, 565–576

McIntyre, J. C. and Sleight, R. G. (1991) Fluorescence assay for phospholipid membrane asymmetry. *Biochemistry*, 30, 11819-11827.

Moreno, M. J.; Estronca, L. M. B. B. and Vaz, W. L. C. (2006) Translocation of phospholipids and dithionite permeability in liquid-ordered and liquid-disordered membranes. *Biophysical Journal*, 91, 873−881

Moreno, M. J.; Bastos, M. And Velazquez-Campoy, A. (2010) Partition of amphiphilic molecules to lipid bilayers by isothermal titration calorimetry. *Analytical Biochemistry*, 399, 44-47

Nörtemann, K.; Hilland and J.; Kaatze, U. (1997) Dielectric properties of aqueous NaCl solutions at microwave frequencies. *Journal of Physical Chemistry A*, 101, 6864−6869

Ozbek, H. Viscosity of Aqueous Sodium Chloride Solutions from 0−150 °C. Accessed on 21/12/2011, Lawrence Berkeley National Laboratory, LBNL paper LBL-5931; http://escholarship.org/uc/item/3jp6n2bf

Pautot, S.; Frisken, B. J. and Weitz, D. A. (2003) Engineering asymmetric vesicles. *Proceedings of the National Academy of Sciences USA*, 100, 10718-10721

Perozzo, R.; Folkers, G.; Scapozza, L. Thermodynamics of protein–ligand interactions: History, presence, and future aspects. J. Recept. Sig. Transd. 2004, 24, 1–52

Taylor, R. P.; Broccoli, A. V. and Grisham, C. M. (1978) Enzymatic and colorimetric determination of total serum cholesterol. An undergraduate biochemistry laboratory experiment. *Journal of Chemical Education*, 55, 63-64

Tsamaloukas, A. D.; Keller, S. and Heerklotz, H. (2007) Uptake and release protocol for assessing membrane binding and permeation by way of isothermal titration calorimetry. *Nature Protocols*, 2, 695−704

Velazquez-Campoy, A. and Freire, E. (2005) ITC in the post-genomic era…? Priceless. *Biophysical Chemistry*, 115, 115−124

Velazquez-Campoy, A. and Freire, E. (2006) Isothermal titration calorimetry to determine association constants for high-affinity ligands. *Nature Protocols*, 1, 186−191

Zhang, F. L: and Rowe, E. S. (1992) Titration calorimetric and differential scanning calorimetric studies of the interactions of normal-butanol with several phases of dipalmitoylphosphatidylcholine. *Biochemistry*, 31, 2005–2011

Zhou, X.; Sun, Q.; Kini, R. M. and Sivaraman, J. (2008) A universal method for fishing target proteins from mixtures of biomolecules using isothermal titration calorimetry. *Protein Science*, 17, 1798–1804